NUREG/CR-2956
PNL-4471

Neutron Dosimetry at Commercial Nuclear Plants

Final Report of Subtask B: Dosimeter Response

Prepared by F. M. Cummings, G. W. R. Endres, L. W. Brackenbush

Pacific Northwest Laboratory
Operated by
Battelle Memorial Institute

Prepared for
U.S. Nuclear Regulatory Commission

GPO Printed copy price: $5.50

NUREG/CR-2956
PNL-4471

Neutron Dosimetry at Commercial Nuclear Plants

Final Report of Subtask B: Dosimeter Response

Manuscript Completed: February 1983
Date Published: March 1983

Prepared by
F. M. Cummings, G. W. R. Endres, L. W. Brackenbush

Pacific Northwest Laboratory
Richland, WA 99352

Prepared for
Division of Facility Operations
Office of Nuclear Regulatory Research
U.S. Nuclear Regulatory Commission
Washington, D.C. 20555
NRC FIN B2282

ABSTRACT

As part of a larger program to evaluate personnel neutron dosimetry at commercial nuclear power plants, this study was designed to characterize neutron dosimeter responses inside the containment structure of commercial nuclear plants. In order to characterize those responses, dosimeters were irradiated inside containment at 2 pressurized water reactors and at pipe penetrations outside the biological shield at two boiling water reactors. The reactors were operating at full power during the irradiations. Measurements were also performed with electronic instruments, the tissue equivalent proportional counter (TEPC), and portable remmeters, SNOOPY, RASCAL® and PNR-4®.

Dosimeter irradiations were also performed (1) using monoenergetic neutrons produced by an accelerator and (2) using the filtered reactor beams at the National Bureau of Standards research reactor. Dosimeter response was measured for the various dosimeters as a function of neutron energy. The results of higher energy irradiations (neutron energy between 4 and 5 MeV) showed that using bare neutron sources for dosimeter calibrations without further corrections is inappropriate for reactor neutron dosimetry. The results also indicated that the dosimeters responded inside containment as if the dosimeters were being irradiated with monoenergetic neutrons below 100 keV. CR-39 and polycarbonate track etch dosimeters, used without (n,α) radiators, are inappropriate techniques for personnel dosimetry inside containment. The polycarbonate track etch dosimeter which used (n,α) radiators to produce tracks in the plastic lattice was adequately sensitive, but was judged inadequate because of the variability of the measurements and the fact that two of the dosimeters saturated at low doses. No CR-39 dosimeter was tested which used (n,α) radiators. The most precise (reproducible) dosimeters for the irradiations were the TLD-albedos. Of those, two dosimeters were in reasonable agreement with the SNOOPY remmeter: a TLD-albedo dosimeter calibrated using a D_2O-moderated ^{252}Cf source and the Hankins dosimeter calibrated according to the 9 in. to 3 in. sphere ratios. None of the dosimeters exhibited an accurate dosimetric response compared to the TEPC measurements.

® Eberline Instruments, Santa Fe, New Mexico.

SUMMARY

This study is part of a larger program to evaluate personnel neutron dosimetry at commercial nuclear power plants. The first phase of the program, subtask A, was designed to measure neutron energy spectra, dose equivalents, and various parameters necessary to calibrate neutron dosimeters (e.g., 9 in. to 3 in. sphere response ratios) at six nuclear power plants (5 pressurized water reactors, PWRs, and 1 boiling water reactor, BWR). Multisphere measurements indicated that the average neutron energies inside containment at the PWRs were, generally, below 100 keV (Endres et al. 1981). The average energies at the pipe penetrations outside the biological shield at the BWR were 155 keV or above (Endres et al. 1981). During those measurements it was noted that NTA-film dosimeters predominantly in use at the time as personnel neutron dosimeters failed to positively respond at any of the measurement locations, even when dose equivalents exceeded 3 rem. It was determined by Schwartz in a related study that the threshold for NTA film under field conditions was above 0.6 MeV (Schwartz et al 1982).

The objective of the second phase of the project, subtask B, was to accurately characterize the responses of several types of personnel neutron dosimeters currently in use at nuclear power plants and relate those responses to reactor environments. In order to accomplish that task, three types of dosimeters (TLD-albedo, CR-39 and polycarbonate) from five commercial vendors and two U.S. DOE contractors were irradiated in groups of five dosimeters from each participant. Irradiations were conducted using water phantoms inside containment at two PWRs and at two pipe penetrations at a BWR plant. Dose equivalent rate measurements were performed at each location at the time of dosimeter irradiation using a tissue equivalent proportional counter (TEPC), and several types of commercially available remmeters, including a SNOOPY, RASCAL and PNR-4. All of the dosimeter measurements were compared to the TEPC and SNOOPY measurements in order to judge the appropriateness of each type of dosimeter.

The criteria for evaluating dosimeters for use inside containment of nuclear power plants included sensitivity and precision. Because the calibration techniques determine accuracy, and because accuracy may be improved by site specific calibration, accuracy was not used as a criterion for adequacy of dosimeter technique.

The TLD-albedo dosimeters were all adequately sensitive to neutrons inside containment in the personnel dosimetry range of doses. While most of the TLD-albedo dosimeters exhibited good precision, several of them showed a definite lack of precision (reproducibility) indicating the need for careful analysis and interpretation no matter what technique is used. Of the dosimeters which showed good precision, two dosimeters compared very favorably with SNOOPY measurements: the TLD-albedo dosimeter which was calibrated using a D_2O-moderated ^{252}Cf source and the Hankins type TLD-albedo dosimeter corrected using the 9 in. to 3 in. sphere response ratio technique.

The polycarbonate dosimeter which used natural-boron loaded (n,α) radiators was adequately sensitive and agreed with SNOOPY measurements on the average. However, this dosimeter was judged inadequate for use inside containment because of its high variability and because 2 of the 40 dosimeters in irradiated inside containment saturated at low doses.

The dosimeters which lacked sensitivity adequate for personnel neutron dosimetry included NTA film (Endres et al. 1981), CR-39 and polycarbonate track etch films irradiated without the use of (n,α) radiators (boron-loaded) for track enhancement. No CR-39 track etch dosimeter which used (n,α) radiators was available for evaluation during this study.

In addition to the reactor irradiations, dosimeters were irradiated using a Van de Graaff accelerator producing monoenergetic neutron beams with the following energies: 0.070, 0.096, 0.110, 0.161, 0.264, 0.358, 0.448, 4.09, 4.45, and 4.88 MeV. The dosimeters were also irradiated using the monoenergetic filtered reactor beams at the National Bureau of Standards research reactor which included the following energies: thermal, 0.002, 0.024 and 0.144 MeV. All the monoenergetic irradiations were performed on water phantoms and were carefully controlled in order to accurately assess neutron energy and delivered dose equivalent.

The responses were characterized for each type of dosimeter and were as follows:

- TLD-albedo

  All the TLD-albedo dosimeters exhibited a linear (straight line) relationship between the natural log of the response and the natural log of the neutron energy between neutron energies of 0.024 MeV and 0.500 MeV. The responses in this range increased with decreasing neutron energy. Outside this range, the response flattened out as reported by Alsmiller and Barish (1974).

- CR-39 Track Etch

  The CR-39 track etch responded high in the range of neutron energies between 0.1 and 0.5 MeV, but decreased rapidly to zero as neutron energies went below 0.1 MeV.

- Polycarbonate Track Etch

  Used without (n,α) radiators, the polycarbonate track etch dosimeter failed to respond, even to neutrons with energies between 4 and 5 MeV produced on the accelerator. It was expected that the polycarbonate would have detected neutrons at the high energies because the stated threshold of detection is 1.5 MeV (Brackenbush et al. 1980).

When (n,α) radiators were used to enhance track formation in the polycarbonate film, the response was flat over the range of neutron energies investigated in this study. The response of this dosimeter was variable.

Comparing the dosimeter responses from the monoenergetic irradiations with the dosimeter responses from the reactor irradiations confirmed subtask A results that the energies of neutrons found inside containment are predominantly below 0.100 MeV.

Comparing the responses of the portable instruments during the reactor irradiations indicates the necessity of making careful measurements of neutron dose equivalents and neutron energy spectra inside containment at nuclear power plants (this issue will be addressed in detail in future phases of this program during subtasks C and D). It was shown that the portable remmeters responded high, compared to the TEPC. Calibrating dosimeters to portable remmeters will therefore result in dose equivalents assigned to personnel being conservative on the high side.

CONTENTS

FIGURES

TABLES

ACKNOWLEDGMENTS

We would like to thank Bob Schwartz of the National Bureau of Standards for his help and cooperation in this study. Particularly, we are grateful for his careful handling and irradiation of the many dosimeters we used.

We should also like to thank Messrs. Leo Faust, Dan Haggard, Bob Scherpelz and Joe Aldrich for their parts in the measurements at the nuclear plants and their analyses of that data.

Additionally, there are those staff members of the represented power companies and dosimeter vendors whose cooperation and support made this study possible.

1.0 INTRODUCTION

This report discusses subtask B which is the second part of a larger four-phase project to evaluate neutron dosimetry techniques at commercial nuclear power plants. This study, subtask B, was designed to characterize the response of personnel neutron dosimeters at the power plants.

The first phase, subtask A, finished in FY 1981, involved the characterization of neutron energy spectra and dose equivalent rates at six plants (5 PWR's and 1 BWR). The measurement techniques which were employed under the first phase included the Bonner multisphere system, the tissue equivalent proportional counter (TEPC), the ^{3}He spectrometer, various portable neutron rem-meters and several types of neutron dosimeters (Endres et al. 1981).

During the second phase of this project, started in FY 1980, multiple dosimeters of each type of neutron dosimeter were irradiated at three of the sites visited previously (2 PWR's and 1 BWR), at the Hanford Accelerator Facility and at the National Bureau of Standards (NBS) research reactor. The neutron dosimeter measurements are evaluated herein by comparing them to portable instrument measurements and TEPC measurements (reactor irradiations) and calculations from fluence measurements (accelerator and NBS irradiations).

The criteria which are used to evaluate dosimeter adequacy include sensitivity and precision. A dosimeter may not be sensitive enough to use for personnel neutron dosimetry if it has a threshold below which it cannot detect neutrons regardless of the number of neutrons present, or if the reactions in the dosimeter require so many neutrons that dose equivalents in the 0-100 mrem range cannot be measured. For instance, some nuclear power plants still employ NTA film neutron dosimeters. While NTA film was not evaluated in this subtask, related studies attest to the inadequacy of NTA-film for use as a personnel neutron dosimeter inside containment of nuclear power plants because NTA film exhibits a threshold of 0.6 MeV which means that NTA-film cannot detect neutrons with energies below 0.6 MeV (Endres et al. 1981; Schwartz et al. 1982; Ryan et al. 1982).

Another factor in neutron dosimetry is the precision of the measurement. For instance, one type of dosimeter may achieve a high degree of accuracy when averaged over many irradiations, but individual dosimeter results may vary from the mean as much as an order of magnitude. The object then is to find a dosimeter type with good precision (i.e., a dosimeter which faithfully reproduces its response under similar conditions) and adequate sensitivity.

This work was performed for the U.S. Nuclear Regulatory Commission (USNRC) under Contract No. DE-AC06-76RLO 1830. Dosimeter irradiations were conducted at commercial nuclear power plants, the Van de Graaff accelerator at Hanford and at the NBS research reactor using filtered neutron beams. Each dosimeter processor or vendor analyzed its own dosimeters and provided the results reported herein.

2.0 DOSIMETER MEASUREMENTS

Personnel neutron dosimeters are passive devices used to collect and record radiation doses to persons. These devices operate in a variety of ways and will be described in some detail for each dosimeter tested in this study. In this study two kinds of dosimeters were tested, thermoluminescence (TLD) albedo dosimeters and track etch dosimeters. A general discussion of the principles behind each of these techniques follows. Five dosimetry vendors and two USDOE labs submitted dosimeters for evaluation in this study.

2.1 DOSIMETER DESCRIPTIONS

2.1.1 TLD - Albedo Dosimeters

TLD's are crystals which are constructed so that radiation interacting with an atom liberates an electron (ionization) and the "liberated" electron moves away to occupy an interstitial site. The "occupation of interstitial sites" means that the electron is shared by several atoms and the most probable location of the electron at any given time is the volume between those atoms. These sites are called traps. Heating the crystal to the right temperature allows the trapped electrons to move through the crystal and recombine with electron deficient atoms. The energy that an electron loses when it recombines with an atom is given up as a "particle" of light. These light pulses can be counted by using a photomultiplier tube. For gamma rays between 100 keV and 2 MeV the number of light pulses per interaction is roughly constant. That is not the case for neutrons of different energies, though.

The most common TLD for neutron detection uses lithium-6 in either lithium fluoride (LiF) or in lithium borate ($Li_2B_4O_7$). When a neutron interacts with the lithium, the reaction of interest is the splitting of the lithium into an alpha particle (helium-4 nucleus) and a triton (tritium nucleus). This is written as $^6Li(n,\alpha)^3H$. The α and ^3H recoiling particles ionize atoms in their path freeing electrons to become trapped. The difficulty with interpreting this interaction is that a thermal neutron will interact with ^6Li one thousand times more frequently than a neutron with a million times the energy. For this reason TLDs are "neutron energy dependent."

The term "albedo" means "reflected." Its use in this case refers to the detection of the neutrons which have been moderated by a person's body and reflected back into the dosimeter. This technique greatly increases the sensitivity of TLD's, but also complicates the interpretation of the neutron dose.

2.1.2 Track Etch Films

The track-etch dosimeters used in this study used either allyl diglycol carbonate (CR-39®) or polycarbonate plastic. They work in essentially the same manner. A neutron interacts with an atom in the plastic lattice or in a

®Registered trademark of Pittsburgh Plate Glass.

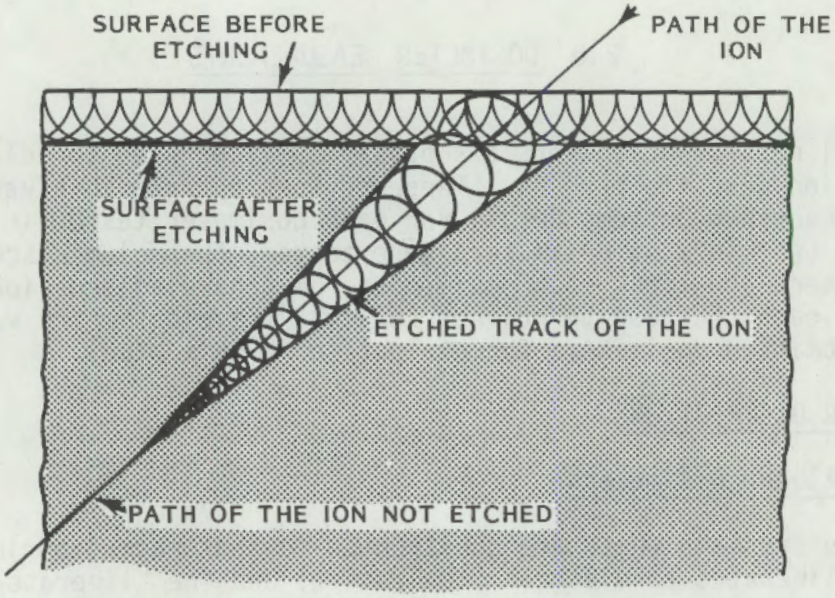

FIGURE 1. Side View of An Etched Track (Enge 1980)

material adjacent to the plastic (radiator) producing a charged recoil particle. The recoiling atom may be a proton, an alpha particle or a carbon atom which ionizes other atoms as it travels through the plastic lattice (see Figure 1). These plastic films are insensitive to photon radiation.

To analyze the tracks (paths of ionization) requires chemical etching of the plastic surfaces. An electrical field is sometimes applied across the film during etching to produce high localized electric fields at sites where the lattice has been deformed by the recoiling atoms. The plastic along the tracks then is preferentially etched producing pits. The number of pits in a given area are counted manually using a microscope or a microfiche reader. The density of tracks, or pits, is proportional to the dose. A typical etched-film is shown in Figure 2 with the tracks clearly defined. Additional techniques include pre-etching the films and using microprocessor controlled cell-colony counters. (For a discussion of track-etch principles, the reader is referred to the publication, Nuclear Tracks, dedicated to reporting research efforts with nuclear track detectors. Specifically refer to Volume 4, Number 4, Page 283 in which W. Enge gives an introduction to nuclear track detectors; Enge 1980).

2.1.3 Vendor A (TLD-Albedo)

Vendor A's dosimeter relies on neutron interactions with ^{6}Li in natural LiF. When the chip is heated, the number of light pulses, or photo-tube current is plotted versus the temperature of the planchette on which the chip rests. The resulting curve is called a "glow curve." Figure 3 shows a glow curve with two glow peaks, A and B, which occur around temperatures T_a and T_b respectively. Glow peak A is due to the interactions with gamma rays in

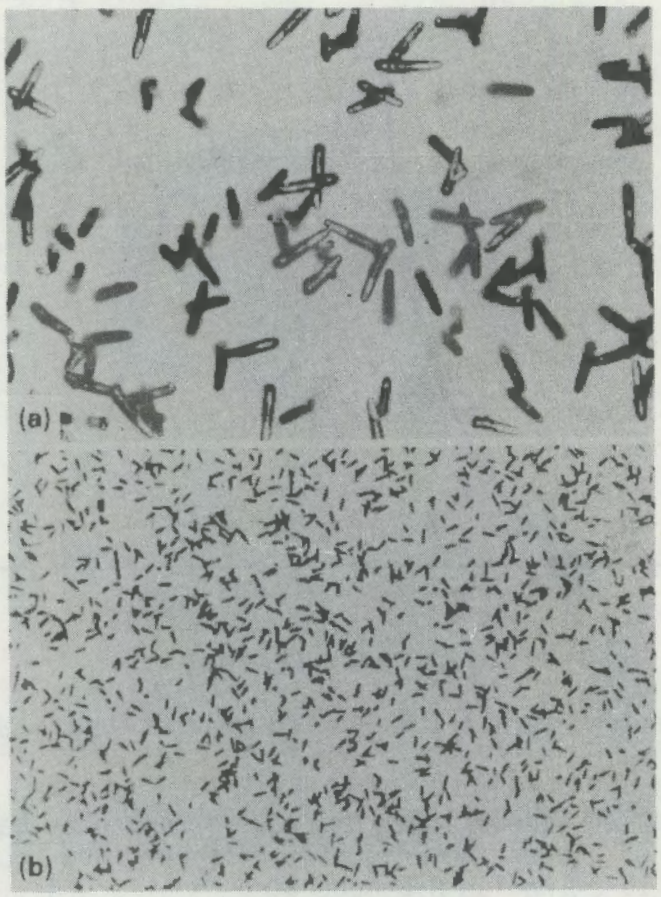

FIGURE 2. Fission Tracks in Polycarbonate. 2.a. is magnified 450X, b. is magnified 100X (Enge 1980).

the LiF crystal. Peak B is due to neutron and gamma interactions. A comparison of the two peaks leads to an estimate of the neutron interactions in the crystal and, when the proper calibration factor is applied, also to the dose. This technique is called "deep trap analysis" and is the technique used by Vendor A.

The calibration factors for the irradiations in this study were unknown to Vendor A as the neutron energy spectra were also unknown, hence Vendor A's data appear as net reader counts, not as dose equivalents.

2.1.4 Vendor B (TLD-Albedo, CR-39, Polycarbonate)

The TLD-albedo portion of this dosimeter consists of a pair of LiF chips. The Li in one chip has been enriched in the isotope ^{6}Li to greater than 95 percent while the other chip is enriched in ^{7}Li to greater than 99 percent. The neutron interactions are evaluated by comparing the light output from the neutron-sensitive ^{6}LiF chip to the light output from the neutron-insensitive ^{7}LiF chip. The light output is related to dose equivalent

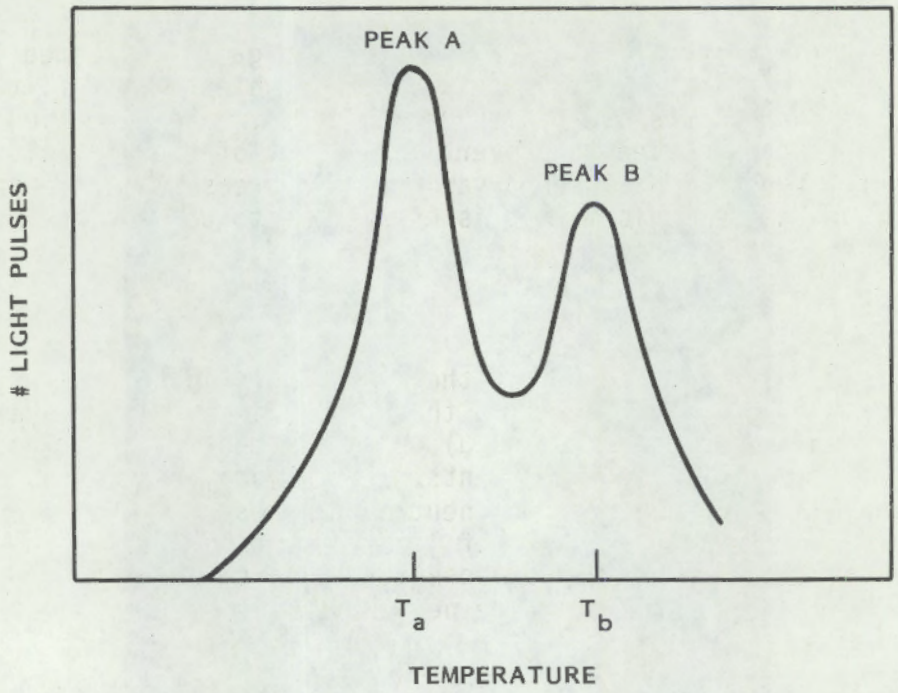

FIGURE 3. Representative TLD Glow Curve from Deep-Trap TLD Analysis

through the calibration source. In this case, the vendor had previously determined the response of his dosimeter to two different neutron sources, a bare ^{252}Cf source and a 15 cm radius D_2O-moderated ^{252}Cf source. The dose equivalents noted in the data and summary tables in the appendix for each irradiation used the same raw counts from the TLDs, but different calibration factors as is verified by the ratio of the two reported results at each irradiation (see appendix).

The CR-39 film in this dosimeter is actually a block of plastic which is placed inside the dosimeter holder with the TLDs. The inside of the holder is lined with cadmium to reduce the thermal neutron flux reaching the TLDs. The CR-39 has a threshold of approximately 100 keV, which means that neutrons with energies less than 100 keV will not be detected by the CR-39. The cadmium effectively shields the detectors only from the neutrons with energies less than 0.5 eV.

The thin polycarbonate film is placed in a paper envelope and attached to the outside-front of the dosimeter. This part of the dosimeter is used to detect neutrons with energies above 1.5 MeV where the TLD portion has a smaller probability of detecting neutrons.

2.1.5 Vendor C (TLD-Albedo)

Vendor C's dosimeter consists of LiF impregnated into a plastic substrate. The neutron detection is similar to other types of TLD-albedos, however, the

analysis of results differs. Vendor C compares the gamma-corrected light output of ^{6}Li which is behind a cadmium filter to ^{6}Li which is not filtered. The ratio of the two outputs is related graphically to a calibration factor. The calibration factor is used to convert the output of the unshielded LiF to dose equivalent. Vendor C has used a variety of sources to derive the calibration factor and hence, this method is an attempt to correct the neutron response for energy differences.

2.1.6 Vendor D (TLD-Albedo)

Vendor D's dosimeter differs from the other TLD's in several ways. First the TLD materials used are different in that the dosimeter incorporates copper doped natural lithium borate ($Li_2B_4O_7$:Cu) as two elements and dysprosium doped calcium sulfate ($CaSO_4$:Dy) as two elements. The natural $Li_2B_4O_7$:Cu elements contain ^{6}Li and ^{10}B which enhances the neutron response. The dose equivalent is determined by comparing the ratios of light output between the two $Li_2B_4O_7$ chips and the $CaSO_4$ chips. Based on those ratios, a calibration factor is multiplied with the light output of the neutron-sensitive element to arrive at dose equivalent.

2.1.7 Vendor E (Polycarbonate)

Vendor E uses polycarbonate film as the basis of its dosimeter. The difference between this dosimeter and the polycarbonate used by Vendor B is that E does not rely solely on the interaction of neutrons with the plastic lattice for track production. The polycarbonate film is placed behind filters containing material such as ^{10}B which produces an alpha particle under neutron interaction (written as $^{10}B(n,\alpha)^{7}Li$). Tracks in the plastic are caused by the alpha particles instead of neutrons. As the neutron energy goes above 1.5 MeV the neutrons have sufficient energy to leave tracks in the plastic by interacting with carbon atoms directly in the lattice itself as explained in the previous section covering the general theory of neutron detection by plastic track etch dosimeters.

2.1.8 HMPD (TLD)

The HMPD dosimeter compares the reading of a cadmium shielded ^{6}LiF chip to that of an unshielded ^{6}LiF chip. The dose equivalent is defined below (Thorson and Endres 1981).

$$DE = A \cdot R_1 - B \cdot R_\gamma - C \cdot (R_2 - R_1)$$

where

DE = dose equivalent in mrem
A,B,C = proportionality constants
R_1 = reading on the cadmium filtered ^{6}LiF chip (neutron-sensitive)
R_γ = reading on the tin filtered ^{7}LiF chip (neutron-insensitive)
(R_2-R_1) = difference between the tin-filtered ^{6}LiF chip and the Cd filtered ^{6}LiF chip; proportional to the thermal neutron flux.

This dosimeter is energy dependent as are other TLD-albedo dosimeters. The HMPD was calibrated using the bare ^{252}Cf source at NBS.

2.1.9 LLL (TLD)

This is the Hankins dosimeter described extensively in open literature, (Griffith et al. 1979). The dose equivalent estimated using dosimeter data is adjusted by a calibration factor related to the 9 in. to 3 in. sphere response technique (Hankins 1975; Hankins 1977; Griffith 1979). It is very important to realize that the calibration factor relates the dosimeter response to a moderated portable instrument response. The effect is that this dosimeter will give results which approximate the SNOOPY or PNR-4 very closely. LLL did not participate in the accelerator measurements.

2.2 IRRADIATION CONDITIONS

Great care was taken to irradiate the dosimeters from each participant under as similar conditions as possible. For instance, all the dosimeters (TLD-albedo and track-etch) were irradiated on water phantoms facing the main source of neutron radiation even though only the TLD-albedo dosimeters required a phantom. The dosimeters were irradiated at an accelerator, at the NBS research reactor and at the commercial nuclear power plants. At the accelerator, only three dosimeters of each type were irradiated at any given neutron energy because the irradiation conditions were easily controlled and because irradiation times were long. The neutron energies were chosen to reflect the energies of neutrons encountered inside containment at nuclear power plants.

At the NBS research reactor, dosimeters were irradiated on a phantom using a scanner. The scanner is programmed to move the phantom across the neutron beam at various heights in order to achieve a simulated uniform irradiation field.

The locations chosen in the power plants were representative of routine work locations. The irradiation conditions for these three situations are described in the paragraphs that follow.

2.2.1 Accelerator Irradiations

The accelerator used for these irradiations was a 2.0 MeV Van de Graaff positive ion accelerator. The ions that were accelerated included protons and deuterons.

2.2.1.1 Irradiation Configuration

Dosimeters were placed on a 37 cm x 37 cm x 18 cm-thick water-filled phantom at 45° relative to the beam line (Figure 4). Distances were measured from the center of the target holder on the end of the proton beam tube to 1) the center of the phantom and 2) the edges of the phantom (18.5 cm from center). Those distances are 75.0 cm from target to phantom center and 78.9 cm from target to phantom edge.

For the irradiations between 0.16 and 0.50 MeV a ^{3}He spectrometer was placed so its longitudinal axis was at 45° relative to the beam line and its geometrical center was 50 cm from the center of the target holder. The precision long counter was positioned at 45° and the nearest face of the long counter was 91.7 cm from the center of the target holder. All reference points (center of long counter front face, vertical center of ^{3}He spectrometer, center of target face and center of phantom) were 106.2 cm from the floor. Irradiations were performed at 135° relative to the beam line for the 0.110 and 0.096 MeV irradiations and 105° relative to the beam line for the 0.07 MeV irradiation, with the same distances being maintained. During the high energy irradiations ($E_n \geq 4.0$ MeV) the long counter was placed at 120° while the dosimeters and phantom were at 0° relative to the beam line.

The target used was a copper-backed titanium hydride (TiH) disk 0.56 mg/cm^2 thick. This target was chosen because it was known to yield very nearly monoenergetic neutrons from the interaction between the accelerated ion and the hydride target atom without degrading the ion energy too much. For the irradiations using neutrons with energies between 0.07 and 0.5 MeV, the hydride in the target was tritium (^{3}H) and the accelerated ion was a proton. For the 4 to 5 MeV irradiations, the hydride was deuterium (^{2}H) and the accelerated ion was also deuterium.

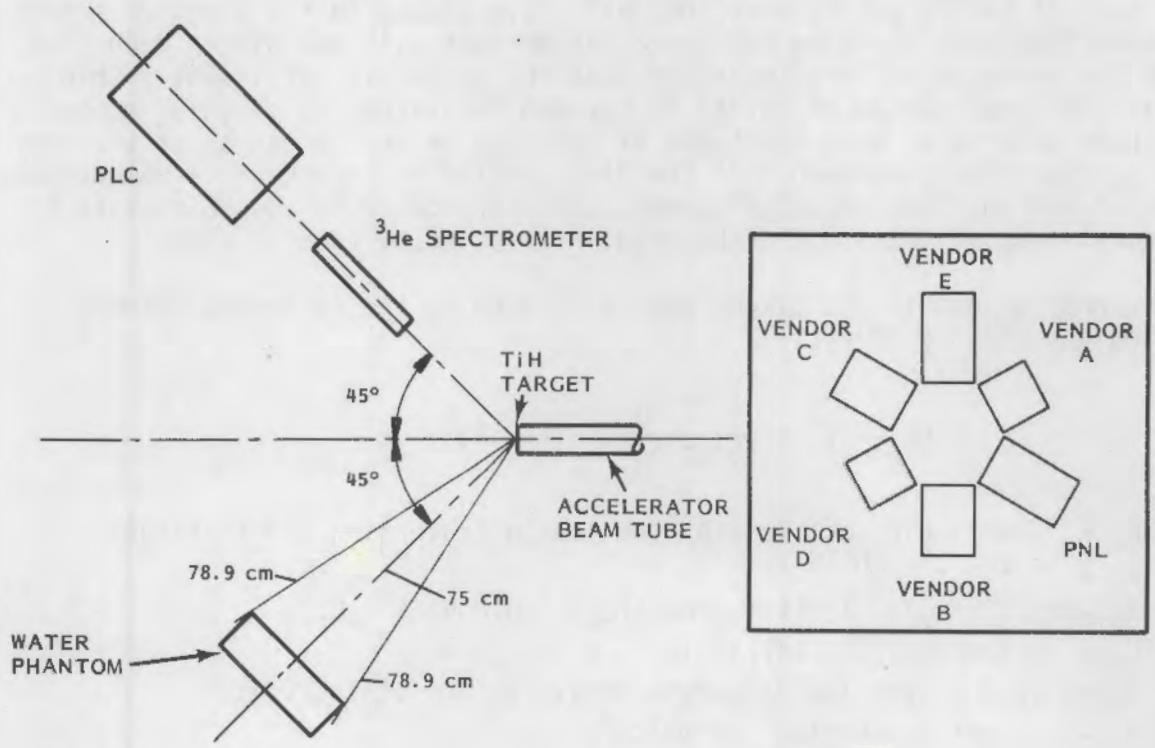

FIGURE 4. Irradiation Configuration and Dosimeter Placement on the Water Phantom for Accelerator Irradiations

2.2.1.2 Neutron Energy Determination

The neutron energy distribution is a result of the $^{3}H(p,n)^{3}He$ reaction in the $Ti^{3}H$ target or the $^{2}H(^{2}H,n)^{3}He$ reaction in the $Ti^{2}H$ target. The energy of the neutron produced is a function of 1) the bombarding energy of the ion, and 2) the scattering angle. The first consideration will be the bombarding energy of the ion.

The energy of the ion beam reaching the target is a function of the magnetic field produced by the bending magnet and the accelerating voltage produced by the belt of the Van de Graff accelerator. The accelerating voltage is calibrated using comparisons of various electronic measurements, and the magnet is calibrated by using a known energy threshold reaction. The shape of the energy spectrum of the ion beam reaching the target is a steeply sloped Gaussian curve around the average energy, varying by less than 10 keV at energies between 1.0 and 2.0 MeV. For that reason, the ion beam is considered to be monoenergetic when it reaches the target.

The cross-section of interaction for the neutron-producing reactions is very small, so the entire beam may be considered to traverse the target without interaction. Some of the accelerated ions, however, will interact with atoms in the target and produce neutrons. The ions that interact with atoms after traversing the target will have a lower energy than those which interact at the face of the target because they will have slowed in the titanium matrix. The interaction cross-section for the degraded ions will not differ much from that of the nondegraded ions, provided that the target is sufficiently thin. Also, if the distribution of ^{2}H and ^{3}H through the target is roughly homogenous, there will be as many reactions at the face of the target as at the rear of the target. It is assumed that the distribution of ^{2}H and ^{3}H is homogenous because of the way the target is constructed and because ^{2}H and ^{3}H migrate to the warmest spot in the target (the area intersected by the ion beam).

The energy lost in the target was calculated by the following formula (Anderson and Ziegler 1977):

$$dE_p(\text{keV}) = \frac{S_L \cdot S_H}{(S_L + S_H)} \cdot (12.58) \cdot dx$$

where dE_p = energy (in keV) lost by the ion in traversing the Ti target

$S_L = 5.496 \cdot (E_p^{0.45})$

$S_H = (5165/E_p) \cdot \ln [1 + (568.5/E_p) + 0.009474 \cdot E_p)]$

E_p = ion energy (in keV/amu)

12.58 is a conversion factor to arrive at the stated units

dx = target thickness, .56 mg/cm^2.

The scatter angle was measured with an accuracy of 0.01 radians.

The neutron energy can be calculated from reaction kinematics. Figure 5 is a schematic representation of the reaction and illustrates the neutron energy determination. The various components are: M_1 = mass of the incident ion, E_I = ion energy, M_2 = mass of the target atom, M_3 = mass of the neutron, E_3 = energy of the neutron, M_4 = mass of the ^{3}He recoil atom, E_4 = energy of the recoil ^{3}He, and Q = mass defect for the reaction.

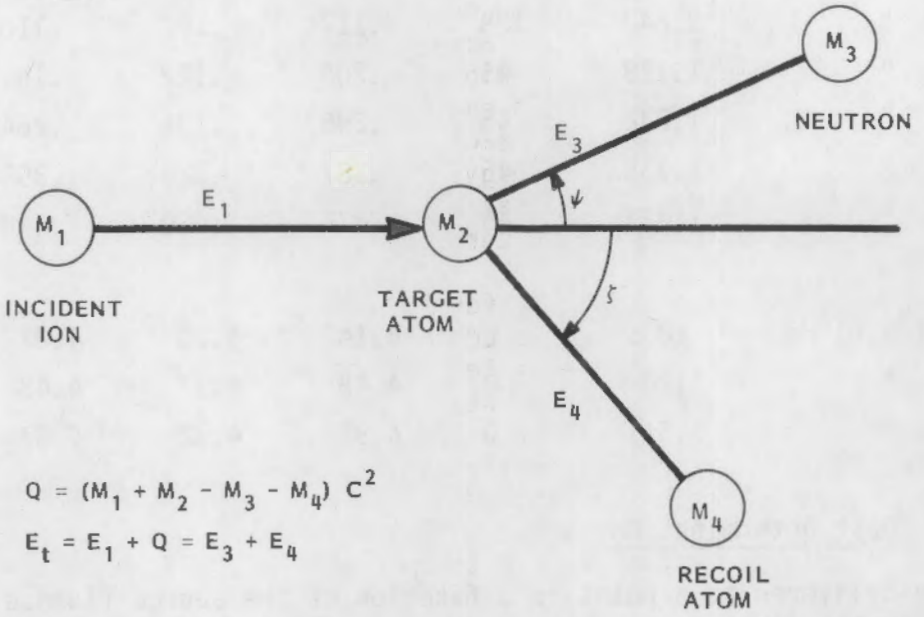

FIGURE 5. Kinematics of Nuclear Reactions and Scattering (Anderson and Ziegler 1977)

The neutron energy is determined by (Anderson and Ziegler 1977):

$$E_3 = (E_I + Q) \cdot B \cdot [\cos \psi + (D/B - \sin^2 \psi)^{1/2}]^2$$

where

E_I = the energy of the accelerated ion

$$B = \frac{M_1 \cdot M_3 \cdot [E_I/(E_I + Q)]}{(M_1 + M_2) \cdot (M_3 + M_4)}$$

$$D = \frac{M_2 \cdot M_4 \cdot (1 + [M_1 \cdot Q]/[M_2 \cdot (E_I + Q)])}{(M_1 + M_2) \cdot (M_3 + M_4)}$$

Because the numbers of neutrons created at the front of the target and at the rear of the target are roughly the same, the reference neutron energy is the average of the two. The neutron energy at the face is determined by setting $E_I = E_p$, and at the rear by setting $E_I = E_p - dE_p$. The range of ion and neutron energies is summarized in Table 1.

TABLE 1. Neutron Energy Data for the Accelerator Irradiations

Accelerated Ion Energy MeV		Degraded Ion Energy MeV	ψ deg.	Neutron Energies, MeV Maximum	Minimum	Average
1.400	$^{3}H(p,n)^{3}He$	1.335	105	.083	.057	.070
1.650	"	1.591	135	.104	.088	.096
1.700	"	1.642	135	.117	.102	.110
1.200	"	1.128	45	.200	.122	.161
1.300	"	1.232	45	.296	.231	.264
1.400	"	1.335	45	.387	.328	.358
1.500	"	1.437	45	.475	.420	.448
1.000	$^{2}H(^{2}H,n)^{3}He$	.885	0	4.14	4.00	4.07
1.300	"	1.20	0	4.48	4.37	4.43
1.700	"	1.61	0	4.92	4.82	4.87

2.2.1.3 Dose Determination

The dose delivered at a point is a function of the source fluence (neutrons/cm^2), the distance from the source and the energy distribution of the neutrons. The dose equivalent is also a function of the neutron energy, especially where the quality factor is changing rapidly in the range between 0.1 and 0.5 MeV.

Several assumptions are needed in determining the dose equivalent at a point. First, the reference dose from neutrons is deposited at the center of the phantom face which is set at some reference angle relative to the beam line and 75 cm from the target. Second, the target is considered to be a point source. Third, the long counter is considered to be a point detector (that point being a function of neutron energy). Finally, the long counter is an absolute neutron fluence counter.

The neutron fluence measured by the long counter can be adjusted by $1/r^2$ to find the fluence at the center of the face of the phantom. The fluence may be converted to dose equivalent by use of an analytical fit of flux-to-dose-equivalent conversions found in NCRP (1971). The analytical fit constitutes a logarithmic interpolation and is described in ANS/ANSI 6.1.1 (ANSI 1977), and summarized in Table 2.

In order to use these conversions, they must be divided by 3.6 to convert from flux to fluence and rem to millirem. Table 3 summarizes the fluence and dose equivalent values used for the Van de Graaff irradiations.

TABLE 2. Neutron Flux-to-Dose Equivalent Rate Conversions

Neutron Energy, MeV	Flux-to-Dose Equivalent Rate Factors	
	NCRP[a] (rem/hr)/(n/cm^2-sec)	ANSI[b] (rem/hr)/(n/cm^2-sec)
0.070	--	1.64×10^{-5}
0.097	--	2.12×10^{-5}
0.100	2.17×10^{-5}	2.17×10^{-5}
0.110	--	2.37×10^{-5}
0.161	--	3.34×10^{-5}
0.264	--	5.21×10^{-5}
0.358	--	6.85×10^{-5}
0.448	--	8.39×10^{-5}
0.500	9.26×10^{-5}	9.26×10^{-5}
4.090	--	1.47×10^{-4}
4.450	--	1.50×10^{-4}
4.880	1.56×10^{-4} (5 MeV)	1.55×10^{-4}

(a) NCRP 1971.
(b) ANSI 6.1.1 (ANSI 1977).
* Table only shows conversion comparisons for neutron energies in the scope of this study.

Finally, some small variations may occur due to geometry considerations (e.g., the actual position of dosimeter on phantom). Those variations are small compared to the variations produced by the dosimeter systems.

During the accelerator irradiations, two unusual conditions arose. First, the second irradiation of the 448 keV group was allowed to exceed the target dose. For purposes of response averaging, the dosimeter response for each of these irradiations is determined prior to averaging. For presentation of raw data in Table A.21, that irradiation is presented separately. The second unusual condition arose when Vender E's dosimeters were improperly irradiated at the accelerator. The protective film covering the polycarbonate was left in place during the irradiations. For that reason, another set of Vendor E's dosimeters was irradiated by themselves, three at a time. As before, the three dosimeters were placed radially around the center point of the phantom face.

TABLE 3. Fluence and Dose Equivalent Values from Van de Graaff Irradiations

E_n, (a) MeV	ϕ_{LC}, (b) n/cm^2	D_{LC}, (c) cm	ϕ_{Ph}, (d) n/cm^2	DF, (e) $mrem/(n/cm^2)$	Dose Equiv. (f) mrem
0.070	5.72×10^6	99.6	3.46×10^7	4.56×10^{-6}	46
0.097	4.77×10^6	99.6	4.09×10^6	5.90×10^{-6}	50
0.110	5.23×10^6	99.6	9.22×10^6	6.58×10^{-6}	61
0.161	2.16×10^6	99.7	3.82×10^6	9.28×10^{-6}	35
0.264	2.15×10^6	99.8	3.81×10^6	1.45×10^{-5}	55
0.358	1.99×10^6	99.9	3.53×10^6	1.90×10^{-5}	67
0.448	2.52×10^6	100.0	4.48×10^6	2.33×10^{-5}	104
4.070	2.32×10^6	104.0	4.46×10^6	4.07×10^{-5}	54
4.430	2.30×10^6	104.4	4.46×10^6	4.18×10^{-5}	54
4.870	2.21×10^6	104.9	4.33×10^6	4.31×10^{-5}	54

(a) Neutron energy.
(b) Neutron fluence at the long counter.
(c) Distance of the long counter = 91.7 + (7.8 + 1.1 En).
(d) ϕ_{Ph} = fluence at phantom = $\phi_{LC} \cdot (D_{LC}^2/75^2)$.
(e) DF = DF (from Table 2)/3.6.
(f) Dose Equivalent = $\phi_{Ph} \cdot$ DF.

Other than the aforementioned, no unusual occurences arose. The vendors were not supplied with irradiation energies or doses prior to analysis, so results represent field results as closely as possible. A summary of dosimeter data is found in Table A.26.

2.2.2 NBS Filtered Beam Irradiations

Irradiations at the National Bureau of Standards utilized neutrons from the core of the NBS research reactor. Columns of ultra-pure metals have been built into the containment walls. These metals all have anti-resonances, that is they do not absorb neutrons of a certain energy. Hence, the metal acts as both a neutron beam channel and a filter. Figure 6 illustrates that scandium has a probability for absorption of 1 keV neutrons which is very much smaller than that for other energies (roughly 1/100).

For the irradiations, the dosimeters are placed on a water phantom on a "scanner." The scanner moves the phantom across the neutron beam so that the entire surface of the phantom is eventually irradiated. The neutron fluences are known, and dose equivalents are calculated by using fluence to dose equivalent conversion factors.

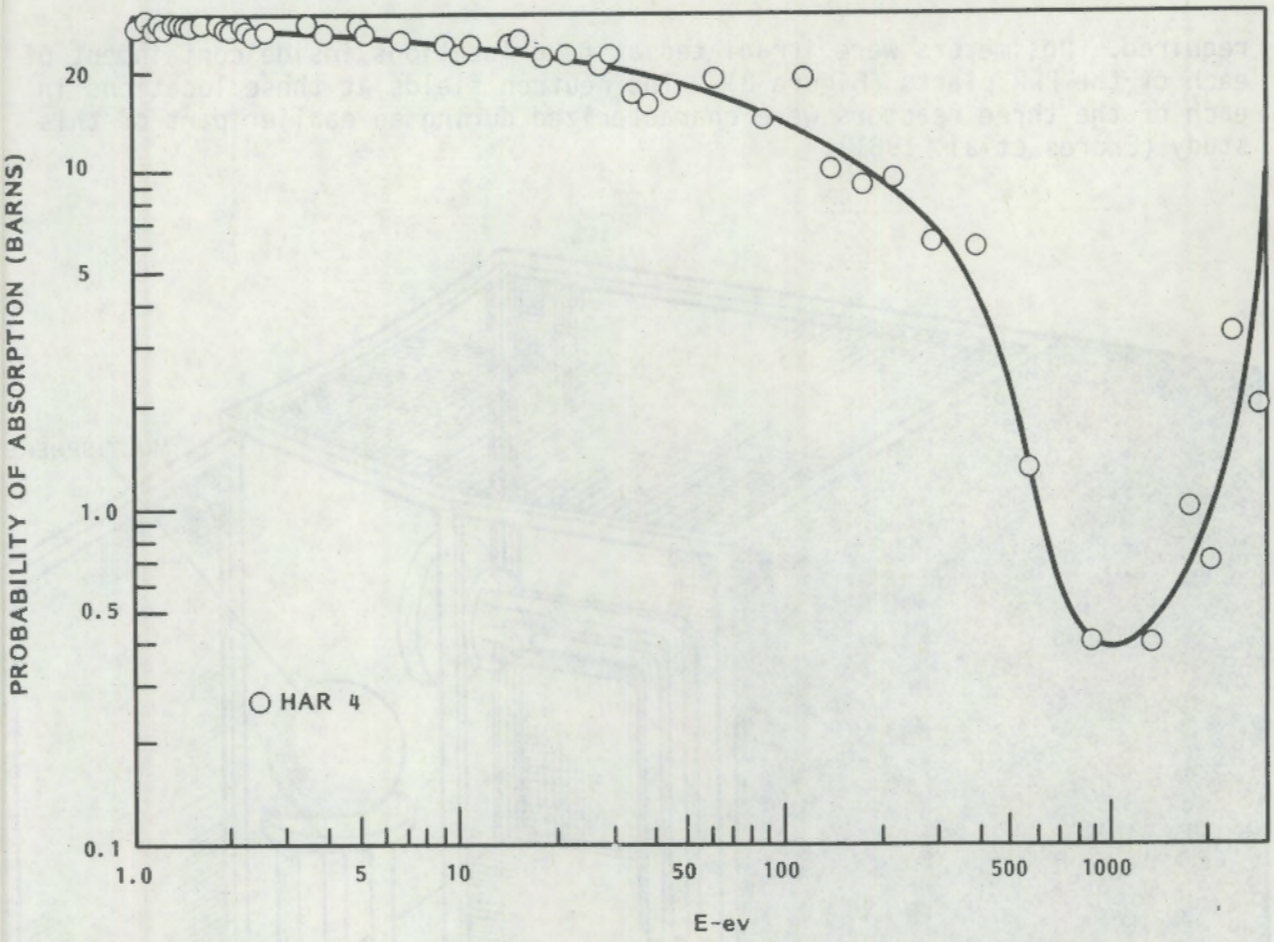

FIGURE 6. Probability of Absorption of Neutrons in Scandium as a Function of Neutron Energy (BNL-325)

The delivered dose equivalents were 50 mrem for the thermal, 2 (scandium filter), 24 (iron filter) and 144 (silicon filter) keV irradiations. A summary of dosimeter data for these irradiators is found in Table A.26.

No measurements were performed by PNL at the NBS reactor beam facility. The dose equivalents given to the dosimeters are based on measured neutron fluences and were supplied by NBS.

2.2.3 Irradiations Inside Reactor Containment

The nuclear power plants at which irradiations were performed are designated as Site E (BWR), Site G (PWR), and Site I (PWR). All irradiations were performed in locations where routine entry is made and while the reactors were at 100 percent power. The dosimeters were irradiated inside two units at the BWR plant and both locations were at sample-line pipe penetrations through the biological shield (Figure 7). Since dose equivalent rates were on the order of a millirem per hour (mrem/hr) at both locations, long irradiation times were

required. Dosimeters were irradiated at four locations inside containment of each of the PWR plants (Figure 8). The neutron fields at these locations in each of the three reactors were characterized during an earlier part of this study (Endres et al. 1981).

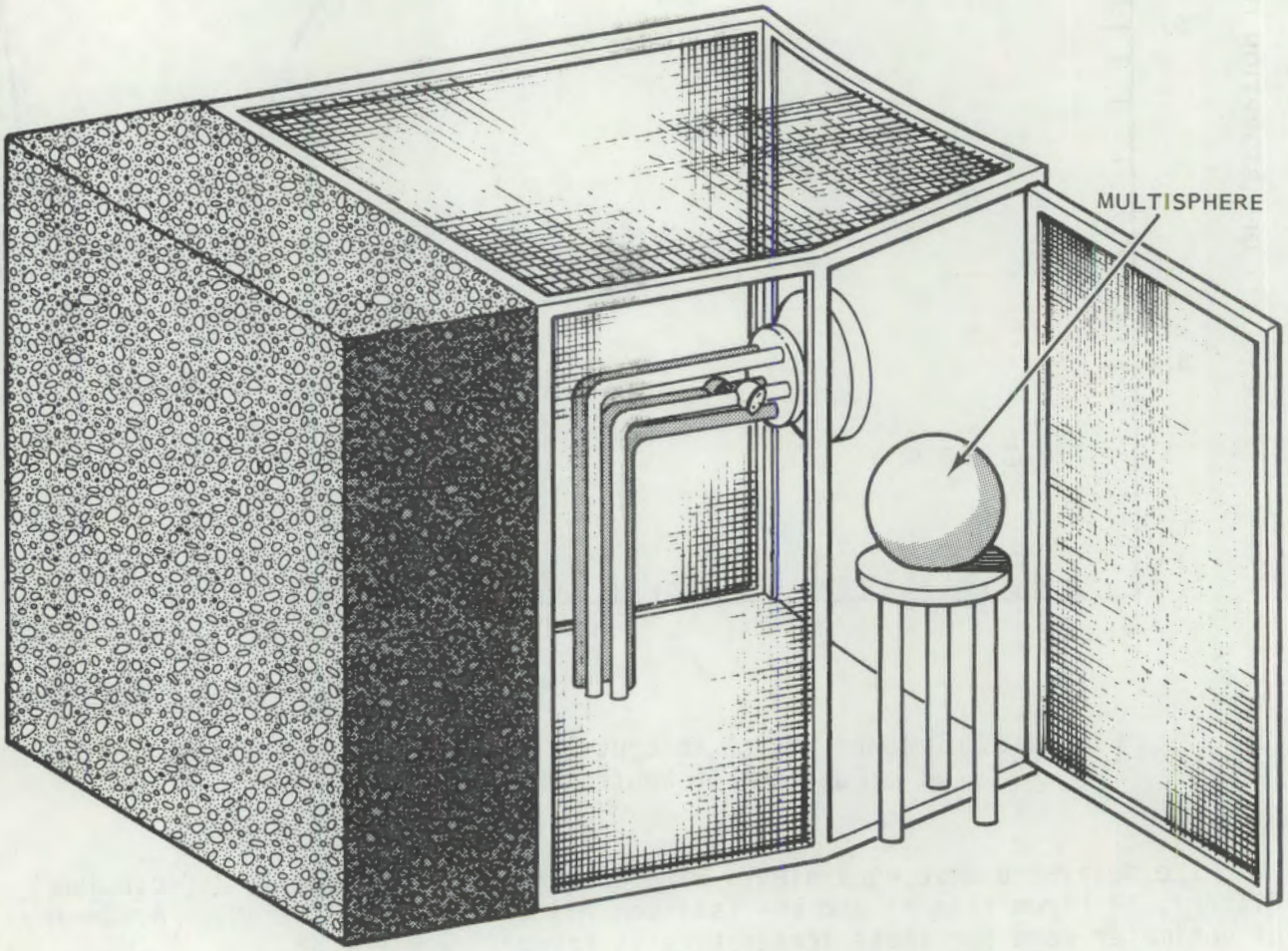

FIGURE 7. View of Pipe Penetration at Site E

All the dosimeters were placed centrally on a 37 x 37 x 18-cm thick water-filled phantom. Since five dosimeters of each type were irradiated together to improve the precision of measurement, there was only enough space on the phantom for four types of dosimeters at a time. Hence, two sets of irradiations had to be performed at each location in order to include all the dosimeters.

SITE G

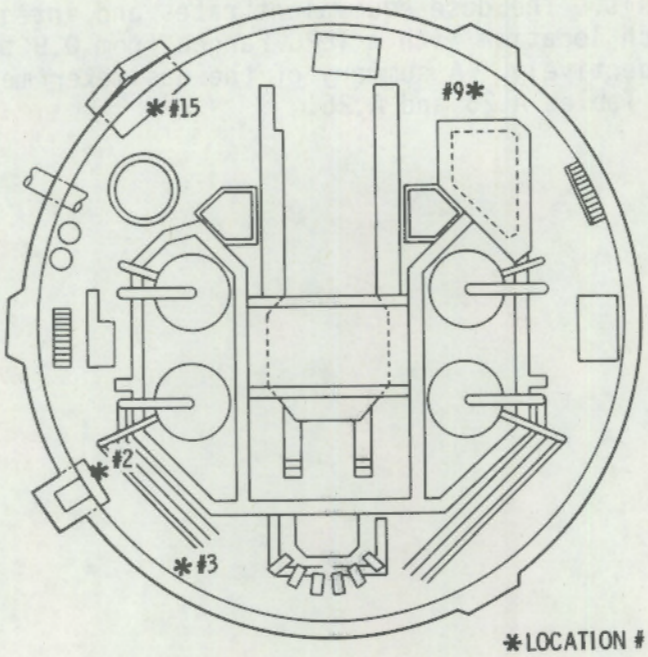

SITE I

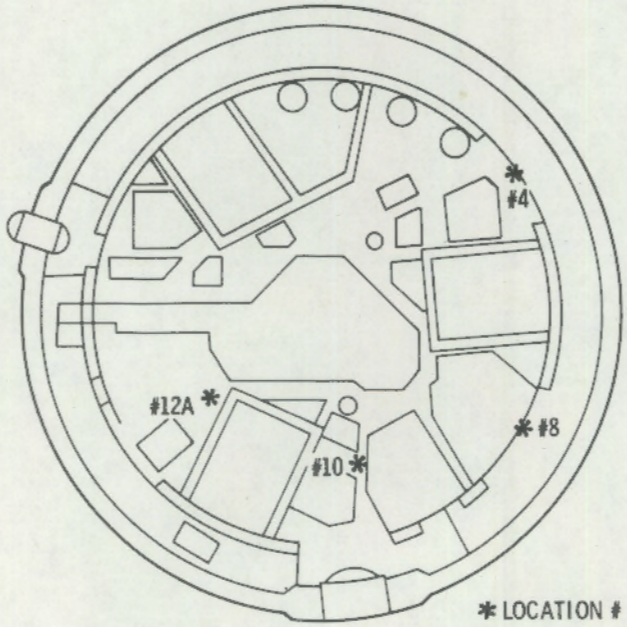

FIGURE 8. Irradiation Locations Inside Containment at (a) Site G and (b) Site I

After the irradiations were made, the dosimeters were mailed back to the processors for analysis. The dose equivalent rates and integral dose equivalents measured at each location with a TEPC ranged from 0.9 to 190 mrem/hr and 19 to 3300 mrem, respectively. A summary of the dosimeter measurements may be found in Appendix A, Tables A.25 and A.26.

3.0 INSTRUMENT MEASUREMENTS

The adequacy and applicability of personnel neutron dosimeters can only be judged against measured or calculated dose equivalents. The response of the dosimeter will depend on the response of the particular reference instrument. Therefore, it is desirable that the instrument accurately measure the dose equivalent. Unfortunately, little is known of the actual neutron energy spectra to allow a high degree of measurement accuracy. In this section, the particular instruments used to measure dose equivalent and the interpretations of those measurements are discussed.

3.1 INSTRUMENT DESCRIPTIONS

3.1.1 Tissue Equivalent Proportional Counter (TEPC)

One of the best summaries of the TEPC is found in NUREG/CR-1769 (Endres et al. 1981). It is reproduced here for description of the TEPC system. The TEPC system is shown in Figure 9. The TEPC is spherical but is shown in the protective cylindrical can in which it is sealed.

FIGURE 9. Tissue Equivalent Proportional Counter (TEPC) With Associated Electronics, Multi-Channel Analyzer and Cassette Deck Readout

"The electronic system components include detector, preamplifier, amplifier, and high-voltage power supply. The multi-channel analyzer (MCA) used with the TEPC has a log display, which greatly assists in the analytical interpretation of the unanalyzed data.

"The TEPC is a hollow sphere of tissue-equivalent plastic (Shonka A150 muscle-equivalent plastic) with the 3.2-mm thick walls filled with methane-based tissue-equivalent gas. Details of plastic and gas composition and methods of construction can be found in Report 26 of the International Commission of Radiation Units and Measurements (ICRU 1977). This form of TEPC, called a Rossi counter, has a helical grid around the central anode wire. The helical grid establishes uniform electric field strength along the entire length of the anode. This produces the needed uniformity in gas amplification at all points along the anode for proper pulse height analysis. The plastic sphere is contained inside a metal pressure vessel with a valve for admitting tissue-equivalent gas. The gas pressure is maintained at a pressure of 5.6 mm Hg (for the 5-in. counter) absolute so that charged particles crossing the cavity lose only a small amount of energy as they traverse the counter. Energy deposited in the cavity is then equal to the linear energy transfer (LET) of the particle times the path length. At these low pressures, the gas-filled cavity has the same mass-stopping power as a sphere of tissue (ρ = 1 gm/cm^3) with a diameter of about 1 μm and is said to have an 'equivalent diameter' of 1 μm.

"The TEPC becomes self-calibrating when the proton drop point is identified. A proton drop point corresponds to a slow proton recoil having the highest LET or stopping power traversing the diameter of the spherical cavity and is independent of the initial energy of the neutron producing the event. According to the data of Glass and Samsky (1967), this point occurs at about 100 keV/μm and is a slowly varying function of tissue-equivalent gas pressure.

"Multiplying the number of events of a given size by the energy of the event gives the absorbed energy distribution in the tissue-equivalent gas, which is a direct measure of absorbed dose. Following the nomenclature in ICRU (1977), this is stated in the following equation:

$$D = 1.602 \times 10^{-8} \frac{k}{V \cdot \rho} \sum_{h_1}^{h_2} h \cdot N(h)$$

where

D = absorbed dose in rad
h = the measured pulse height expressed as channel number
N(h) = the number of pulses accumulated in channel h; h_1 and h_2 are the limits in pulse height between which the absorbed dose is to be determined
ρ = the gas density in gm/cm^3
V = the sensitive volume of the cavity in cm^3

k = the calibration relating energy to channel number, which was determined from the proton drop point (keV/channel number)."

"For calculational purposes, the lower limit of event size, h_1, is defined as the minimum between photon- and neutron-induced events, which occurs at an event size of about 15 keV/μm; h_2 is the upper limit of the event-size spectrum. The summation over N(h) between h_1 and h_2 is the total energy absorbed in the gas cavity due to the high LET events. The measured neutron dose, D, is the energy absorbed in the gas cavity divided by the mass of tissue-equivalent gas inside the sphere.

"The TEPC event spectrum (Figure 10) shows the number of events per channel, commonly referred to as the event-size spectrum. Also shown in Figure 10 are the three parameters needed to analyze TEPC data: h_1 (the lower limit), h_2 (the upper limit), and the proton drop point.

"The only general method that has been developed for the measurement of the distribution of dose in LET is based on an analysis of the frequency distribution of the event size due to individual particles in a spherical volume of tissue, that is, the N(y) distribution. Actual distributions are different from those derived with the assumptions that energy loss is continuous and that particles travel in straight lines and have a range that is much larger than the cavity diameter. In the practical application of the TEPC, these assumptions are not entirely correct. Some events 'start' and 'stop' in the cavity, especially when many intermediate energy neutrons are present.

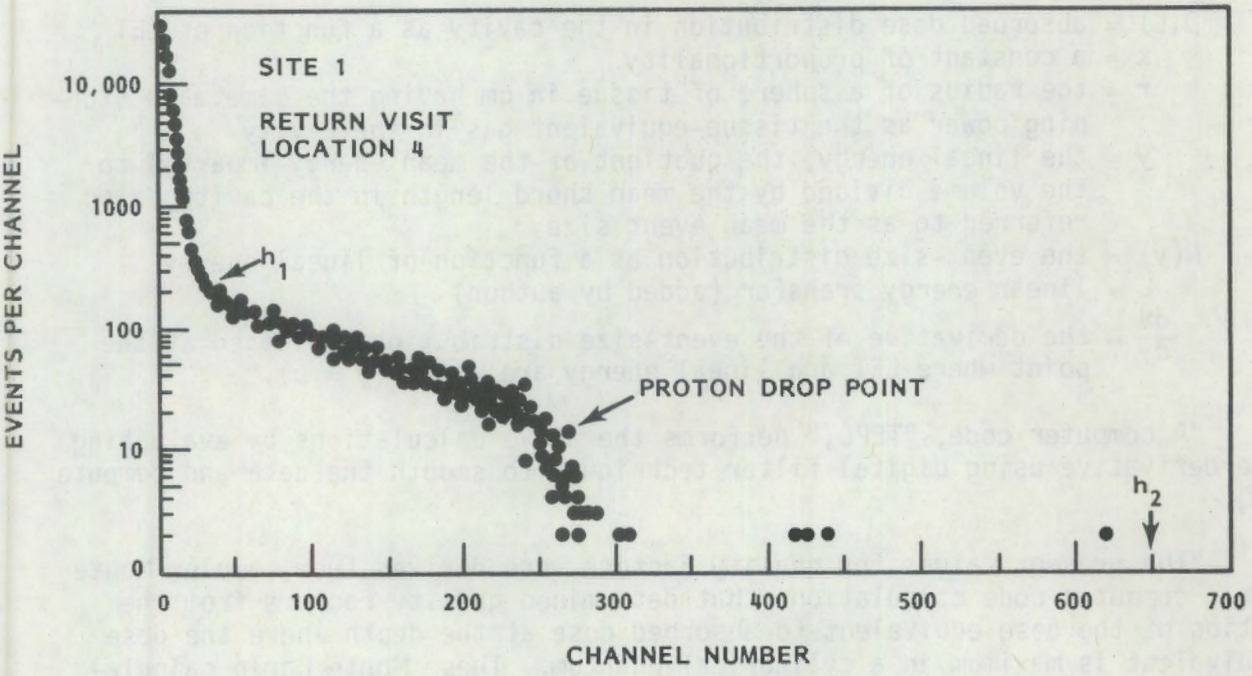

FIGURE 10. TEPC Event-Size Spectrum

Therefore, some error is introduced when deriving the LET spectrum from the event-size spectrum. X-rays, electrons, $H(n,\gamma)D$ reactions, and positrons are assigned a Q of 1, which does not add significantly to the calculated dose equivalent. Most of these events are below the lower limit (h_1) used in TEPC analysis. However, discrepancies between experimental and theoretical spectra are usually sufficiently small to be acceptable for purposes of radiation protection. It has been Rossi's development of this technique, using the previously mentioned assumptions, that has led to a determination of dose-equivalent rates with the TEPC by calculating absorbed dose as a function of LET and by using Q as a function of LET as described in ICRU (1976) and ICRU (1977)."

"Rossi devised a relatively simple model to determine the absorbed dose distribution as a function of LET (Rossi 1968). In ICRU 26, the quality factor Q is defined in terms of LET, which makes it possible to determine dose-equivalent rates and Q from a single TEPC measurement. The Rossi model employs a spherical counter with neutron recoils arising within the walls and assumes that they have a constant, uniform energy loss along a straight line and that they completely cross the cavity. Under these assumptions, the absorbed dose distribution within the cavity as a function of LET, D(L) can be calculated by the following equation (Rossi 1968).

$$D(L) = \frac{k}{r^2}\left[y\,N(y) - y^2\,\frac{dN}{dy}\right]_{y=L}$$

where

$D(L)$ = absorbed dose distribution in the cavity as a function of LET
k = a constant of proportionality
r = the radius of a sphere of tissue in cm having the same mass stopping power as the tissue-equivalent gas in the cavity
y = the lineal energy; the quotient of the mean energy imparted to the volume divided by the mean chord length in the cavity, also referred to as the mean event size
$N(y)$ = the event-size distribution as a function of lineal energy
L = linear energy transfer (added by author)
$\frac{dN}{dy}$ = the derivative of the event-size distribution evaluated at the point where LET and lineal energy are equal ($y = L$)."

"A computer code, "TEPC," performs the above calculations by evaluating the derivative using digital filter techniques to smooth the data and compute a Q.

"The present values for quality factors were derived from complex Monte Carlo computer code calculations that determined quality factors from the ratios of the dose equivalent to absorbed dose at the depth where the dose equivalent is maximum in a cylindrical phantom. These Monte Carlo calculations include the contributions from elastic scattering of hydrogen, charged particle reactions and $H(n,\gamma)D$ reactions. At low neutron energies (approximately 10 keV or lower) the contribution to dose equivalent from gamma rays

produced by the absorption of neutrons by hydrogen becomes significant. In fact the contribution to dose equivalent from the induced gamma-ray reactions is significant for any neutron energy below about 100 keV. In the Monte Carlo computer code calculations, the dose equivalent attributable to the gamma rays from $H(n,\gamma)D$ reactions is included as part of the neutron dose equivalent.

"In a tissue-equivalent proportional counter (TEPC), it is not possible to distinguish between photons originating from $H(n,\gamma)D$ reactions in a phantom of the walls of the tissue-equivalent proportional counter and photons from external gamma sources. Therefore, all low-energy photon events are excluded from the analysis of the TEPC data. This procedure makes it impossible to directly compare quality factors from TEPC measurements with those based on the Monte Carlo computer code calculations for low-energy neutrons. Above 200 keV, the contribution from $H(n,\gamma)D$ reactions becomes negligible, and the TEPC measurements agree quite well with the Monte Carlo calculations (Brackenbush et al. 1979). The Rossi analysis can be applied to the TEPC data to determine the effective quality factors for neutron and gamma-ray fields, but the relative contributions from $H(n,\gamma)D$ reactions cannot be determined from a single TEPC measurement."

Since all photon events are excluded from our analysis of TEPC data, the resulting quality factors derived from TEPC data tend to have higher value than those calculated by Monte Carlo computer programs. However, multiplying these quality factors by the measured absorbed neutron dose, which also has all photon contributions excluded, gives a dose-equivalent value that is reasonably close to the dose-equivalent value derived from the Monte Carlo computer calculations and multisphere spectrometer measurements.

Additionally, the TEPC measurement of dose equivalent from monoenergetic neutrons (produced on a Van de Graaff) between 0.1 MeV and 8 MeV is within 3 percent of the calculated dose equivalent; or $R = 1.03 \pm (0.09)$ (Brackenbush et al. 1979). For that reason, additional TEPC measurements were not made for the Van de Graaff irradiations.

3.1.2 Multisphere Spectrometer System

While we did not employ the multispheres during this part of the study, the following description from NUREG/CR-1769 (Endres et al. 1981) is included. The multispheres have been the benchmark measurement for this program and will be used to explain response differences from location to location (see the next section). The multisphere neutron system is shown in Figure 11.

"The detector is a cylindrical $^{6}LiI(Eu)$ scintillation crystal, 1.27 cm in diameter by 1.27 cm long. It is optically coupled to a 20.3-cm light pipe, which in turn is optically coupled to a photomultipler tube (PMT). The detector and its integral components are hermetically sealed in an aluminum tube with walls 0.16 cm thick. The PMT is surrounded by a brass sleeve for protection and support for cable connectors. A single cable carries both the high-voltage and output signals, connecting the detector to a preamplifier. The preamplifier decouples the signals and feeds them into the MCA. The analyzer

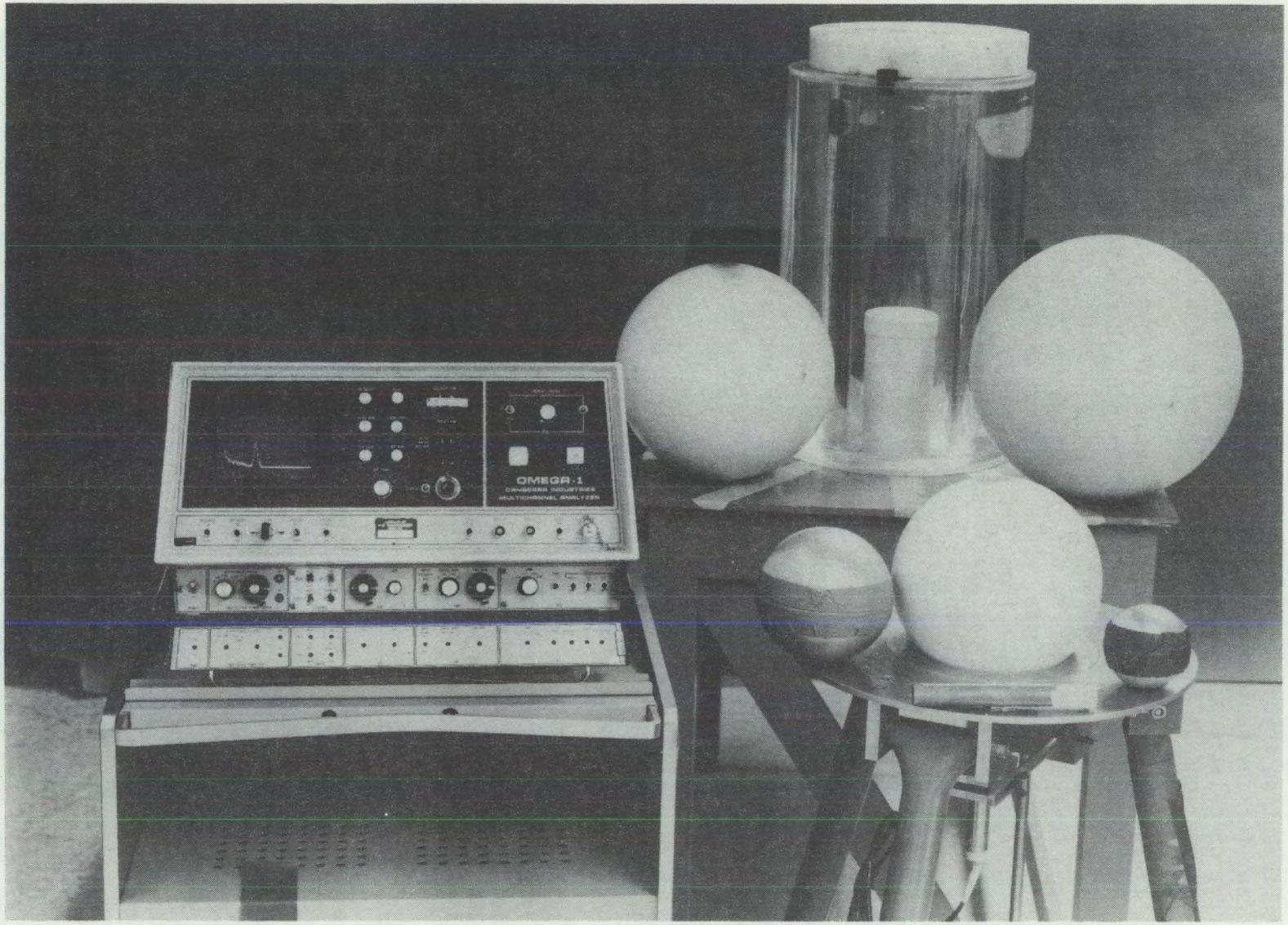

FIGURE 11. Multisphere System Shown with a Water-Filled Cylinder Used to Moderate Neutron Sources

has three built-in systems as integral parts: amplifier, high-voltage power supply, and discriminators. The unanalyzed data is obtained directly from the MCA and fed to a printer for hard copy.

"The neutron detection mechanism of the ^{6}LiI(Eu) crystal is the $^{6}Li(n,\alpha)^{3}H$ reaction, which has a positive energy release value of 4.8 MeV. Thermal neutrons absorbed in the scintillator produce a distinct peak in the pulse-height spectrum shown on the MCA. There are no other competing peaks in the spectrum. An exponential background continuum is subtracted from the full-width-peak area. The full-width-peak area is defined by the point at which the (n,α) reaction begins to be detected, the peak, and the high-energy point at which the reaction ceases to be detected.

"Data for the neutron energy spectrum analysis were obtained by taking counts 1) with a bare, unshielded scintillation crystal, 2) with the crystal in a cadmium shell (0.051 cm thick), and 3) with the crystal moderated by spheres of high-density polyethylene (7.6, 12.7, 20.3, 25.5, and 30.5 cm in diameter). The fast-neutron response of this system increases with sphere size because the larger polyethylene spheres moderate the fast neutrons to lower energies where they have a greater probability of being detected by the ^{6}LiI(Eu) scintillator. Cadmium shells placed around the 7.6 and 12.7 cm spheres suppress response to external thermal neutron fields and improve the detectability of the system to moderated fast neutrons above the cadmium cutoff (0.4 eV) (Hankins and Griffith 1978).

"Using the responses from the seven detector configurations (bare, cadmium-covered, and with 7.6, 12.7, 20.3, 25.5, and 30.5 cm moderators), the spectrum is unfolded with the aid of the LOUHI computer code. LOUHI is a FORTRAN program written to solve Fredholm integral equations of the first kind by using a generalized least-squares procedure with a nonnegative solution. With LOUHI, the spectral solution is not dependent on the choice of the initial approximation. Through prior knowledge of the flux in a particular part of the spectrum, the solution in the appropriate energy bin can be "tied" to that point (Hankins and Griffith 1978). The energy bin referred to is the twenty-sixth bin or upper limit of the energy range over which the spectrum is to be calculated. This becomes the "tied" point and is based on the response of the 17.7 cm sphere. For this study, this feature is used to place the high-energy bin at a realistic value that reflects the lack of source neutrons above 14 MeV (Hankins and Griffith 1978; Hajnal et al. 1979).

"Consideration was given to potential multiplicative errors introduced through overlapping responses between different sizes of spheres (Griffith et al. 1977; Zaidins et al. 1978; Routti 1969). Multiplicative errors are those errors associated with each sphere response multiplied together as the code unfolds through several iterations developing a 26-point spectrum. The mathematics of LOUHI, when compared to the mathematics-of-error calculations developed for foil activation unfolding codes (Robkin 1968), indicate similar inherent error problems. LOUHI minimizes these errors by weighting functions and varying the emphasis of each detector response. Neutron energy response functions calculated by Sanna (1973) are used as input for the unfolding process. Sanna's calculations are based on one-dimensional spherical geometries

and were verified empirically in the energy range from 100 keV to 20 MeV (Griffith and Fisher 1976). To make the sphere responses equal to Sanna's calculations in this energy range, density corrections for the spheres are performed by the LOUHI code.

"Essentially, the basic equations of LOUHI solve for neutron flux, abosrbed dose, average neutron energy, and dose-equivalent rate. LOUHI used the following (complex set of) equation(s) to determine neutron flux in the j^{th} energy band, ϕ_j:

$$A_i = \sum_{j=1}^{26} R_{ij}\, \phi_j$$

where

A_i = the count rate with the i^{th} detector configuration, and is obtained by integrating under the peak using a log background subtraction continuum and dividing that value by the count time for each individual detector configuration, and

R_{ij} = one of the response functions to the i^{th} detector in the j^{th} energy calculated by Sanna (1973), and is directly available from his tabulations.

The average neutron energy calculation incorporates a weighting function shown in the following:

$$E_{av} = \sum_{j=1}^{n} w_j \cdot E_j \cdot F_j \cdot F_s^{-1}$$

where

E_{av} = average neutron energy
j = energy band (1 to 26)
n = total number of energy bands (26)
w_j = weighting function of j^{th} energy band
E_j = energy value at the j^{th} point, in MeV
F_j = the solution at point j
F_s = total flux.

The dose-equivalent rate equation uses a weighting function and a precalculated ratio for conversion of neutron flux to dose equivalent:

$$DS = \sum_{j=1}^{n} w_j \cdot d_j \cdot F_j$$

where

DS = dose-equivalent rate
d_j = factor for conversion of neutron flux to dose equivalent.

"Flux-to-dose-equivalent conversion factors are compiled as a subroutine in the LOUHI program and have been taken directly from tables in Publication 21 of the International Commission on Radiological Protection (ICRP 1971). Absorbed dose calculations are performed in a subroutine called "Element 57 Dose Rate." This model is used to estimate the dose in various regions of an homogeneous anthropomorphic phantom, which was taken as a right cylinder with a radius of 15 cm and a height of 60 cm. The composition of the phantom was assumed to be H, C, N, and O in the proportions of standard man. The cylindrical volume was divided into 150 numbered volume elements, and the average dose per neutron flux in the incident beam was computed for each volume element. The neutron beam was assumed to be broad enough to irradiate the whole phantom and to be monoenergetic and monodirectional with velocity vector parallel to the base of the cylinder (Auxier et al. 1968). The maximum dose rate, in this scheme, is to Element 57. Thus, the Element 57 dose rate is considered to be the best estimate for depth dose rate for the neutron energies measured in reactors. It also is the element usually used to determine dose-equivalent rates.

"Quality factors Q are not directly calculated by the LOUHI unfolding code but can be easily determined by dividing the dose-equivalent rate by the Element 57 absorbed dose rate. A Q value determined by this method will not be the same as the Q value calculated by the TEPC. The significance of this point will become more apparent as it is shown that the systems derive dose-equivalent rates and Q by different methodologies. Further detailed discussion of the LOUHI program is readily available in the literature (Awschalom 1966; Routti and Sandberg 1978; Bramblett et al. 1960)."

3.1.3 Portable Moderated Remmeters

The remmeters described in the following paragraphs were calibrated with unmoderated neutron sources. The SNOOPY and RASCAL, both belonging to PNL, were calibrated using a ^{239}PuBe source on the lowest range of measurement. The instruments were then checked on the higher ranges to verify the calibration. The same SNOOPY and RASCAL were used for all the measurements in this study and subtask A. The PNR-4s used in this study were supplied by the health physics staff at the power plants. The calibration source was unknown, but most probably was ^{252}Cf or ^{241}AmBe. The health physics technicians supplied the PNR-4 readings at the various locations.

3.1.3.1 SNOOPY Remmeter

The SNOOPY (Figure 12) is a portable survey instrument used to measure the neutron dose equivalent rate. The dynamic range of the instrument for dose equivalent rate goes from 0 to 2000 mrem/hr. The neutron detector in the SNOOPY, a boron trifluoride (BF_3) tube, is surrounded by a boron-loaded attenuator and inner and outer polyethlene moderators. The theoretical response of the detector (in counts per millirem) is thought to closely follow the dose equivalence curve. However, the following response curve for the SNOOPY is given to illustrate its dependence on neutron energy (Figure 13).

FIGURE 12. SNOOPY Neutron Remmeter

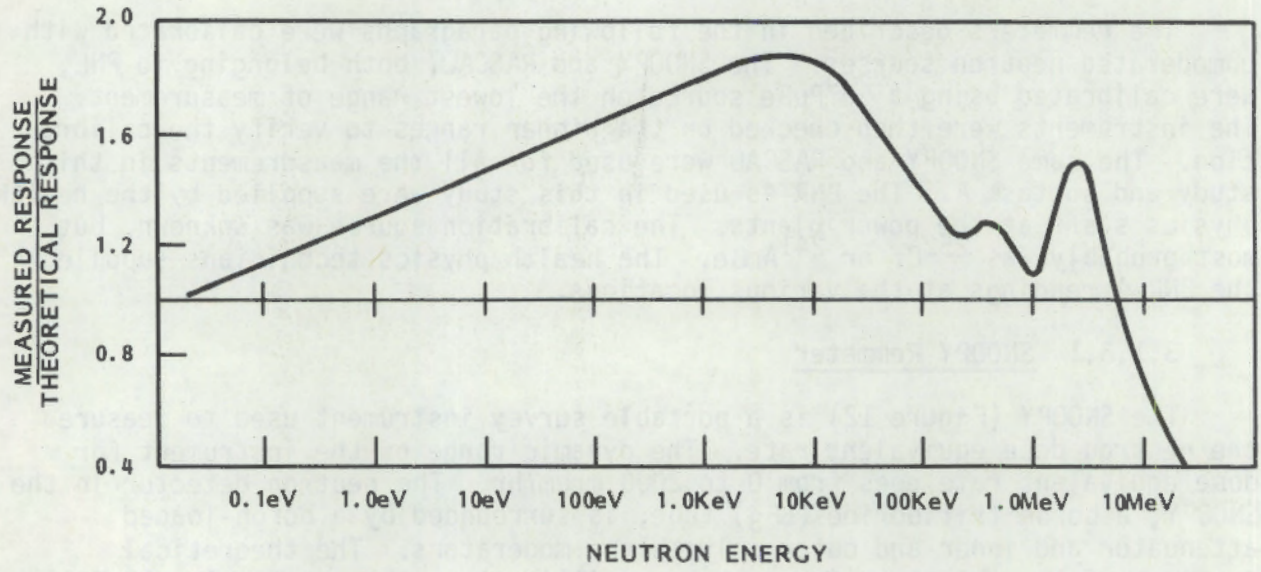

FIGURE 13. Neutron Energy Dependence for the SNOOPY (BNW 1972)

The SNOOPY also exhibits some temperature dependence, but for the situations encountered during the study, that correction would be small (<4 percent).

3.1.3.2 RASCAL and PNR-4

The RASCAL and PNR-4 are basically the same as the SNOOPY except that the BF_3 tube protrudes into the center of a 9 in. polyethylene sphere. The RASCAL and PNR-4 differ in their respective display of dose equivalent rates. The RASCAL has a digital display of dose equivalent rate (Figure 14) while the PNR-4 has a dose meter display which shows the dose equivalent rate on a linear scale and logarithmic scale simultaneously using two pointers.

The RASCAL was used to collect the 9 in. and 3 in. sphere measurements. Both the remmeter configuration and the 9 in. and 3 in. sphere configuration are shown in Figure 14.

The PNR-4s and the PNR-4 measurements were supplied by the health physics staff at the power plants.

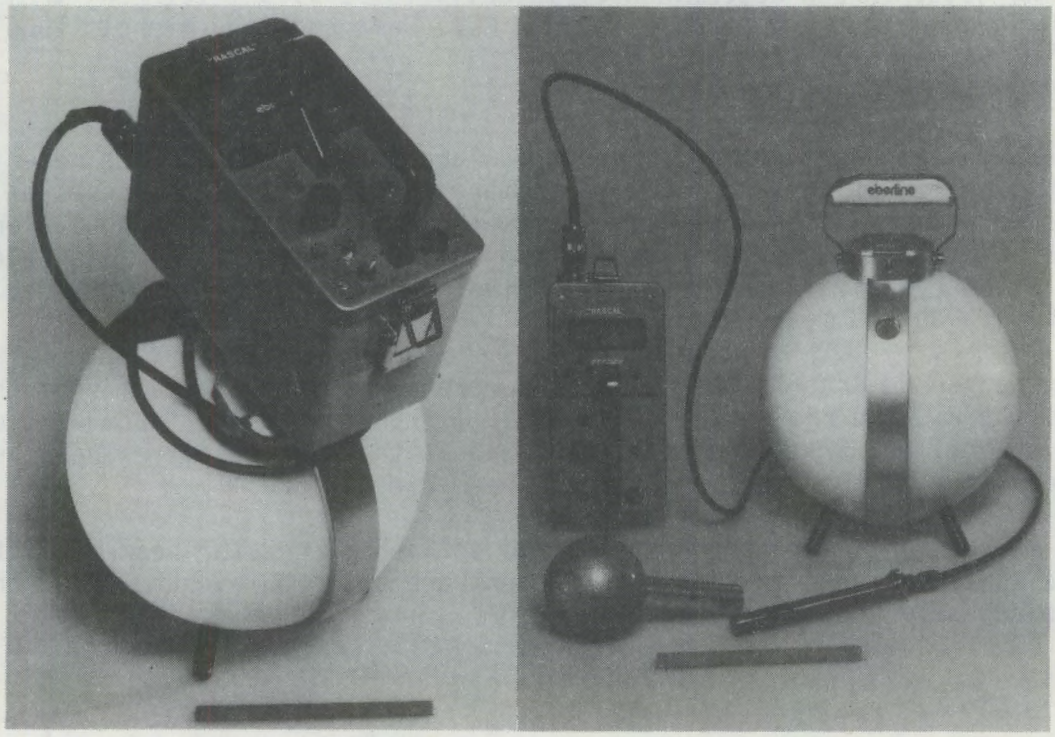

FIGURE 14. The RASCAL Neutron Remmeter in the (a) 9-in. Remmeter Configuration and (b) 9-in. to 3-in. Sphere Response Configuration

The 9 in. spherical remmeters have response functions similar to the SNOOPY and response function. All of the remmeters respond high to neutrons encountered inside containment of nuclear power plants.

A summary of measurements is found in Table 6.

3.1.3.3 Precision Long Counter (PLC)

The PLC was used to measure the neutron fluence for the Van de Graaff irradiations. Fluence-to-dose equivalent conversions were used as specified in Table 3 to calculate dose.

The PLC consists of a large diameter BF_3 tube (Figure 15). As with the portable instruments, neutrons are moderated by the polyethylene and thermalized. The PLC behaves as a "point detector;" that is, when neutrons of a given energy interact wth the polyethylene, they are thermalized and detected around a given depth in the counter. The flux is then calculated by knowing the distance between the front face of the detector, the energy of the neutron beam and the response function. For our purposes, the distance of the effective point detector was determined empirically to be 99.5 + 1.1 [En] from the target, where En is the neutron energy in MeV (DePangher and Nichols 1966).

3.2 IRRADIATIONS CONDITIONS

The physical conditions of irradiation are noted under the Dosimeter Measurements section of this report. In summary, instrument measurements at the reactors were made at the same location as the dosimeters. Dose equivalent rates were integrated over the irradiation time to determine dose equivalents. At Site E, dose equivalent rates were on the order of 1 mrem/hr which required long irradiation and measurement times.

At the Van de Graaff, the dosimeters were irradiated at 75 cm from the target. The PLC and ^3He were located at ~1 m from the target (dependent on neutron energy) and 52 cm, respectively, and at the same relative angle as the dosimeters, but on the other side of the beam (see Figure 4).

No measurements were performed by PNL at the NBS reactor beam facility. The dose equivalents given to the dosimeters are based on measured neutron fluences and were supplied by NBS.

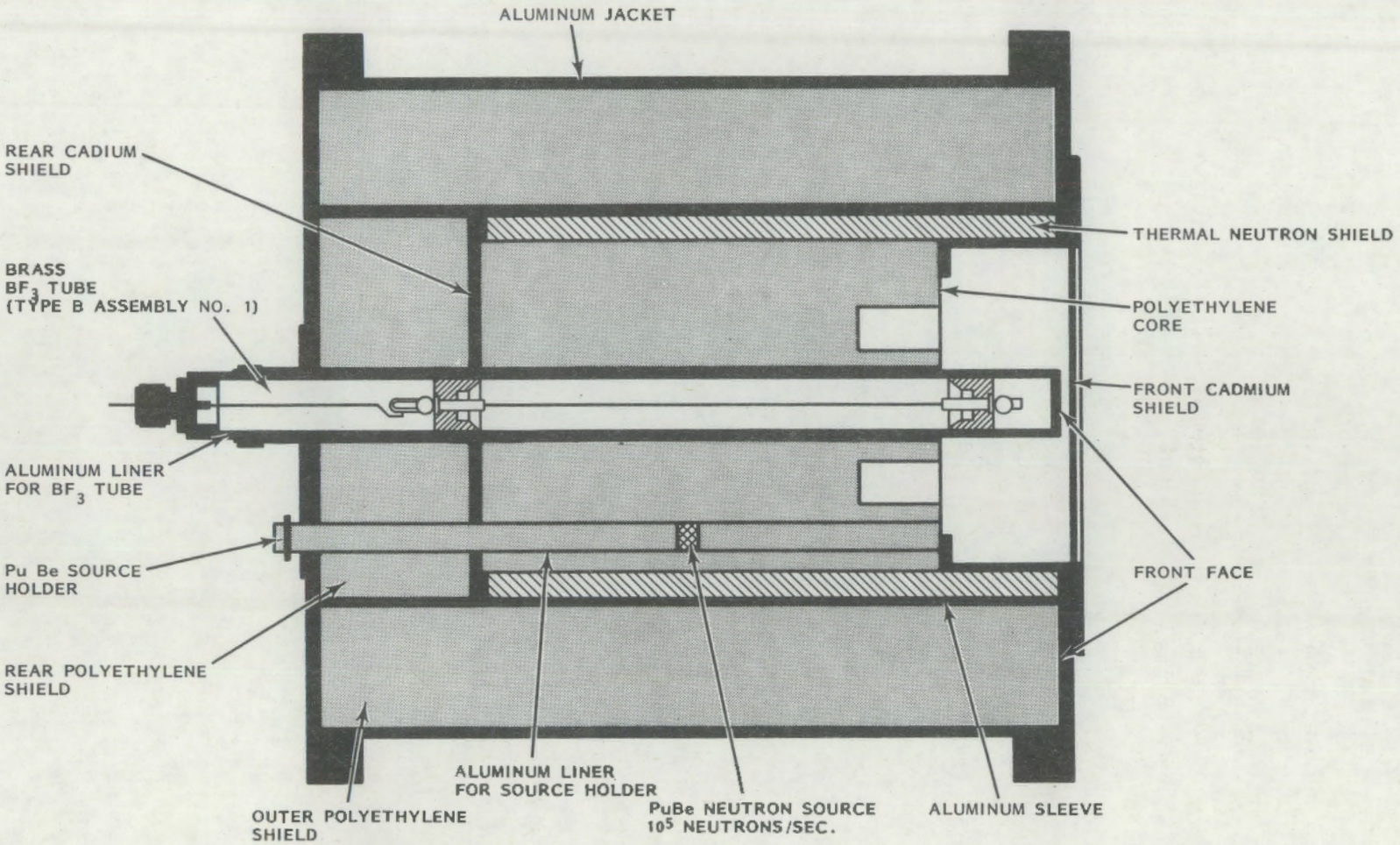

FIGURE 15. Sketch of PLC Showing BF_3 Tube and Removable Internal Neutron Check Source (Depangher and Nichols 1966)

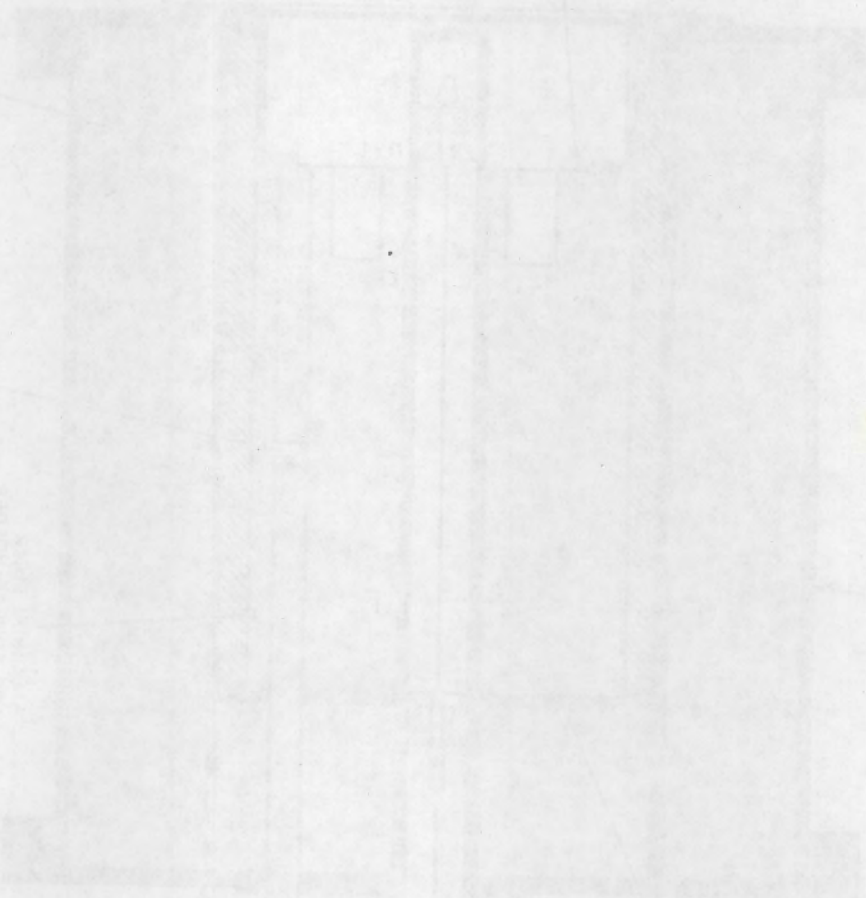

4.0 DOSIMETER RESPONSE

The objective of this study is to characterize the responses of personnel neutron dosimeters inside containment at commercial nuclear power plants. The response, defined as the ratio of the dose equivalent measured using the dosimeter to the dose equivalent measured using some instrument, is dependent upon which instrument is used as the reference.

The reference measurement from Subtask A has been the multisphere system. Since the TEPC measurements agreed well with the multisphere, it was chosen to be a substitute measurement during subtask A. The justification for this substitution is developed in the following paragraphs. Additionally, using the TEPC allowed for more dosimeter irradiations because only a single measurement is necessary at a location using the TEPC where multiple measurements are necessary when the multisphere system is used.

Because the choice of reference instrument is so important, the instrument responses will be discussed before the dosimeter responses.

In addition, Cutie Pie (CP) measurements are given to verify that unusually high gamma fields were not encountered during the reactor irradiations. The CP is a portable ion chamber which measures gamma exposure rates.

4.1 COMPARISON OF INSTRUMENT RESPONSES

Multisphere and TEPC measurements were made at the locations listed in Table 4 (Endres et al. 1981) during the execution of Subtask A. The agreement between the two techniques is close for all the measurements, with the greatest

TABLE 4. Multisphere and TEPC Measurements from Subtask A

	Multisphere		TEPC
Location	Neutron Energy keV	Dose Eq. Rate mrem/hr	Dose Eq. Rate mrem/hr
F-10	10	2.4	3.6
F-11	1	0.9	1.7
G-2	50	16	11
I (initial visit)			
1	77	45	48[a]
3	53	8.6	10
I (second visit)			
4	56	17	16
7	30	3.5	3.6
8	49	23	29

(a) average of 2 measurements

disagreement occuring when the average neutron energy (measured by the multispheres) was less than or equal to 10 keV. One would expect some difference in that those events below 10 keV/μ are discarded in the TEPC analysis, which results in lowering the absorbed dose and raising the average quality factor (see page 28).

The TEPC measurements between Subtasks A and B agree very well except at Site G (Table 5). The reduction in dose equivalent rate at Site G from Subtask A to Subtask B was noted by D. L. Haggard,[a] and was the result of the installation of retrofit bioshields at the reactor after the measurements made during Subtask A. The portable instruments verified the TEPC measurements and showed a reduction of ~40 percent in the dose equivalent rate. Because of its agreement with Multisphere data, and its demonstrated consistency between subtasks, the TEPC is felt to be the most appropriate measurement as a reference to relate reactor irradiations and the monoenergetic response functions.

The 9-in. remmeter is the most prevalent dose equivalent instrument in use at power reactors. Its energy response is similar to that of the SNOOPY shown in Figure 13 but generally higher. The instrument measurements are summarized in Table 6, while in Figure 16 the ratio of the instrument measurements to the TEPC are plotted . [note: In order to reproduce the data points,

TABLE 5. Comparison of TEPC Measurements Made During Subtask A and Subtask B

	Subtask A		Subtask B
	Multisphere	TEPC	TEPC
Location	D. E. Rate mrem/hr	D. E. Rate mrem/hr	D. E. Rate mrem/hr
E1	0.9	--	1.0
E3	0.9	--	0.4
G2	16	11	2.7*
G3	19	--	7.0*
G9	98	--	40*
G15	--	--	65*
I4	17	16	17
I8	23	29	26
I10	--	--	180
I12A	--	100	78

*After retrofit installation of bioshields.

(a) Report of measurement results to plant HP, Site G by D. L. Haggard, dated 1/8/81.

TABLE 6. Summary of Instrument Measurements for Subtask B

Location	Gamma Measurements CP mR/hr	TEPC mrem/hr	SNOOPY mrem/hr	PNR-4 mrem/hr	RASCAL mrem/hr	Average 9"/3" Ratio
Site E						
1x-29	0	1.0	1.2	NA	1.6	0.22
3x-29	0	0.4	0.7	NA	0.6	0.22
Site G						
2	10	2.7	13	8	NA	0.10
3	8	7.0	15	13	NA	0.10
9	25	40	100	75	NA	0.12
15	35	65	120	100	NA	0.12
Site I						
4	50	17	80	100	62	0.11
8	40	26	130	150	97	0.11
10	250	180	1300	1000	930	0.09
12A	75	78	360	300	240	

NA = Not available. Site G 9-in./3-in. sphere ratios were used from an earlier trip because the RASCAL malfunctioned during these measurements.

1) the average response of a particular instrument was determined over all ten locations, and 2) individual ratios were normalized by dividing them by the average]. The lines are eyeguides only and not meant to infer information relative to locations between the locations of measurement.

The noteworthy item is the greater response of the portable instruments at Site I as compared to the other sites visited during subtask B. There are two possible explanations of the increased response: 1) the TEPC malfunctioned and measured less than the actual dose equivalent, or 2) the energy of neutrons was such that the remmeters responded high. The consistency of the TEPC measurements in subtasks A and B (Tables 4 and 5) demonstrate that the TEPC did not malfunction. The second explanation is more probable because the remmeters exhibit a demonstrated energy dependence (Figure 13) and because the licensee had installed a great deal of shielding at Site I.

Quoting from Subtask A (Enders et al. 1981):

"... the borated polyethylene was replaced with a new neutron attenuation material, a silicon-based elastomer with a hydrogen density of approximately 0.06 gm/cm^3 (4.3 percent by weight) impregnated with boron to a density of 0.02 gm/cm^3 (1.5 percent by weight)..."

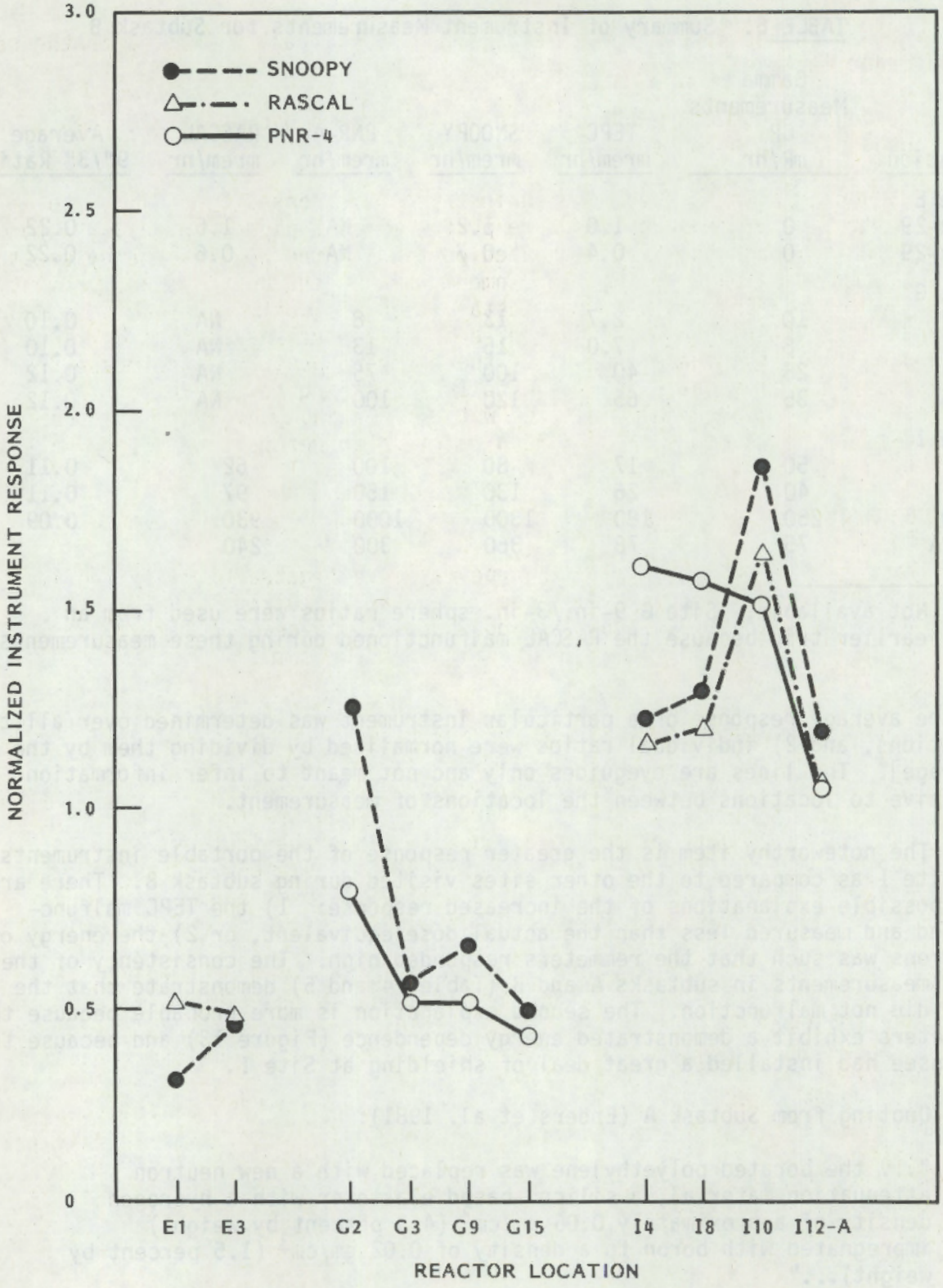

FIGURE 16. Response Ratio of Portable Instrument Readings at Each Site Relative to the TEPC

Another change in neutron shielding at Site I dealt with gaps in the concrete crane material Permali Type JN,

> "...densified beech wood laminate incorporating 6 percent hydrogen and 3 percent boron (by weight)..."

Noteworthy also is the trend in instrument responses from Site E to Site I. At Site E, measurements were performed at a pipe penetration into containment which means that the moderated portion of the neutron energy spectrum was selectively removed by the containment wall at the point of measurement. At Site G, new bioshields had been installed inside containment which allowed for greater scattering and moderation, but not as much as at Site I. Thus, one would expect the "hardness"[a] of the neutron spectrum to decrease from measurement locations at site E to G to I. Referring to Figure 13, the response of the SNOOPY would increase with decreasing hardness. Therefore, the moderated instruments respond high relative to reference dose equivalent measured using the TEPC.

4.2 COMPARISON OF DOSIMETER RESULTS

The response of each dosimeter type was investigated by analyzing its energy dependence using the monoenergetic beams of neutrons, and 2) its performance at the power reactors. Individual and average dosimeter results are included in Appendix Table A.1 through A.24 and summaries are found in Tables A.25 and A.26.

4.2.1 Accelerator/NBS Filtered Beam Irradiations

The response of a dosimeter is the dose equivalent reported by the vendor divided by the reference dose equivalent, either measured or calculated. TLD's are known to be strongly dependent on the energy of the incident neutron; while plastic track etch dosimeters exhibit thresholds at neutron energies below which they are unable to detect neutrons regardless of the number of neutrons. This will be made evident in the following discussion.

Dosimeters were irradiated to monoenergetic neutrons, the responses calculated and plotted, to illustrate the energy response of each dosimeter. The following tables give the dose equivalent response of each dosimeter for the particular neutron energy. That response is the average dosimeter measurement divided by the calculated dose equivalent. The error bars are the one standard deviation value of the dosimeter measurements divided by the calculated dose equivalent. The response equations for each dosimeter are given in each summary table. R is the dosimeter response, E_n is the neutron average in keV and r^2 is the correlation coefficient. The response functions are derived by linear regression analysis over the range of neutron energies between 0.024 and 0.448 MeV as this range is the normally reported range of linearity for TLD albedo dosimeters.

(a) Hardness is a qualitative measure of the relative energy of neutrons. One spectrum is harder than another if it has a greater average energy.

4.2.1.1 Vendor A (TLD)

Vendor A's dosimeter exhibited the response as plotted in Figure 17. Table 7 gives the data points and the equation of the response function between 20 keV and 500 keV (determined by linear regression from a log-log display). The response of Vendor A's dosimeter is in units of counts per millirem.

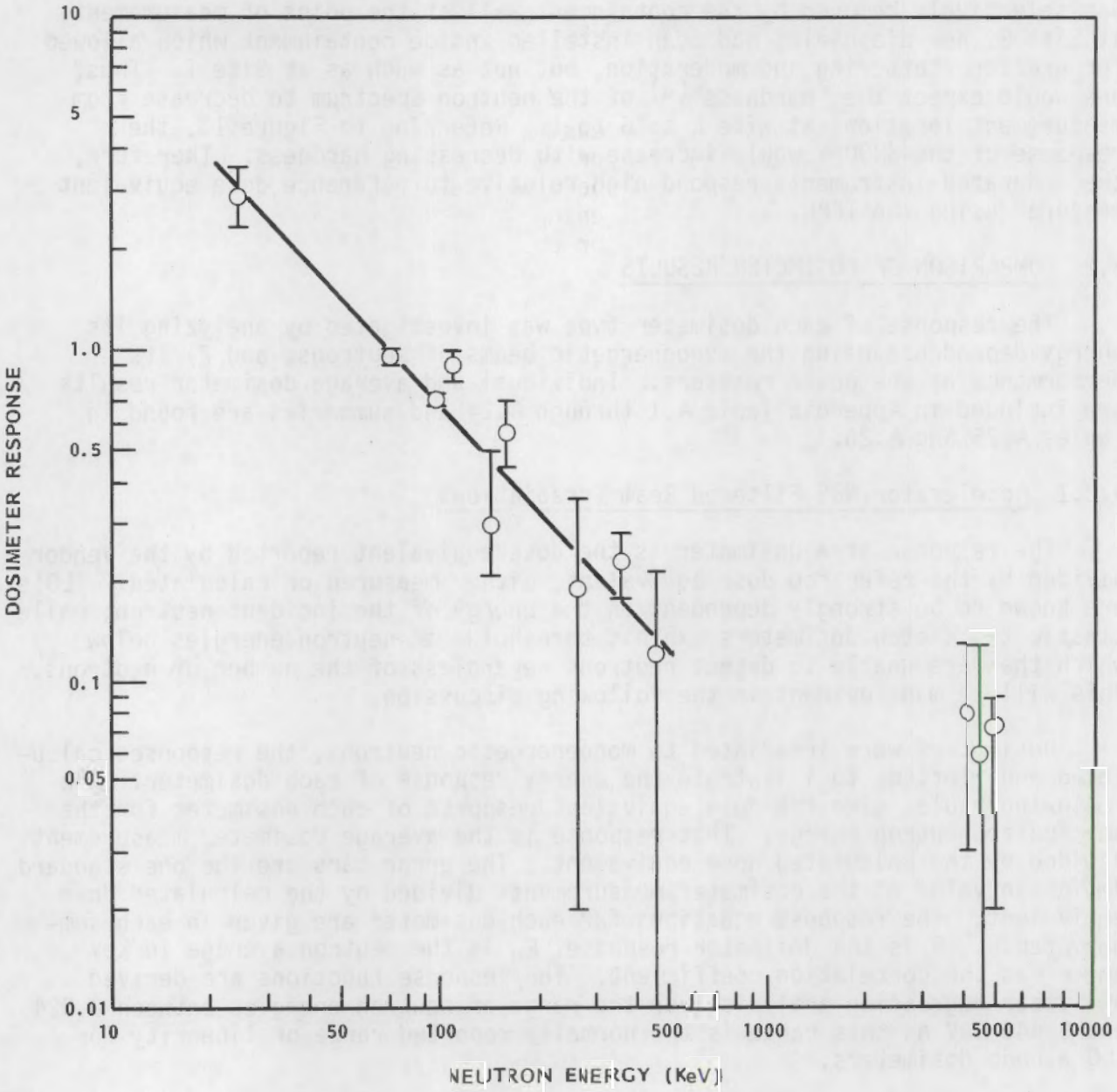

FIGURE 17. Vendor A Dosimeter (TLD) Response Curve

TABLE 7. Response Function for Vendor A

	Neutron Energy, keV													
	Thermal	2	24	70	97	110	144	161	264	358	448	4100	4500	4900
Response	32.6	6.3	2.9	0.96	0.71	0.90	0.30	0.57	0.19	0.23	0.12	0.08	0.06	0.07
1 S.D.	0.94	1.2	0.6	0.04	0.02	0.10	0.19	0.13	0.17	0.05	0.11	0.05	0.07	0.05

Response Function $R = 90.4\ E_n^{-1.06}$ $r^2 = .9237$

(response = reported net neutron counts/delivered dose equivalent)

It is important to note the increasing response with decreasing neutron energy. This was the primary trend for all the TLD's. Also note that the curve flattens out above 0.5 MeV and below 20 keV (referring to the 2 keV and thermal irradiations). Similar flattening is described in depth by Alsmiller and Barish in the literature (Alsmiller and Barish 1974).

4.2.1.2 Vendor B (TLD)

Figures 18 and 19 are the response curves for the TLD portion of Vendor B's dosimeter. Note that while the responses are different, the slopes of the curves are identical, showing the difference between the D_2O-moderated ^{252}Cf calibration and the bare, or unmoderated ^{252}Cf calibration. Table 8 contains the dosimeter response data.

TABLE 8. Response Function for Vendor B-TLD

	Neutron Energy, keV													
	Thermal	2	24	70	97	110	144	161	264	358	448	4100	4500	4900
D_2O Calibration	0	1.78	2.02	0.71	0.55	0.64	0.52	0.44	0.35	0.20	0.15	0.03	0	0.02
1 S.D.	0	0.17	0.35	0.03	0.02	0.06	0.05	0.02	0.02	0.02	0.04	0.04	0	0.03

D_2O Response Function: $R = 27.6\ E_n^{-0.83}$ $r^2 = 0.9631$

Bare Calibration	0	32.8	38.2	13.1	10.2	11.8	9.88	8.09	6.22	3.76	2.79	0.52	0.58	0.29
1 S.D.	0	3.22	6.77	0.68	0.40	1.08	1.07	0.34	0.43	0.37	0.59	0.90	0.12	0.50

Bare Response Function: $R = 527E_n^{-0.83}$ $r^2 = 0.9666$

(response = reported dose equivalent/delivered dose equivalent)

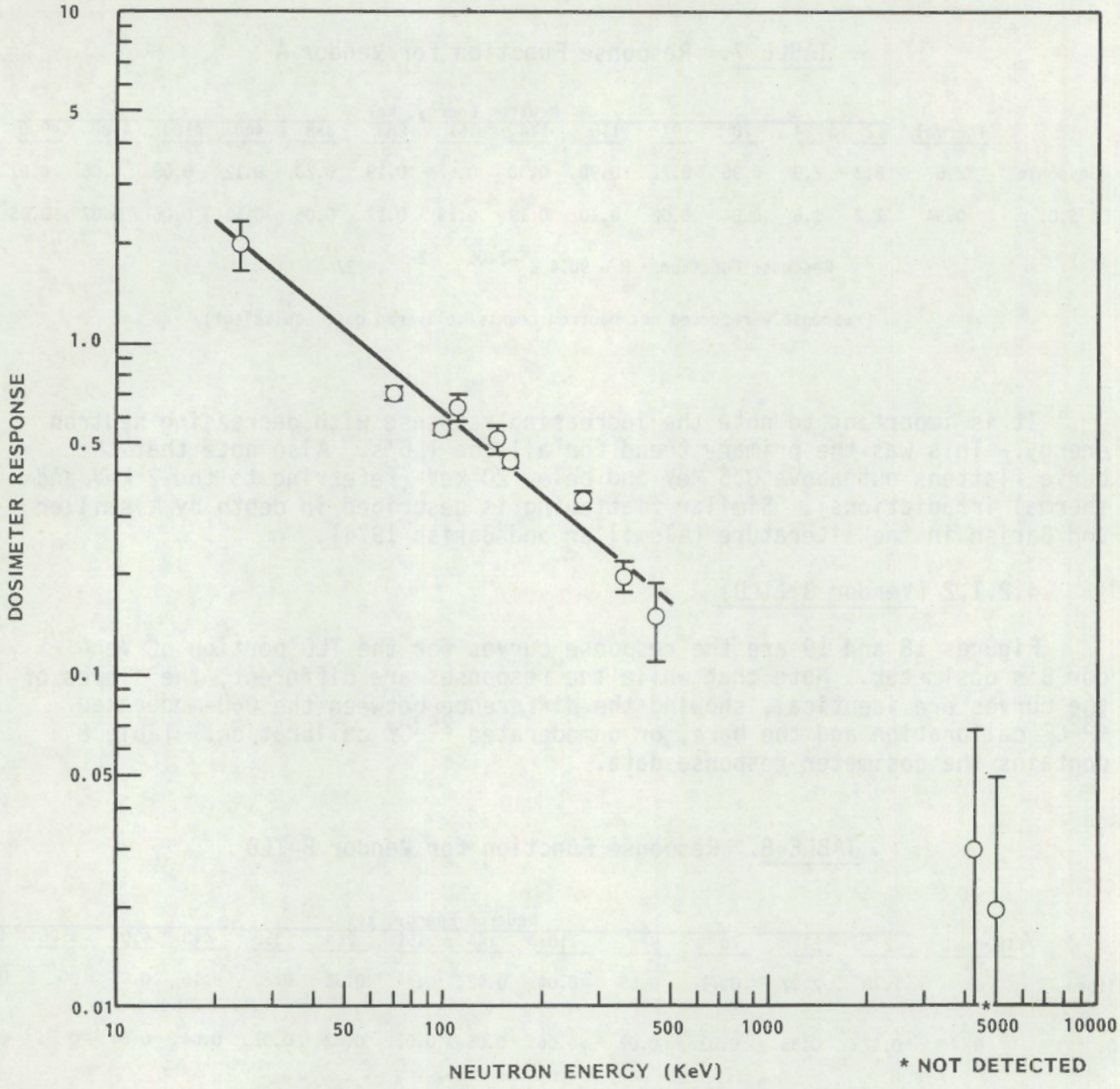

FIGURE 18. Vendor B Dosimeter (TLD-D_2O) Response Curve

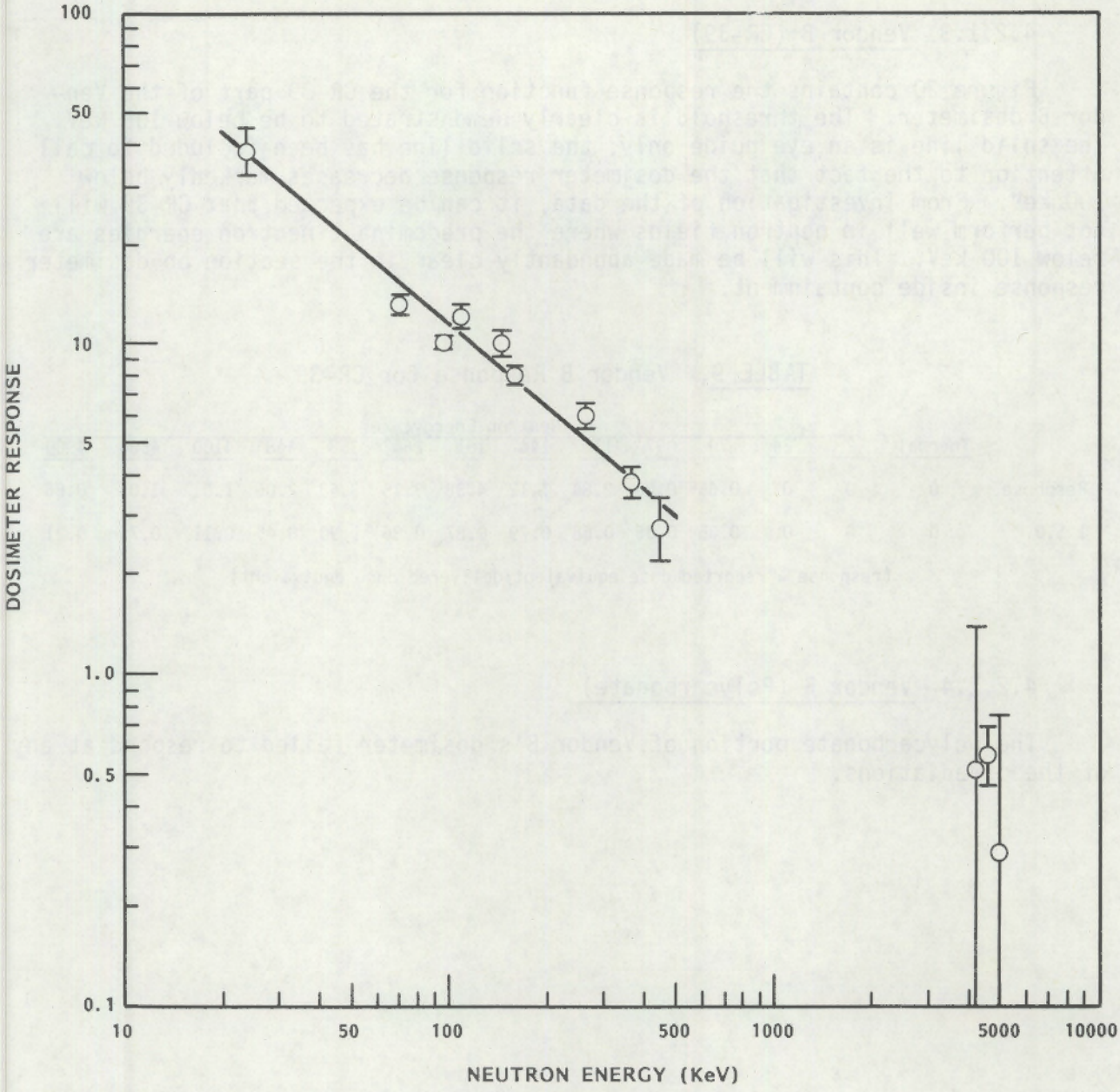

FIGURE 19. Vendor B Dosimeter (TLD-Bare) Response Curve

4.2.1.3 Vendor B (CR-39)

Figure 20 contains the response function for the CR-39 part of the Vendor B dosimeter. The threshold is clearly demonstrated to be below 100 keV. The solid line is an eye guide only; the solid line has been included to call attention to the fact that the dosimeter response decreases markedly below 100 keV. From investigation of the data, it can be expected that CR-39 will not perform well in neutron fields where the predominant neutron energies are below 100 keV. This will be made abundantly clear in the section on dosimeter response inside containment.

TABLE 9. Vendor B Response for CR-39

	Neutron Energy, keV													
	Thermal	2	24	70	97	110	144	161	264	358	448	4100	4500	4900
Response	0	0	0	0.65	0.20	2.84	1.12	4.38	3.15	3.63	2.06	1.01	1.05	0.86
1 S.D.	0	0	0	0.65	0.35	0.68	0.79	0.87	0.86	1.90	0.45	0.11	0.75	0.21

(response = reported dose equivalent/delivered dose equivalent)

4.2.1.4 Vendor B (Polycarbonate)

The polycarbonate portion of Vendor B's dosimeter failed to respond at any of the irradiations.

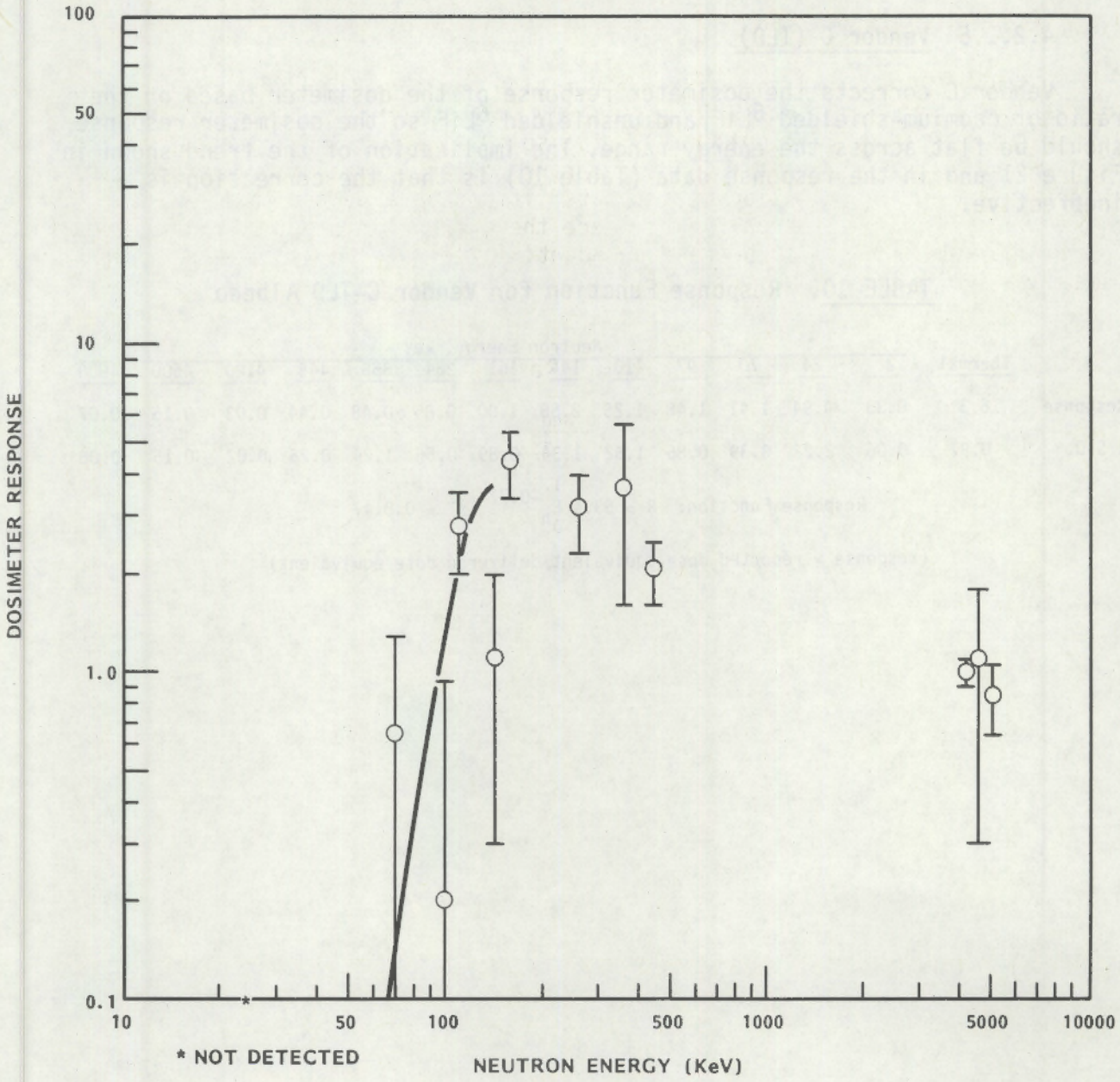

FIGURE 20. Vendor B Dosimeter (CR-39) Response Curve Demonstrating the Decrease in Sensitivity to Neutrons with Energy Below 100 keV

4.2.1.5 Vendor C (TLD)

Vendor C corrects the dosimeter response of the dosimeter based on the ratio of cadmium-shielded ^{6}LiF and unshielded ^{6}LiF so the dosimeter response should be flat across the energy range. The implication of the trend shown in Figure 21 and in the response data (Table 10) is that the correction is ineffective.

TABLE 10. Response Function for Vendor C-TLD Albedo

	Neutron Energy, keV													
	Thermal	2	24	70	97	110	144	161	264	358	448	4100	4500	4900
Response	16.3	0.33	4.94	1.41	1.48	1.25	2.58	1.00	0.85	0.48	0.44	0.03	0.15	0.07
1 S.D.	0.97	0.06	2.22	0.39	0.86	1.62	1.34	0.89	0.56	1.24	0.26	0.02	0.15	0.06

Response Function: $R = 53.4\ E_n^{-0.77}$ $r^2 = 0.8147$

(response = reported dose equivalent/delivered dose equivalent)

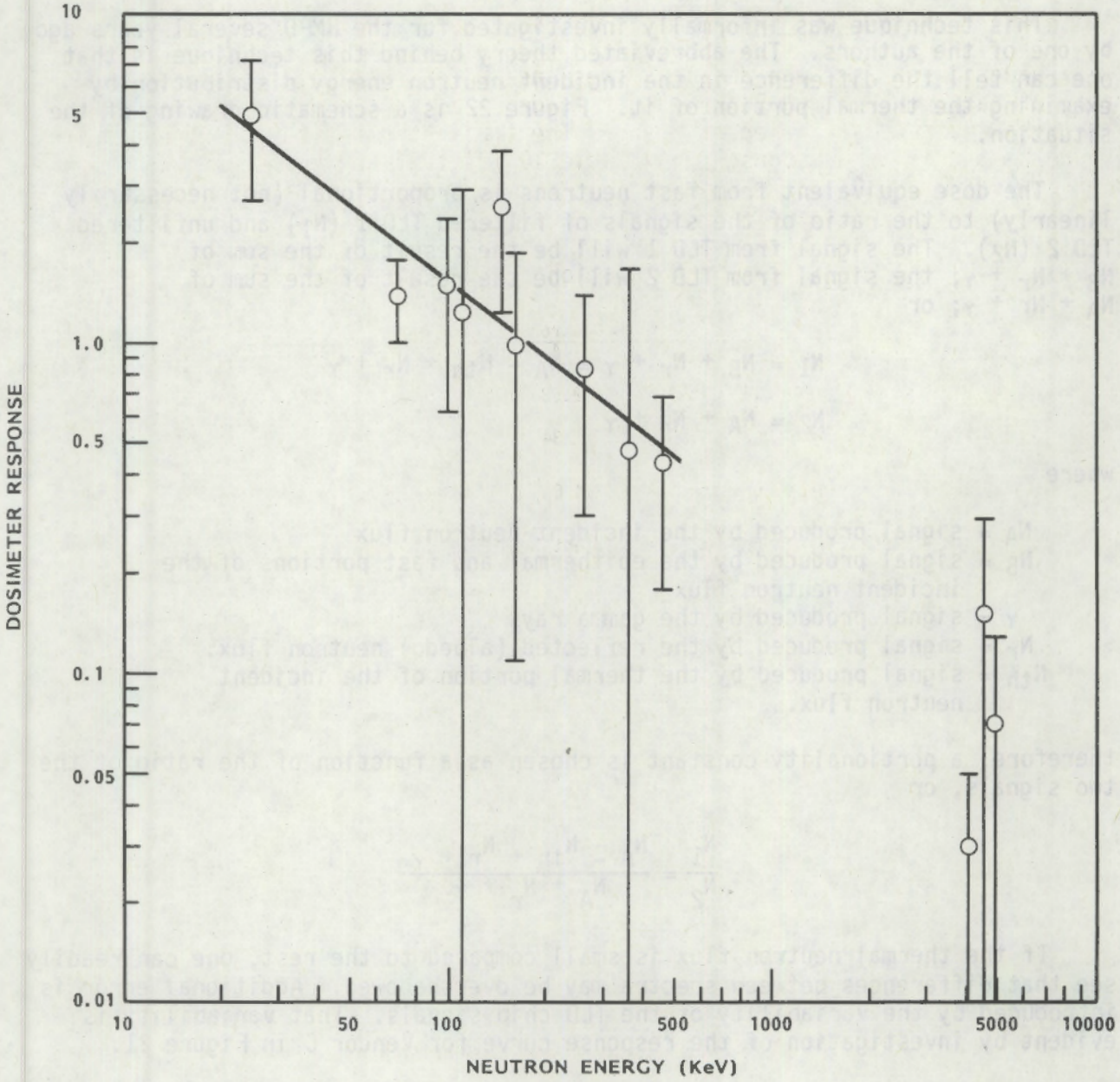

FIGURE 21. Vendor C Dosimeter (TLD) Response Curve

This technique was informally investigated for the HMPD several years ago by one of the authors. The abbreviated theory behind this technique is that one can tell the difference in the incident neutron energy distribution by examining the thermal portion of it. Figure 22 is a schematic drawing of the situation.

The dose equivalent from fast neutrons is proportional (not necessarily linearly) to the ratio of the signals of filtered TLD 1 (N_1) and unfiltered TLD 2 (N_2). The signal from TLD 1 will be the result of the sum of $N_B + N_r + \gamma$; the signal from TLD 2 will be the result of the sum of $N_A + Nr + \gamma$; or

$$N_1 = N_B + N_r + \gamma = N_A - N_{th} + N_r + \gamma$$

$$N_2 = N_A + N_r + \gamma$$

where

N_A = signal produced by the incident neutron flux
N_B = signal produced by the epithermal and fast portions of the incident neutron flux
γ = signal produced by the gamma rays
N_r = signal produced by the reflected (albedo) neutron flux.
N_{th} = signal produced by the thermal portion of the incident neutron flux.

therefore, a portionality constant is chosen as a function of the ratio of the two signals, or

$$\frac{N_1}{N_2} = \frac{N_A - N_{th} + N_r + \gamma}{N_A + N_r + \gamma}$$

If the thermal neutron flux is small compared to the rest, one can readily see that differences between spectra may be overshadowed. Additional error is introduced by the variability of the TLD chip signals. That variability is evident by investigation of the response curve for Vendor C in Figure 21.

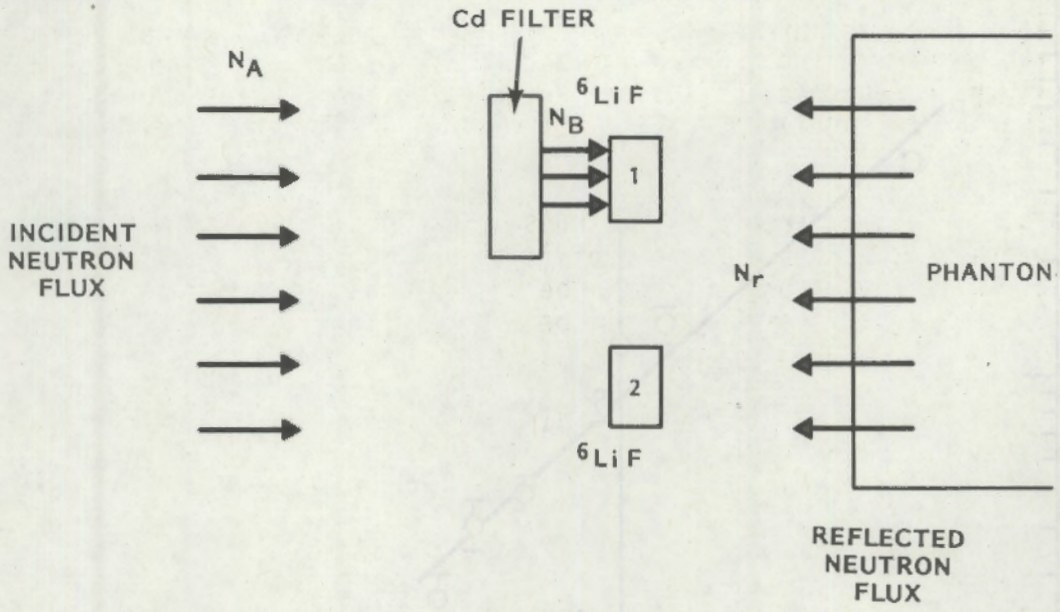

FIGURE 22. Schematic Representation of Neutrons Incident on TLD Albedo Dosimeter

4.2.1.6 Vendor D (TLD)

The response curve for Vendor D (Figure 23) is similar to that of other TLD's. There are less points because Vendor D did not participate in all the Van de Graaff irradiations. The additional data points though would change the response function only slightly. Table 11 contains the response data.

TABLE 11. Response Function for Vendor D

	Neutron Energy, keV						
	24	110	144	161	264	358	448
Response	3.55	1.36	1.18	0.83	0.49	0.41	0.21
1 S.D.	0.06	0.16	1.27	0.07	0.05	0.06	0.04

Response Function: $R = 69.8\ E_n^{-0.88}$ $r^2 = 0.9542$

(response = reported dose equivalent/delivered dose equivalent)

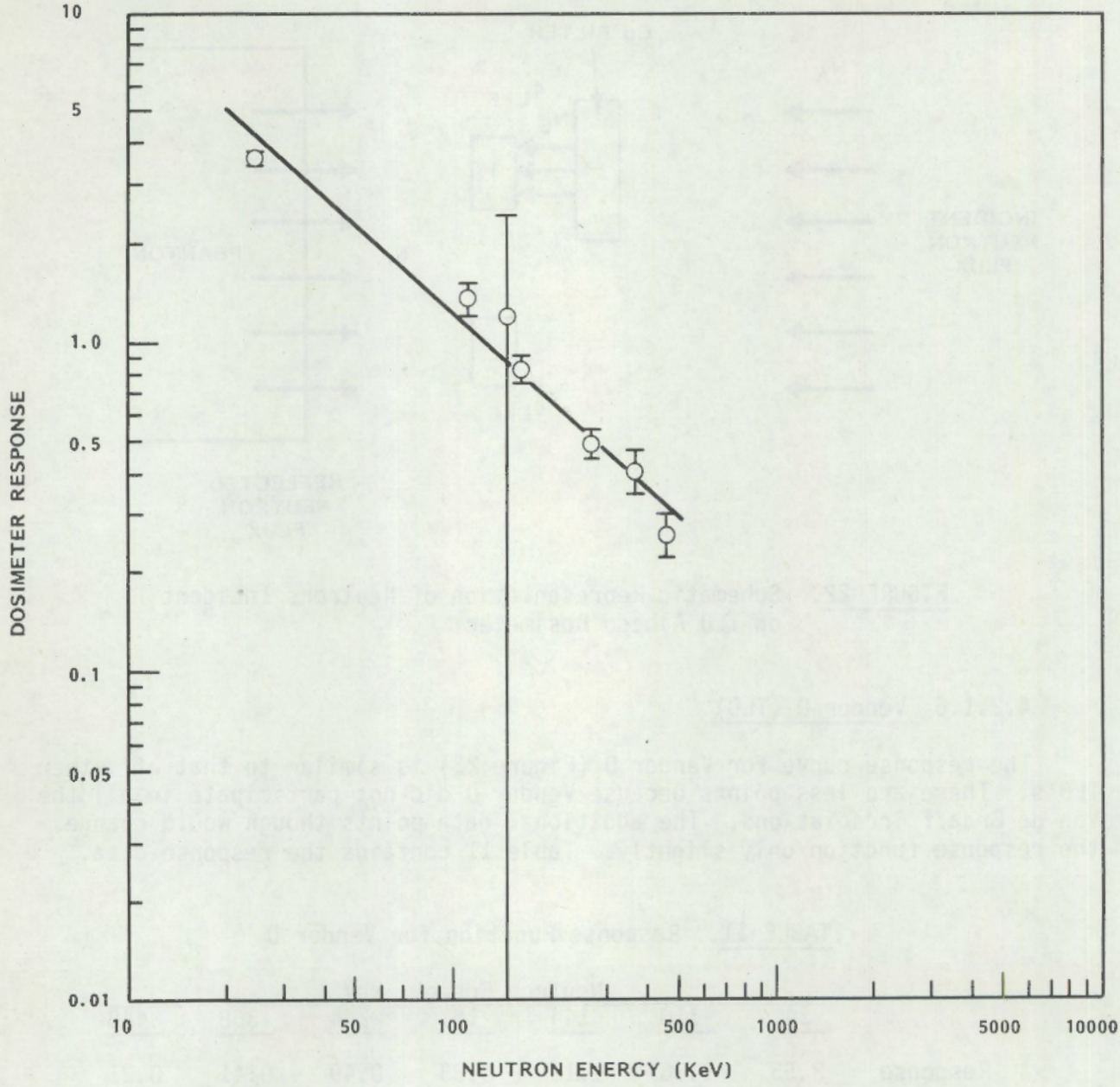

FIGURE 23. Vendor D Dosimeter (TLD) Response Curve

4.2.1.7 Vendor E (Polycarbonate + Radiators)

It would be expected that the response function for this dosimeter would follow the TLD response as (n,α) radiators (^{10}B) are used to generate tracks in polycarbonate. However, due to an energy correction based on the comparison of various filtered and unfiltered areas of the polycarbonate film, that part of the response function due to the (n,α) reactions is folded into a larger, more complex response function. Investigation of Figure 24 reveals that the dosimeter responds within a factor of 2 of the dose equivalent for the reference energies as demonstrated by the dashed lines. Table 12 contains the response data for Vendor E.

TABLE 12. Response Data for Vendor E

	Neutron Energy, keV											
	24	70	96	110	144	161	264	358	448	4100	4500	4900
Response	0.94	0.65	0.60	2.02	1.36	1.86	0.82	0.92	0.58	0.56	0.56	0.56
1 S.D.	0.13	0.26	0.24	0.24	0.09	0.38	0.16	0.24	0.10	0.28	0.28	0.28

(response = reported dose equivalent/delivered dose equivalent)

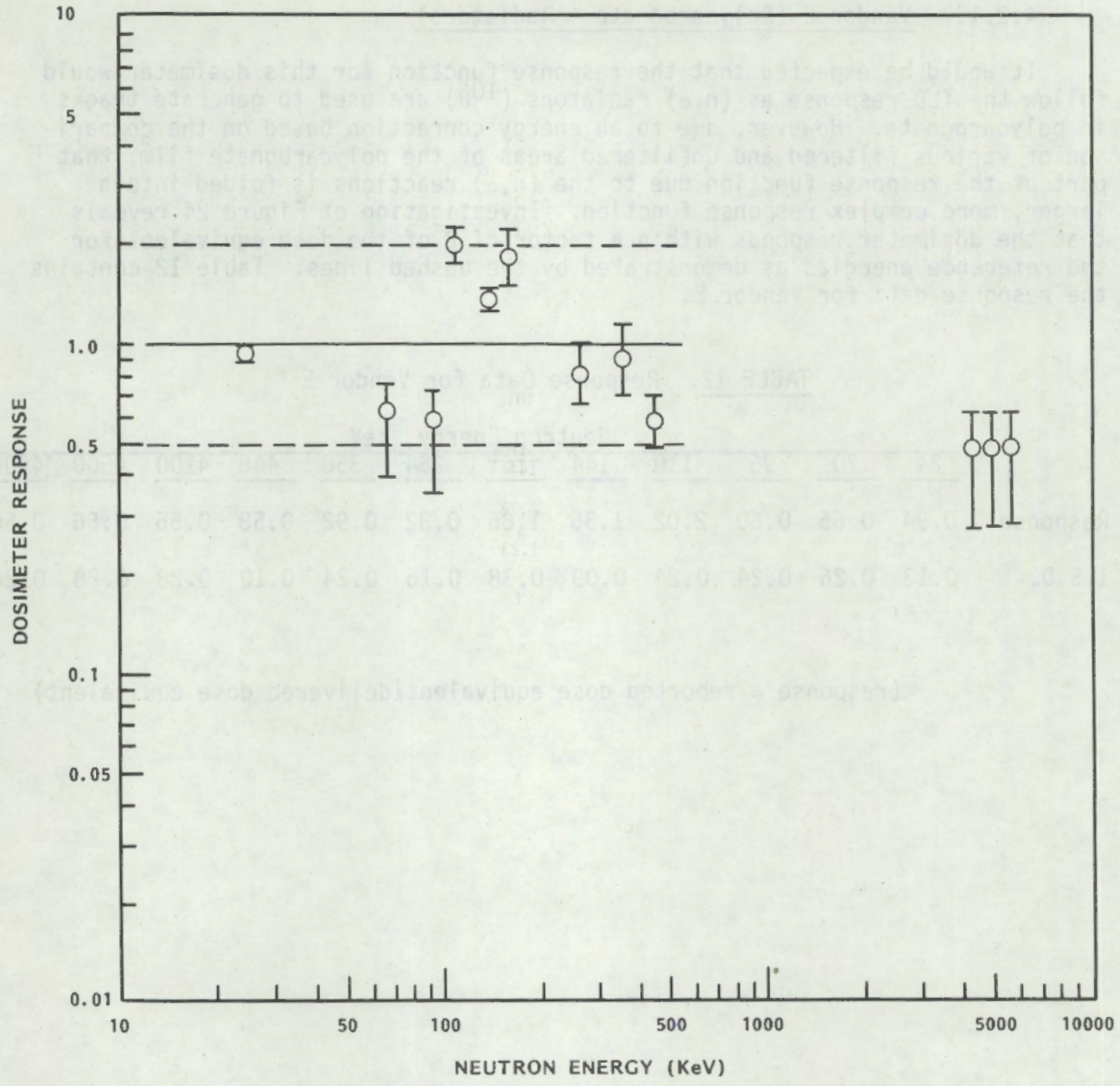

FIGURE 24. Vendor E Dosimeter (Polycarbonate + Radiators) Response

4.2.1.8 HMPD (TLD)

The neutron energy response function of the HMPD is similar to other TLDs. Figure 25 is the plotted response function while Table 13 has the response data. The HMPD fairly well demonstrates the effect of calibrating a dosimeter with a high energy neutron source, bare ^{252}Cf, and using it in a low energy neutron field. Investigation of the data plotted in Figure 25 shows that a response of 1.0 (the response at the energy of calibration) occurs at 0.6 MeV. The HMPD has been irradiated in the past using the D_2O moderated ^{252}Cf source at NBS. The relative energy of calibration for that source is between 50 and 100 keV.

TABLE 13. Response Function for the HMPD

	Neutron Energy, keV													
	Thermal	2	24	70	97	110	144	161	264	358	448	4100	4500	4900
Response	1.86	43.0	27.2	9.81	7.87	5.13	8.78	4.83	2.27	1.72	1.29	0.86	0.75	0.79
1 S.D.	0.19	11.3	3.22	2.14	0.84	0.79	1.23	0.53	0.19	0.09	0.44	0.22	0.13	0.09

Response Function: $R = 850\ E_n^{-1.04}$ $r^2 = 0.9346$

(response = reported dose equivalent/delivered dose equivalent)

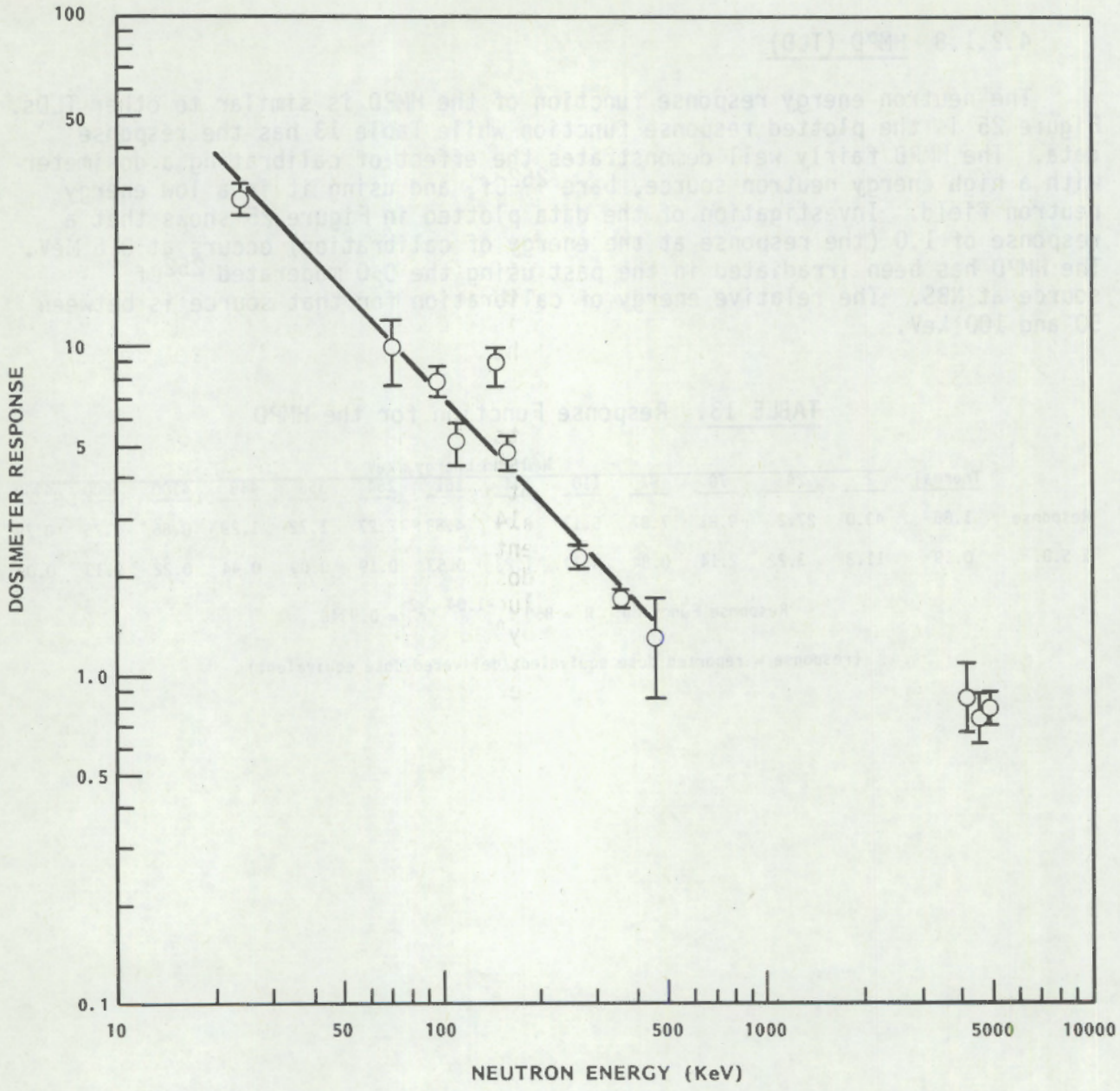

FIGURE 25. HMPD (TLD) Response Curve

4.2.1.8 LLL (TLD)

LLL did not participate in the acceleration irradiations. The reader is directed to the literature for that information (Hankins 1975; Griffith et al. 1979).

4.2.2 Reactor Irradiations

The response of dosimeters inside containment of nuclear power plants is a complex function which depends of the neutron energy spectrum and the reference measurement. For reasons enumerated in the earlier section addressing the instruments used in this study, the TEPC has been chosen as the reference instrument.

The response of dosimeters compared to the SNOOPY will also be displayed for comparison to illustrate the relationship between the dosimeters and the remmeters and also because the TEPC is not yet available as a portable dose equivalent monitoring instrument. Table 14 contains dosimeter response data using the TEPC as the reference measurement; the response is defined as the average dose equivalent measured by the dosimeter divided by the integral dose equivalent measured by the TEPC. The values of one standard deviation of dosimeter measurements are also divided by the TEPC measurement as a measure of the precision of dosimeter measurements. Table 15 contains dosimeter response data using the SNOOPY as the reference.

TABLE 14. Average Dosimeter Response Ratios (by Location) for Reactor Irradiation Using the TEPC as Reference

Vendor	Site E1	Site E3	Site G2	Site G3	Site G9	Site G15	Site I4	Site I8	Site I10	Site I12A
A (TLD)	2.19 (0.21)	3.22 (0.49)	7.86 (1.05)	5.40 (0.88)	5.69 (1.09)	7.27 (1.36)	13.0 (1.90)	9.09 (1.36)	7.06 (1.00)	7.91 (0.70)
B (TLD/D_2O)	0.71 (0.06)	0.98 (0.12)	3.38 (0.16)	2.42 (0.08)	2.73 (0.28)	2.68 (0.11)	4.85 (0.13)	4.55 (0.19)	4.29 (0.17)	4.03 (0.39)
B (TLD/Bare)	15.2 (1.33)	21.1 (2.44)	72.5 (2.75)	51.6 (1.63)	58.2 (6.09)	59.0 (2.32)	105 (2.75)	97.0 (4.06)	91.2 (3.71)	86.6 (8.36)
B (CR-39)	0 (0)	0 (0)	0 (0)	0 (0)	0 (0)	0.02 (0.05)	0.20 (0.45)	0.12 (0.27)	0.08 (0.11)	0 (0)
B (poly-carb)	0 (0)	0 (0)	0 (0)	0 (0)	0 (0)	0 (0)	0 (0)	0 (0)	0 (0)	0 (0)
C (TLD)	2.62 (1.24)	0.89 (1.11)	1.25 (1.00)	0.05 (0.16)	2.55 (0.26)	2.68 (0.40)	5.00 (0.14)	5.00 (0.38)	3.05 (0.28)	4.50 (0.14)
D (TLD)	4.41 (0.73)	7.33 (0.51)	17.5 (0.71)	9.47 (0.37)	10.0 (0.37)	6.32 (0.10)	25.5 (1.5)	23.4 (1.03)	6.50 (0.11)	13.8 (0.16)
E (poly-carb)	0.57 (0.13)	1.33 (0.44)	3.57 (2.70)	1.90 (0.30)	1.69 (0.65)	2.00 (1.73)	4.55 (0.55)	2.30 (2.09)	4.12 (2.41)	4.03 (3.58)
HMPD	5.00 (0.38)	4.56 (1.07)	20.0 (1.15)	15.3 (0.79)	15.5 (2.73)	13.7 (1.32)	24.6 (5.00)	27.2 (3.44)	20.0 (3.70)	21.3 (5.38)
LLNL	1.55 (0.13)	1.78 (0.07)	3.10 (0.76)	2.30 (0.04)	2.15 (0.22)	2.18 (0.05)	5.50 (0.11)	4.85 (0.36)	4.24 (0.18)	4.03 (0.15)

NOTE: Numbers in parentheses are one standard deviation of dosimeter measurements divided by the TEPC measurement.

TABLE 15. Average Dosimeter Response Ratios (by Location) for Reactor Irradiation Using the SNOOPY as Reference

Vendor	Site E1	Site E3	Site G2	Site G3	Site G9	Site G15	Site I4	Site I8	Site I10	Site I12A
A (TLD)	1.77 (0.17)	1.93 (0.29)	1.50 (0.20)	2.08 (0.34)	2.18 (0.42)	4.00 (0.75)	2.60 (0.38)	1.88 (0.28)	1.00 (0.14)	1.71 (0.15)
B (TLD/D_2O)	0.58 (0.05)	0.59 (0.07)	0.68 (0.03)	0.98 (0.03)	1.00 (0.10)	1.46 (0.06)	0.97 (0.03)	0.94 (0.04)	0.61 (0.02)	0.87 (0.08)
B (TLD/Bare)	12.3 (1.08)	12.7 (1.47)	14.5 (0.55)	20.9 (0.66)	21.3 (2.23)	32.0 (1.26)	21.0 (0.55)	20.0 (0.84)	12.9 (0.53)	18.7 (1.81)
B (CR-39)	0 (0)	0 (0)	0 (0)	0 (0)	0 (0)	0.01 (0.03)	0.04 (0.09)	0.03 (0.06)	0.01 (0.02)	0 (0)
B (poly-carb)	0 (0)	0 (0)	0 (0)	0 (0)	0 (0)	0 (0)	0 (0)	0 (0)	0 (0)	0 (0)
C (TLD)	2.12 (1.00)	0.53 (0.67)	0.25 (0.20)	0.02 (0.06)	0.93 (0.09)	1.46 (0.22)	1.00 (0.03)	1.07 (0.08)	0.47 (0.04)	0.97 (0.03)
D (TLD)	3.03 (0.50)	4.40 (0.31)	3.50 (0.14)	3.83 (0.15)	3.67 (0.03)	3.43 (0.05)	5.09 (0.30)	5.00 (0.22)	1.00 (0.02)	2.97 (0.04)
E (poly-carb)	0.46 (0.10)	0.80 (0.27)	0.68 (0.14)	0.73 (0.12)	0.65 (0.25)	1.10 (0.95)	1.00 (0.12)	0.48 (0.43)	0.58 (0.34)	0.87 (0.77)
HMPD	3.44 (0.26)	2.73 (0.64)	4.00 (0.23)	6.17 (0.32)	5.67 (1.00)	7.43 (0.71)	4.91 (1.00)	5.80 (0.73)	3.08 (0.57)	4.59 (1.16)
LLNL	1.06 (0.09)	1.07 (0.04)	0.59 (0.01)	0.88 (0.02)	0.82 (0.08)	1.20 (0.03)	1.10 (0.02)	1.00 (0.08)	0.60 (0.03)	0.87 (0.03)

NOTE: Numbers in parentheses are one standard deviation of dosimeter measurements divided by the SNOOPY measurement.

Figures 26 through 32 are the plotted average response functions for the dosimeters. A trend that is prominent upon investigation of the figures is the general increase in dosimeter response (relative to the TEPC) from Site E (BWR) to Site G (PWR) to Site I (PWR). Since the dosimeter response increases with decreasing neutron energy, it is evident that the spectrum in Site I is very much moderated (lower in energy) compared to Site G and to Site E. From the irradiation conditions, this is the trend one would expect. Referring back to the dosimeter energy response curves (Figures 17 through 25), it is evident that a small shift in neutron energy produces a moderately large shift in dosimeter response.

Lines are drawn between each point to aid in identifying overall trends; the lines are not meant to imply a linear change in dosimeter response as a function of position in going from one irradiation location to another.

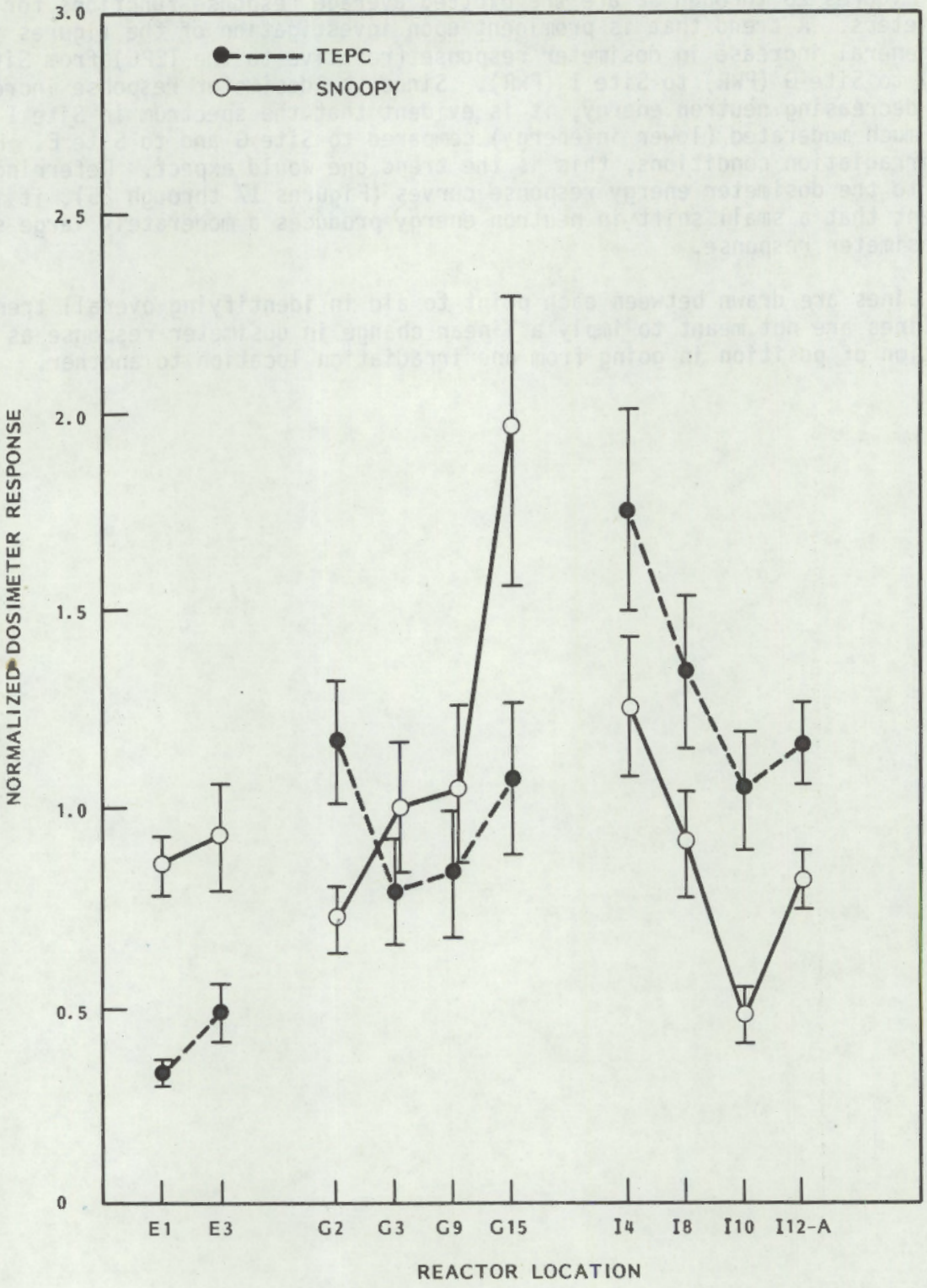

FIGURE 26. Vendor A Dosimeter (TLD) Responses by Reactor Location

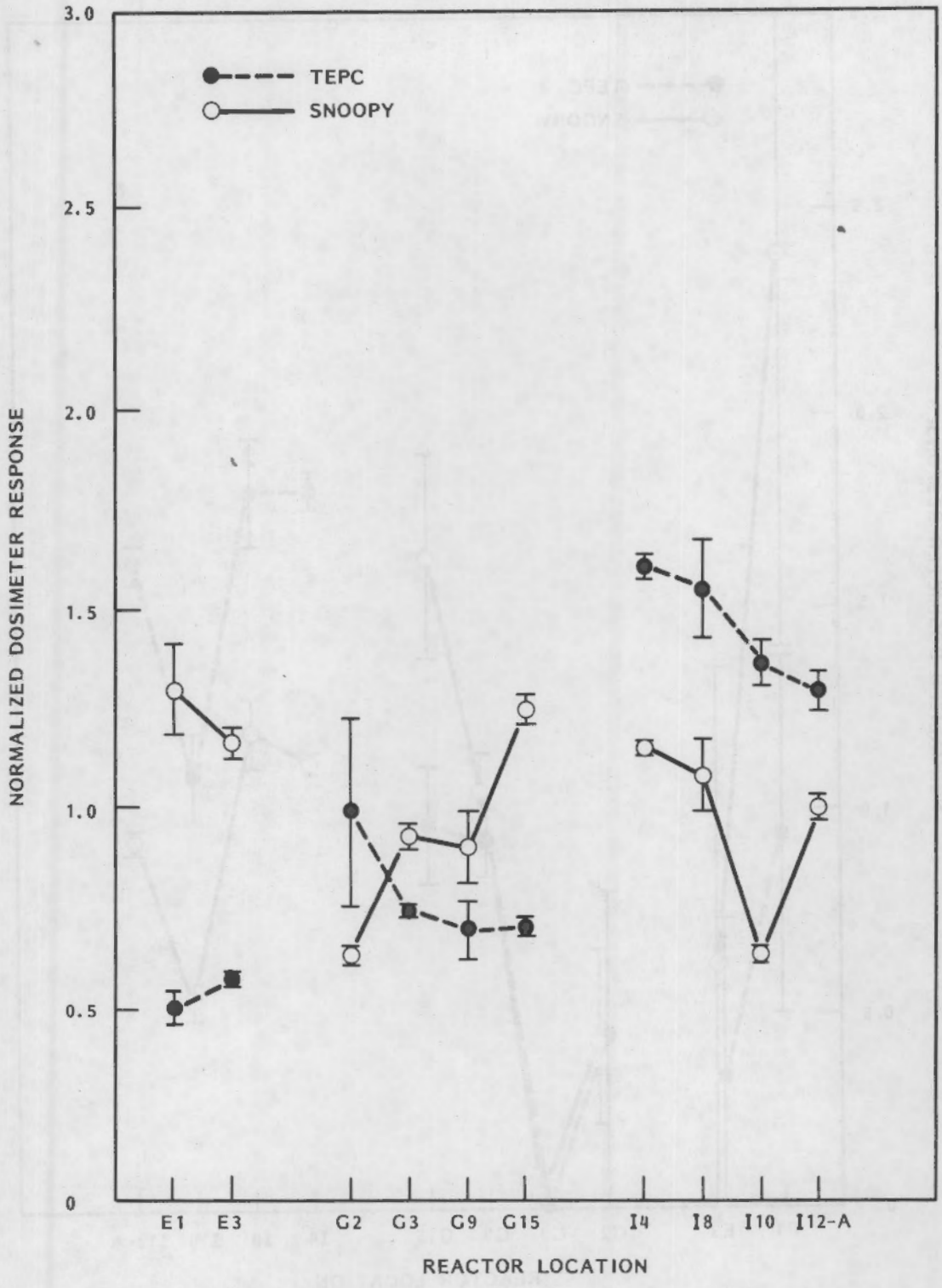

FIGURE 27. Vendor B Dosimeter (TLD) Responses by Reactor Location

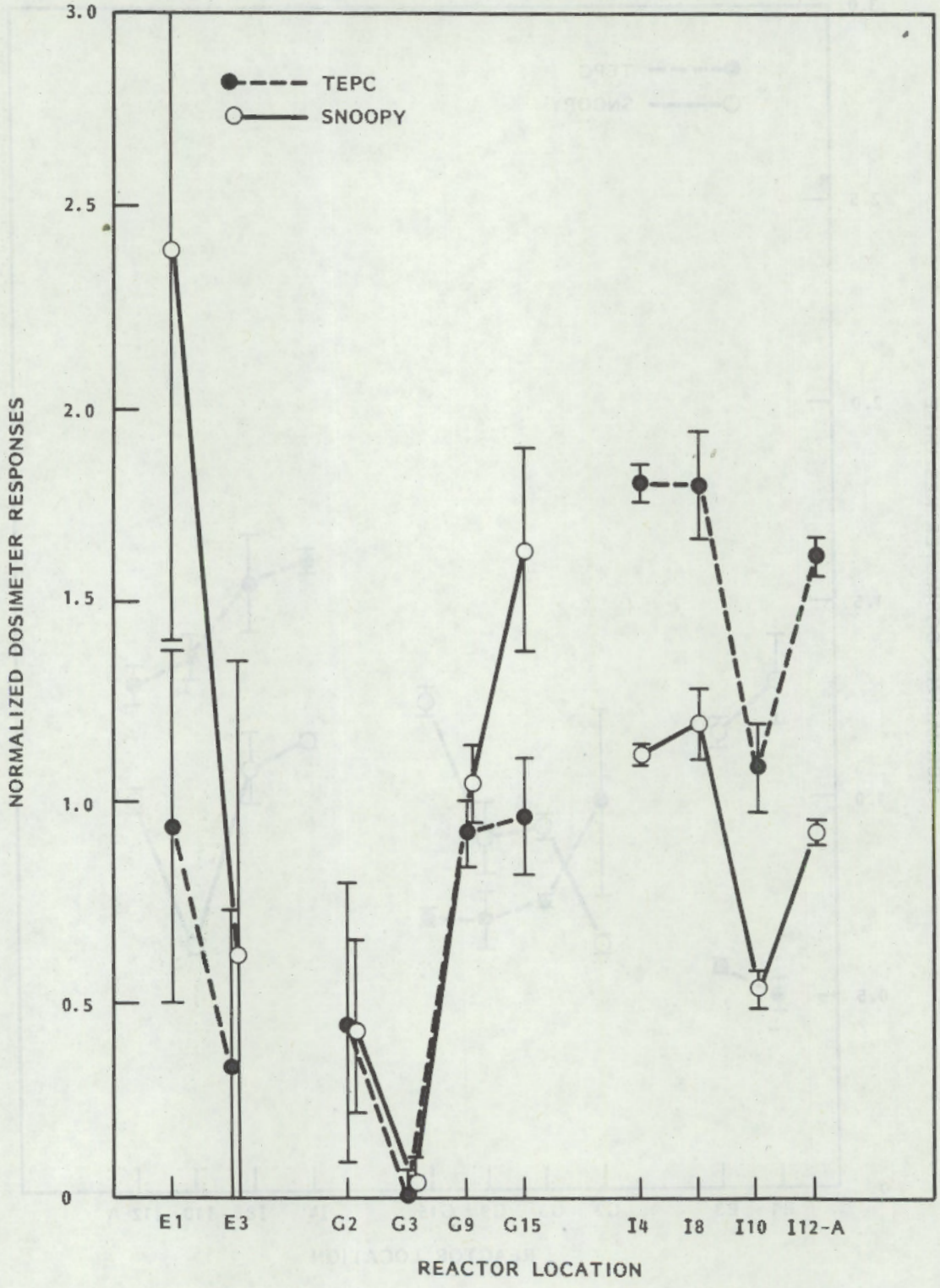

FIGURE 28. Vendor C Dosimeter (TLD) Responses by Reactor Location

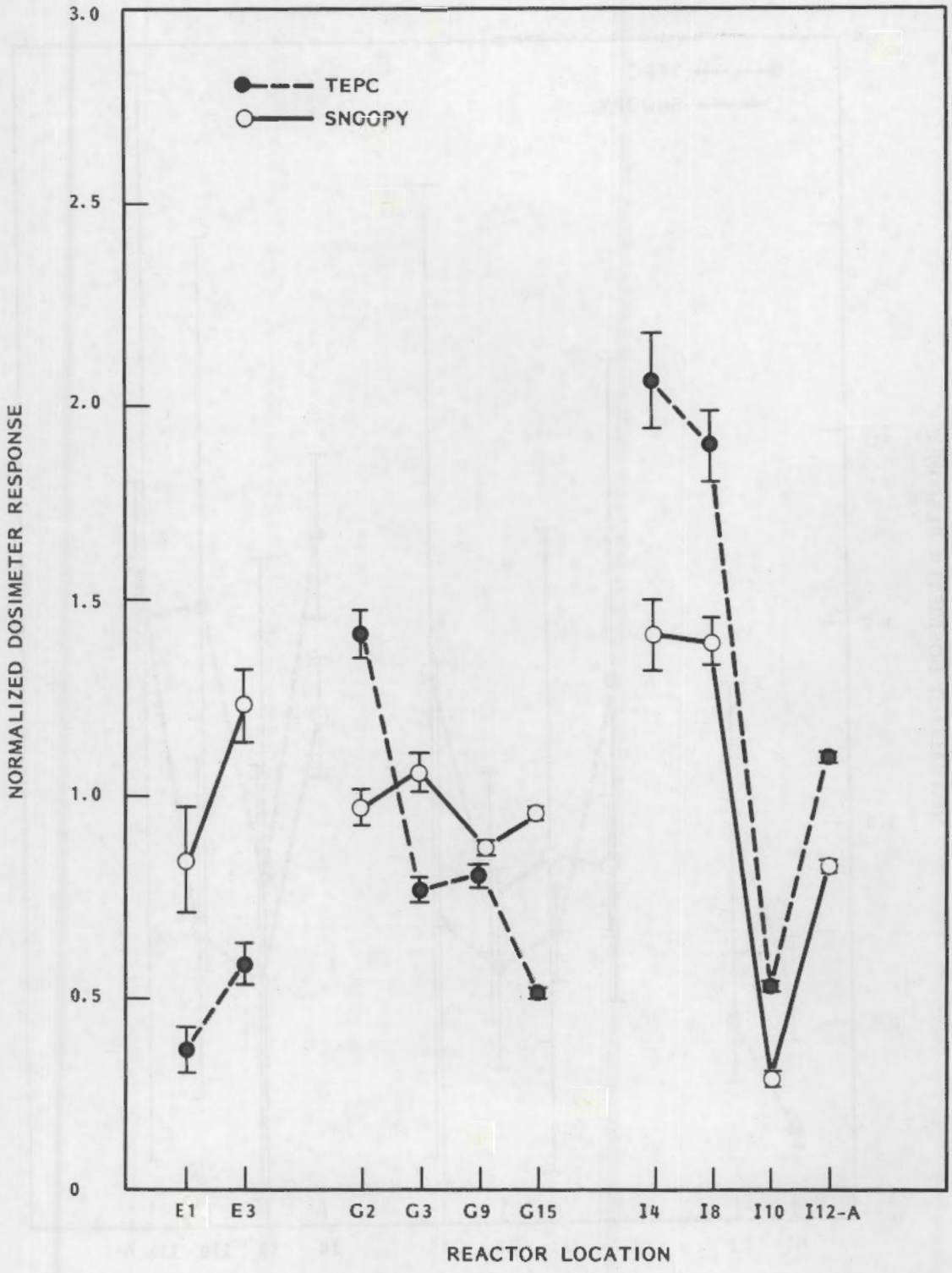

FIGURE 29. Vendor D Dosimeter (TLD) Responses by Reactor Location

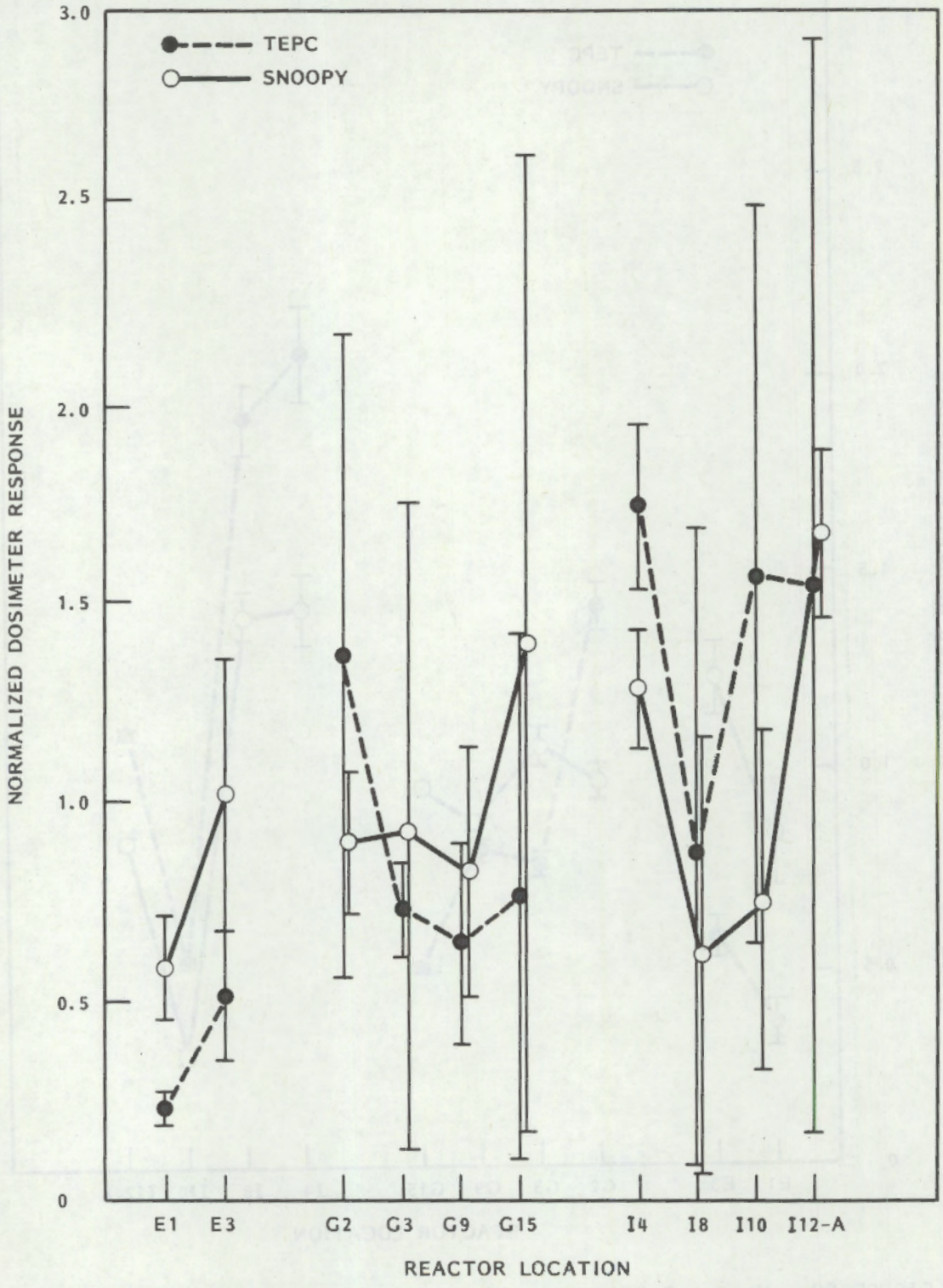

FIGURE 30. Vendor E Dosimeter (Polycarbonate + Radiators) Responses by Reactor Location (average and standard deviation include dosimeters which saturated.)

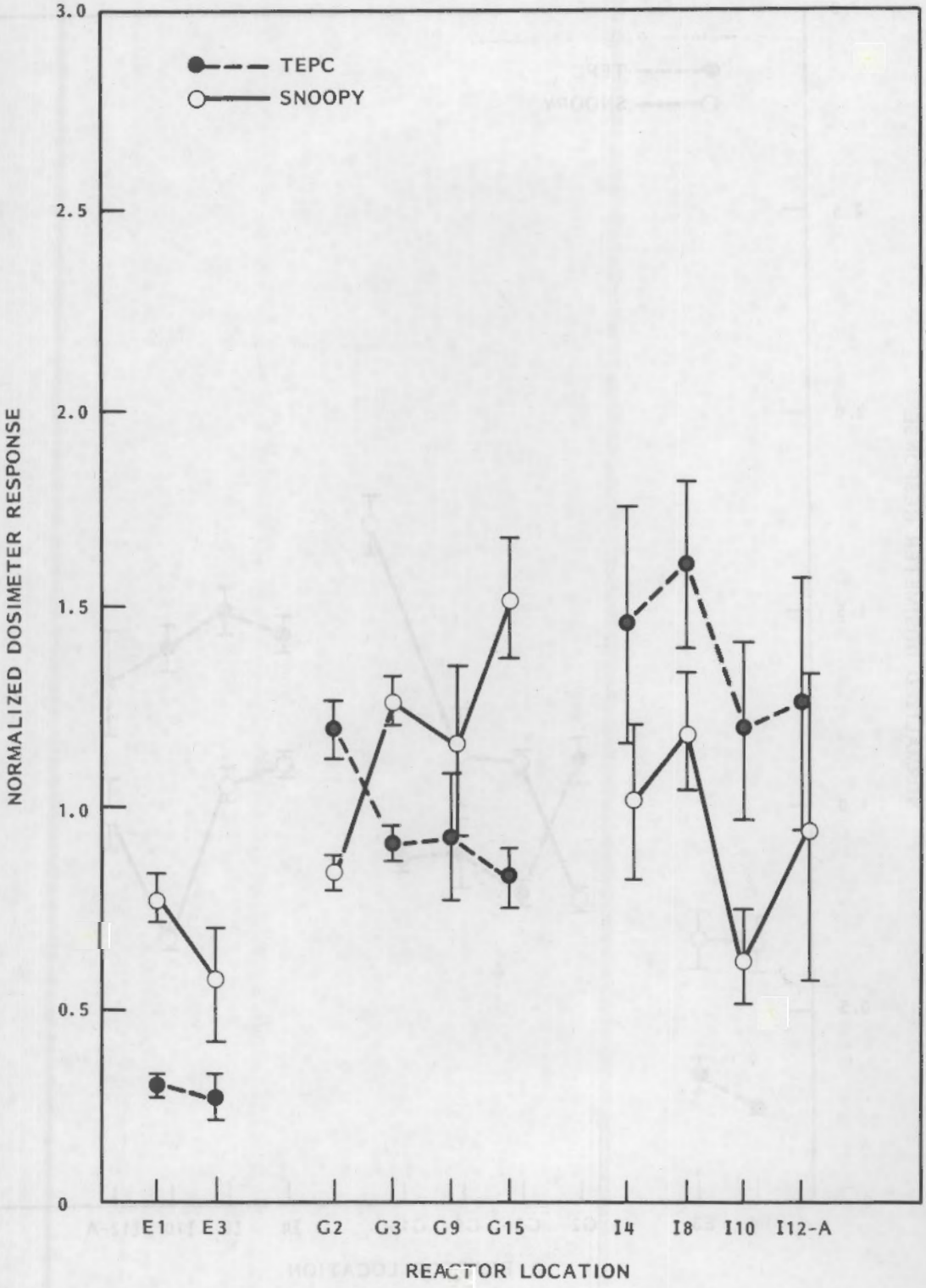

FIGURE 31. HMPD Dosimeter (TLD) Responses by Reactor Location

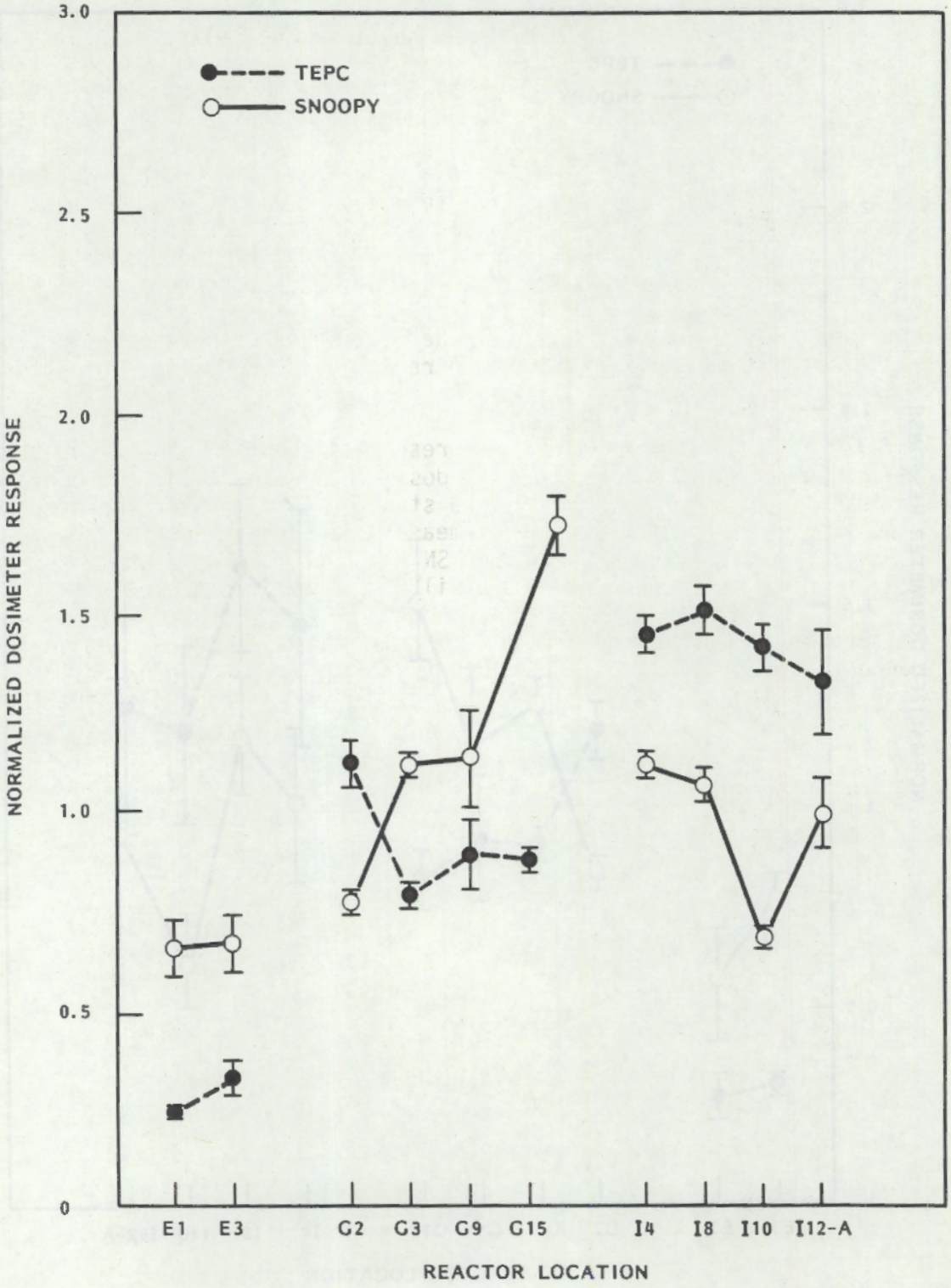

FIGURE 32. LLL Dosimeter (TLD) Responses by Reactor Location

Another trend that is apparent is the shift in the relative position of responses between the TEPC reference and the SNOOPY reference. Noting that: 1) a decrease in neutron energy produces an increase in the dosimeter response and 2) an increase in the instrument measurement produces a decrease in the dosimeter response, the shift in relative position of the TEPC and SNOOPY relationship from site E to G to I may be explained in that the high response of the SNOOPY and the dosimeters compensate for each other at Site I. That is, while the dosimeters respond high compared to the TEPC, the SNOOPY does also, so the combined effect is a lowering of the SNOOPY-referenced dosimeter response in relation to the TEPC-referenced dosimeter response.

A noticeable characteristic of all the dosimeter response data in Figures 26-32 is the wide range of dosimeter response at each site, no matter what instrument is used as a reference.

Table 16 contains average dosimeter responses using the SNOOPY as the reference measurement. The responses of dosimeters at each site were averaged; numbers in parentheses indicate one standard deviation of the average responses. The average response is the measure of how high or low the dosimeter responds (on the average) given the SNOOPY reference dose while the deviation is the precision, or reproducibility, of the measurement.

The information contained in Table 16 is important to relate dosimeter performance to the field instrument currently available and in use at athe reactors. Table 17 presents the same dosimeter data referenced to the TEPC.

TABLE 16. Average Dosimeter Response Ratios (by Site) Using SNOOPY as Reference

Vendor	Location E	G	I	Overall
A	1.85(0.11)	2.44(1.08)	1.80(0.66)	2.07(0.80)
B(D_2O)	0.59(0.01)	1.03(0.32)	0.85(0.16)	0.87(0.27)
B(Bare)	12.5(0.28)	22.2(7.25)	18.2(3.62)	18.6(6.00)
C	1.33(1.12)	0.67(0.66)	0.88(0.27)	0.88(0.61)
D	3.72(0.97)	3.61(0.18)	3.52(1.94)	3.59(1.17)
E	0.63(0.24)	0.79(0.21)	0.73(0.24)	0.74(0.21)
HMPD	3.09(0.50)	5.82(1.42)	4.60(1.13)	4.78(1.50)
LLL	1.07(0.01)	0.87(0.25)	0.89(0.22)	0.92(0.21)

NOTE: Numbers in parentheses are one standard deviation of dosimeter response ratios at each site divided by the integral dose equivalent measured with the SNOOPY.

TABLE 17. Average Dosimeter Response Ratios (by Site) Using TEPC as Reference

Vendor	Location E	G	I	Overall
A	2.71(0.73)	6.56(1.20)	8.97(2.07)	6.75(2.79)
B(D_2O)	0.85(0.19)	2.80(0.41)	4.32(0.22)	3.02(1.38)
B(Bare)	18.3(4.17)	60.3(8.77)	92.6(4.68)	64.8(29.5)
C	1.76(1.22)	1.63(1.24)	4.39(0.92)	2.76(1.71)
D	5.87(2.06)	10.8(4.74)	17.3(8.82)	12.4(7.43)
E	0.95(0.54)	2.29(0.86)	3.75(0.99)	2.61(1.36)
HMPD	4.78(0.31)	16.1(2.71)	23.3(3.26)	16.7(7.54)
LLL	1.67(0.16)	2.43(0.45)	4.53(0.47)	3.12(1.31)

NOTE: Numbers in parentheses are one standard deviation of dosimeter response ratios at each site divided by the integral dose equivalent measured with the TEPC.

Generally, the trend is that the dosimeters exhibit higher response in proportion to the noted amount of moderation. It is important to note that although several dosimeters agreed with SNOOPY measurements at each site, the dosimeter measurements generally do not agree with the TEPC measurements anywhere.

The accuracy of each dosimeter type could be improved at each site by applying a correction, the inverse of the average response at the site. The most important characteristic then, in accurate dose estimation, is the precision of the measurement. Table 18 contains this "normalized" precision (just the standard deviation divided by the response) for comparison.

If the values were all normalized for each dosimeter, information in Table 18 indicates as an example that 67 percent (one standard deviation) of the dosimeters from Vendor A would be within 18 percent of the average dose equivalent (measured using the TEPC) at Site G.

The foregoing discussion is directed to one conclusion, namely that dosimeter response in the field needs to be accurately interpreted based on corrections for spectral differences encountered from plant to plant.

TABLE 18. Normalized Dosimeter Response Deviations

Vendor	Location Standard Deviation in % of Average Response E	G	I
A	27	18	23
B(D_2O)	22	15	5
B(Bare)	23	15	5
C	69	76	21
D	35	44	51
E	57	38	26
HMPD	6	17	14
LLL	10	19	10

As to choosing one dosimeter over another, two issues must be addressed: 1) sensitivity and 2) precision. It has been determined that dosimeters employing NTA film lack adequate sensitivity for use inside containment of nuclear plants (Endres et al. 1981; Schwartz et al. 1982). From this study (Tables 12 and 13, and Appendix Table A.25) it is apparent that Cr-39 and polycarbonate track etch films used without radiators are also inadequate. The rest of the dosimeters tested displayed adequate sensitivity. The two general types of dosimeters which comprise that group are: 1) TLD's and 2) the polycarbonate track etch which was used in conjunction with (n,α) radiators.

The dosimeters which displayed the tightest precision were the dosimeters used by Vendors A (TLD), B (TLD), HMPD (TLD) and LLL (TLD). Of these dosimeters two represent two different techniques for adjusting dosimeter response to account for spectral differences. Vendor B uses D_2O-moderated ^{252}Cf calibration which produces a response more similar to that found inside containment of nuclear power plants (Schwartz et al. 1982). Table 14 shows that the agreement with SNOOPY measurements is very good. LLL uses the Hankins TLD dosimeter and corrects the response based on the 9 in. to 3 in. sphere response technique. This amounts to calibrating the dosimeter to the remmeter for each field situation.

The polycarbonate dosimeter which utilized (n,α) radiators exhibited large variations in precision and saturated at several locations indicating the need for cautious use and analysis of the polycarbonate film. This dosimeter was adequately sensitive though and the authors believe that future improvements may help to render this dosimeter practical for general use.

4.2.3 Neutron Energy

By investigating the dosimeter responses inside containment of the power plants, several characteristics are indicated regarding the energy of neutrons present. If the TEPC-referenced dosimeter response from each reactor irradiation is placed in the dosimeter response function determined from Van de Graff irradiations, a neutron energy may be determined. That neutron energy is the energy of monoenergetic neutron beam which would give the same response as that determined at the particular reactor irradiation. A relative comparison may then be performed from site to site. Table 19 contains the energy data.

TABLE 19. Neutron Energies (in keV) at Reactor Sites Calculated from Dosimeter Response Data and Compared to Multisphere Data

Vendor	Site E	Site G	Site I
A	27	12	9
B (TLD)	66	16	9
B (CR-39)	<100	<100	<100
C	84	93	26
D	17	8	5
HMPD	146	45	31
Multispheres	155	59	53

The trends in Table 17 support the earlier conjecture that the neutron spectra inside containment were progressively moderated from Site E to Site G to Site I. Also, while not being able to use this data to conclusively arrive at an actual average energy, the data do indicate that the predominant number of neutrons are below 100 keV in energy. The information in Table 19 coupled with dosimeter response functions indicates the inappropriateness of using bare neutron sources to calibrate personnel neutron dosimeters for use inside reactor containment. Neutron sources such as $^{239}PuBe$, ^{210}PoB, $^{239}PuF_4$, $^{241}AmBe$, ^{252}Cf, etc., have hard spectra and most of the neutrons emitted from those sources are above 1 MeV. Since the dosimeters respond as if the neutrons are monoenergetic with energies 1 to 2 orders of magnitude smaller than 1 MeV, the use of bare sources as a direct calibration results in the overestimation of personnel neutron dose equivalents by factors of 2 to 100.

5.0 CONCLUSIONS

Three types of personnel neutron dosimeters from five commercial vendors and two DOE labs were irradiated inside nuclear power plants and to monoenergetic neutrons produced using a Van de Graff accelerator and using filtered reactor neutron beams. Dose equivalent rate measurements were conducted simultaneously using the TEPC and portable remmeters at the power plants. Neutron fluences at the accelerator were measured using the precision long counter. Dose equivalents during the accelerator measurements were calculated using fluence-to-dose equivalent conversions. Dose equivalents for the particular filtered beam irradiations were supplied by NBS.

The TEPC was used as the reference measurement as it provided the most accurate measurement of true dose equivalent. The dosimeters used to measure neutron dose equivalents inside the power plants were judged to be adequate or inadequate based on two criteria: 1) whether the dosimeters were sensitive enough to detect neutrons at low doses, and 2) whether the dosimeter results displayed tight precision. Dosimeter accuracy was not chosen as a criterion for adequacy as it is possible for any dosimeter judged adequate, under the previous two criteria, to be calibrated using site specific measurements.

The average dosimeter responses inside the nuclear power plants were used in conjunction with the dosimeter response functions determined from the accelerator and filtered beam irradiations, to draw conclusions about the neutron energy spectrum inside the power plants. From those conclusions, the use of certain high-energy neutron calibration sources was judged for appropriateness.

Additionally certain conclusions have been drawn about the response of portable remmeters and the use of calibrations which relate dosimeter response to remmeter response.

5.1 DOSIMETER RESPONSE

- TLD-Albedo

  All the TLD-albedo dosimeters evluated in this study proved to be adequate from the standpoint of sensitivity. The dosimeters generally responded high compared to the TEPC, in proportion to the amount of moderation present, or the decrease in neutron energy. Additionally, two dosimeter techniques, Vendor B's use of D_2O-moderated californium as a calibration source and LLL's corrections based on 9 in. to 3 in. sphere response ratios, responded closely to SNOOPY measurements.

  From the standpoint of precision the TLD dosimeters generally displayed good precision, the one standard deviation around the average dosimeter response being on the order of 20 percent or less. However, two TLD-albedo dosimeters exhibited precisions which were poorer than the rest, Vendors C and D. Where the other TLD systems

exhibited one standard deviation on the order of 20 percent (Table 18), these two exhibited one standard deviation which averaged 45 to 55 percent of the response. The poor precision demonstrated by these two vendors could be improved by improvements in their analysis techniques.

For these reasons, TLD-albedo dosimeters which display good precision and are appropriately calibrated are recommended for use inside nuclear power plants.

- Polycarbonate Track Etch Film with (n,α) Radiators

  Vendor E used (n,α) radiators to enhance the pit formation in the polycarbonate. This technique proved to be adequately sensitive for use inside nuclear power plants. The precision of results was roughly twice the value of the most precise TLDs and several of the polycarbonate dosimeters "saturated" rendering any evaluation of dose equivalent impossible. For those reasons it is recommended that this kind of dosimeter not be used inside nuclear power plants. At present it is thought that inconsistencies in the composition of the plastics are responsible for the fluctuations of precision. In the future, new techniques could greatly reduce those inconsistencies.

- Polycarbonate Track Etch Film Without (n,α) Radiators

  Because of its lack of sensitivity, polycarbonate film used without radiators was judged to be inadequate for use inside containment of nuclear power plants.

- CR-39 Track Etch Film Without (n,α) Radiators

  CR-39 track etch film was included in a combination TLD-albedo/CR-39/polycarbonate dosimeter. This part of the dosimeter exhibited a threshold at neutron energies of roughly 100 keV, below which it did not respond to neutrons. Additionally, this part of the dosimeter responded very low (when it did respond) to neutrons found inside nuclear power plants. It is therefore not recommended by itself for use inside nuclear power plants. As part of the combination dosimeter, CR-39 will extend the dosimeter response into the range of neutron energies above 1 MeV. The predominant number of neutrons at nuclear power plants was found generally to be less than 100 keV

- NTA Film

  While not evaluated in this study, NTA film is included in this discussion for comparison since it is employed by a large number of licensees. In 3 years of irradiation and evaluation, NTA film was insensitive to neutrons found in reactor containment (Endres et al. 1981) and is therefore not recommended for use inside nuclear power plants.

- Recommendations

  Because of their sensitivity and precision, TLD-albedo dosimeters are the only dosimeters, of those evaluated in this study, adequate for use inside nuclear power plants. Additionally, it is recommended, based on results in Table 17, that a 15-cm D_2O-moderated ^{252}Cf source be used as the calibration source, or that dosimeter measurements be adjusted based on 9 in./3 in. sphere response ratios.

5.2 INSTRUMENT RESPONSE

The TEPC was used as the reference instrument because of its accuracy during accelerator measurements (Brackenbush et al. 1979) and because it responded so closely to the previously conducted multisphere measurements. Since TEPCs are not commercially available as portable instruments yet, and since Subtask O of this project (starting in FY 1982) will focus on the optimization and evaluation of a commercially available TEPC, the SNOOPY (chosen to represent portable remmeters) was also used to compare dosimeter responses.

The portable remmeters generally responded high compared to the TEPC. The amount that the remmeters responded high was a funtion of the amount of moderation present, or the relative hardness of the neutron energy spectrum.

Since the TEPC is not commercially available in a portable model, and because the dosimeter corrections discussed in the preceding recommendations relate the dosimeter response very well to the response of the portable remmeters, it is recommended at this time that the portable remmeters be used for site-specific calibrations instead of the TEPC.

It is also noted that calibration of the portable remmeters with a moderated source, such as the D_2O-moderated ^{252}Cf source, will result in changing the relative response of the portable instruments inside nuclear power plants. We speculate that calibration could make the portable instruments respond more closely to the TEPC and multispheres, however the data to support such a change is not contained in this report, so no recommendation is made relative to the calibration of portable instruments.

5.3 NEUTRON ENERGY

Average neutron energies at each irradiation location inside the nuclear power plants were characterized in Subtask A using multisphere measurements. Using dosimeter response functions determined from monoenergetic neutron irradiations, using the Ven de Graff accelerator and NBS filtered reactor beams, response-weighted average neutron energies inside nuclear power plants were determined. The threshold of response for the track etch and NTA film

dosimeters indicated that neutrons were predominantly below 100 keV. The TLD-albedo response functions were used to determine response-weighted average neutron energies and from that data neutrons were found generally to be between 1 and 100 keV. That is in good agreement with the multisphere measurements from Subtask A and is summarized in Table 19.

The importance of that data is to indicate the necessity of using an appropriate calibration source or calibration technique which relates the dosimeter response to the true dose equivalent. Bare neutron calibration sources are not appropriate because they emit neutrons with energies higher than those found at nuclear power plants.

6.0 REFERENCES

Alsmiller and Barish 1974. Alsmiller, R. G., Jr. and J. Barish. "The Calculated Response of ^{6}LiF Albedo Dosimeters to Neutrons with Energies $\leq$400 MeV." Health Physics 26, 13 (1974).

Auxier et al. 1968. Auxier, J. A., W. S. Snyder and T. D. Jones. "Neutron Interactions and Penetration in Tissue," in Radiation Dosimetry, F. H. Attix and E. Tochilin, Eds. (Academic Press, New York 1968), Vol. 1, 293.

Awschalom 1966. Awschalom, M. "Use of the Multisphere Neutron Oetector for Dosimetry of Mixed Radiaton Fields," in Proceedings of the Symposium on Neutron Monitoring for Radiological Protection, International Atomic Energy Agency, August 29 - September 2, 1966, Vienna, Austria.

BNL-325. Hughes, D. J. and R. B. Schwartz. "Neutron Cross Sections," 2nd Edition, U.S. Atomic Energy Commission Report, BNL-325, July 1958.

BNW 1972. "Portable Radiation Survey Instrument Manual," in External Dose Evaluation, Part 2, BNWL-MA-62 PT 2, Battelle, Pacific Northwest Laboratories, Richland, WA 99352.

Brackenbush et al. 1979. Brackenbush, L. W., G. W. R. Endres and L. G. Faust. "Measuring Neutron Oose and Quality Factors With Tissue Equivalent Proportional Counters," in Proceedings of a Symposium on Advances in Radiation Protection Monitoring, June 26-30, 1978, Stockholm, Sweden.

Brackenbush et al. 1980. Brackenbush, L. W., G. W. R. Endres, J. M. Selby and E. J. Vallario. "Personnel Neutron Dosimetry at Department of Energy Facilities," USDOE Report PNL-3123/UC-41, August 1980.

Bramblett et al. 1960. Bramblett, R. L., R. I. Ewing and T. W. Bonner. "A New Type of Neutron Spectrometer." Nuclear Instrumentation and Methods 9, 1 (1960).

DePangher and Nichols 1966. DePangher, J., and L. L. Nichols. "A Precision Long Counter for Measuring Fast Neutron Flux Density." BNWL-260, Pacific Northwest Laboratory, Richland, Washington.

Endres et al. 1981. Endres, G. W. R., J. M. Aldrich, L. W. Brackenbush and R. V. Griffith. "Neutron Dosimetry at Commercial Nuclear Plants--Final Report of Subtask A: Reactor Containment Measurements," USNRC Report NUREG/CR-1769, May 1981.

Enge 1980. Enge, W. "Introduction to Plastic Nuclear Track Detectors." Nuclear Tracks 4, 283 (1980).

Glass and Samsky 1967. Glass, W. A., and D. N. Samsky. "Ionization in Thin Tissue-Like Gas Layers by Monoenergetic Protons." Radiation Research 32, 138 (1967).

Griffith and Fisher 1976. Griffith, R. V. and J. C. Fisher. "Lawrence Livermore Laboratory Hazards Control Progress Report No. 51, July through December 1975." USDOE Report UCRC-50007-75-2, 1976, Lawrence Livermore National Laboratory, University of California, Livermore, California.

Griffith et al. 1977. Griffith, R. V., D. R. Slaughter, H. W. Patterson, J. L. Beach, E. G. Frank D. W. Rueppel and J. C. Fisher, "Multi-Technique Characterization of Neutron Fields from Moderated ^{252}Cf and $^{239}PuBe$ Sources." USDOE Report UCRL-79483, Lawrence Livermore National Laboratory, University of California, Livermore, California.

Griffith et al. 1979. Griffith, R. V., D. E. Hankins, R. B. Gammage, L. Tommasino and R. V. Wheeler. "Recent Developments in Personnel Neutron Dosimeters - A Review." Health Phys. 36, 235 (1979).

Hajnal et al. 1979. Hajnal, F., R. S. Sanna, R. M. Ryan and E. H. Donnelly. "Stray Neutron Fields Inside the Containment of PWRs," in International Symposium on Occupational Radiation Exposure in Nuclear Fuel Cycle Facilities, IAEA-SM-242/24, June 18-22, 1979, Los Angeles, California.

Hankins, D. E. 1975. "The Effect of Energy Dependence on the Evalutions of Albedo Neutron Dosimeters." p. 861, in Proceedings of the Ninth Midyear Topical Symposium, Health Physics Society, February 9-12, 1977, Denver, Colorado.

Hankins and Griffith 1978. Hankins, D. E., and R. V. Griffith. "A Survey of Neutrons Inside the Containment of a Pressurized Water Reactor," in Radiation Streaming in Power Reactors, USDOE Report ORNL/RSIC-43, Oak Ridge National Laboratory, Oak Ridge, Tennessee.

Hankins 1977. Hankins, D. E., "Energy Deposition Measurements of Rem-Meters and Albedo Dosimeters at Neutron Energies of Thermal and Between 2 keV and 5.67 MeV," p. 553 in Proceedings of the International Radiation Protection Association's IV International Congress, 1977, Paris, France.

ICRU 1976. International Commission on Radiation Units and Measurements (ICRU). 1976. Radiation Protection Instrumentation and Its Application. ICRU Publication 20, International Commission on Radiation Units and Measurements, 7910 Woodmont Avenue, Washington, D. C.

ICRU 1977. International Commission on Radiation Units and Measurements (ICRU). 1977. Neutron Dosimetry for Biology and Medicine. ICRU Publication 26, International Commission on Radiation Units and Measurements, 7910 Woodmont Avenue, Washington, D.C.

Robkin 1968. Robkin, M. A. "An Explicit Error Calculation for Unfolded Spectra Obtained by Foil Activation." Nuclear Instruments and Methods 65, 213 (1968).

Rossi 1968. Rossi, H. H. "Microscopic Energy Distribution in Irradiated Matter," in Radiation Dosimetry, F. H. Attix and E. Tochilin, Eds. (Academic Press, New York 1966), Vol 1, 43.

Routti 1969. Routti, J. T. "High-Energy Neutron Spectroscopy with Activation Detectors, Incorporating New Methods for the Analysis of Ge(Li) Gamma-Ray Spectra and the Solution of Fredholm Integrals Equation." USDOE Report UCRL-18514 (Ph.D. Thesis), Lawrence Radiation Laboratory, University of California, Berkeley, California.

Routti and Sandberg 1978. Routti, J. T. and J. V. Sandberg. "General Purpose Unfolding Program LOUHI78 with Linear and Non-Linear Regularization," Report for Helsinki University of Technology, Department of Technical Physics, TKK-F-A359, SF 02150, ESPOO 15, Finland (1978).

Ryan 1982. Ryan, R. M. "Evaluation of Personnel Neutron Dosimetry at Operating Nuclear Power Plants," USNRC Report NUREG/CR-2454, June 1982.

Sanna 1973. Sanna, R. S. "Thirty One Group Response Matrices for the Multisphere Neutron Spectrometer Over the Energy Range Thermal to 400 MeV," USDOE Report HASL-267, 1973.

Schwartz et al. 1982. Schwartz, R. B., G. W. R. Endres and F. M. Cummings. "Neutron Dosimeter Performance and Associated Calibrations at Nuclear Power Plants," USNRC Report NUREG/CR-2233, April 1982.

Thorson and Endres 1981. Thorson, M. R., and G. W. R. Endres. "Statistical and Low Dose Response," in Hanford Personnel Dosimeter Supporting Studies FY-1980, USDOE Report PNL-3536, February 1981.

Zaidins et al. 1978. Zaidins, C. S., J. B. Martin and F. M. Edwards. "A Least-Squares Technique for Extracting Neutron Spectra from Bonner Sphere Data." Medical Physics 5(1), 42, (1978).

APPENDIX

DOSIMETER DATA FROM IRRADIATIONS AT NUCLEAR POWER PLANTS, AT THE VAN DE GRAAFF ACCELERATOR AND AT THE NATIONAL BUREAU OF STANDARDS RESEARCH REACTOR

TABLE A.1. Neutron Dosimeter Data for Site E, Location IX-29

Vendor	CP mR, γ	SNOOPY mrem, n	Dosimeter ID Number	Gamma Response, mR	Neutron Counts	Response, mrem	D_2O-Cf Response, mrem	Bare-Cf Response, mrem	CR-39 Response, mrem	Polycarbonate mrem
A	0	26	7046	0	52					
			7047	0	42					
			7048	0	45					
			7049	0	43					
			7050							
B	0	26	46				14	295	<10	<10
			47				17	354	<10	<10
			48				15	319	<10	<10
			49				15	330	<10	<10
			50				13	283	<10	<10
C	0	26	E6							
			E7							
			E8	25		55				
			E9							
			E10							
D	0	28	1546	12		76				
			1547	13		102				
			1548	11		111				
			1549	14		111				
			1550	11		83				
E	0	26	E-3							Saturated
			E-4							Saturated
			N-4							15
			N-5							11
			N-6							10
HMPD	0	28	E6	39		96				
			E7	41		102				
			E8	41		106				
			E9	40		119				
			E10	38		106				
LLNL	0	28	235	47		36				
			236	45		32				
			237	38						

Note: <10 means less than the detection limit of the dosimeter.

TABLE A.2. Neutron Dosimeter Data for Site E, Location 3X-29

Vendor	CP mR, γ	SNOOPY mrem,n	Dosimeter ID Number	Gamma Response, mR	Neutron Counts	Response, mrem	D_2O-Cf Response, mrem	Bare-Cf Response, mrem	CR-39 Response, mrem	Polycarbonate mrem
A	0	15	7041	0	34					
			7042	0	29					
			7043	0	30					
			7044	0	30					
			7045	0	22					
B	0	15	41				7	153	<10	<10
			42				9	189	<10	<10
			43				9	210	<10	<10
			44				9	189	<10	<10
			45				10	212	<10	<10
C	0	15	E-1							
			E-2							
			E-3	18		8				
			E-4							
			E-5							
D	0	15	1541	11		69				
			1542	13		65				
			1543	12		58				
			1544	9		67				
			1545	12		69				
E	0	15	E-1							Saturated
			E-2							Saturated
			N-1							8
			N-2							12
			N-3							16
HMPD	0	15	E-1	32		35				
			E-2	34		43				
			E-3	38		28				
			E-4	38		50				
			E-5	38		50				
LLNL	0	15	232	47		16				
			233	52		17				
			234	39		16				

Note: <10 means less than the detection limit of the dosimeter.

TABLE A.3. Neutron Dosimeter Data for Site G, Location 2

Vendor	CP mR, γ	SNOOPY mrem, n	Dosimeter ID Number	Gamma Response, mR	Neutron Counts	Response, mrem	D_2O-Cf Response, mrem	Bare-Cf Response, mrem	CR-39 Response, mrem	Polycarbonate mrem
A	170	220	7021	103	405					
			7022	146	299					
			7023	130	305					
			7024	137	312					
			7025	112	340					
B	30	40	21				28	590	<10	<10
			22				25	543	<10	<10
			23				26	566	<10	<10
			24				28	600	<10	<10
			25				27	578	<10	<10
C	30	40	G-1							
			G-2							
			G-3	29		10				
			G-4							
			G-5							
D	30	40	1521	32		133				
			1522	28		144				
			1523	35		140				
			1524	30		136				
			1525	34		147				
E	170	220	E1							Saturated
			E2							Saturated
			N1							119
			N2							165
			N3							176
HMPD	30	40	G1	28		162				
			G2	28		154				
			G3	29		162				
			G4	30		179				
			G5	32		166				
LLNL	170	220	216	162		137				
			217	171		131				
			218	165		132				
			219	166		137				

Note: <10 means less than the detection limit of the dosimeter.

TABLE A.4. Neutron Dosimeter Data for Site G, Location 3

Vendor	CP mR, γ	SNOOPY mrem,n	Dosimeter ID Number	Gamma Response, mR	Neutron Counts	Response, mrem	D_2O-Cf Response, mrem	Bare-Cf Response, mrem	CR-39 Response, mrem	Polycarbonate mrem
A	140	260	7026	25	434					
			7027	21	555					
			7028	23	506					
			7029	15	548					
			7030	0	675					
B	25	47	26				44	944	<10	<10
			27				45	968	<10	<10
			28				45	968	<10	<10
			29				46	990	<10	<10
			30				48	1027	<10	<10
C	25	47	G6							
			G7							
			G8	22		1				
			G9							
			G10							
D	25	47	1526	15		185				
			1527	15		182				
			1528	16		187				
			1529	14		169				
			1530	14		182				
E	140	260	E3							Saturated
			E4							Saturated
			N4							225
			N5							167
			N6							180
HMPD	25	47	G6	16		274				
			G7	16		282				
			G8	15		282				
			G9	16		310				
			G10	17		301				
LLNL	140	260	220	93		228				
			221	96		220				
			222	95		229				
			223	95		224				

Note: <10 means less than the detection limit of the dosimeter.

TABLE A.5. Neutron Dosimeter Data for Site G, Location 9

Vendor	CP mR, γ	SNOOPY mrem, n	Dosimeter ID Number	Gamma Response, mR	Neutron Counts	Response, mrem	D_2O-Cf Response, mrem	Bare-Cf Response, mrem	CR-39 Response, mrem	Polycarbonate mrem
A	430	1700	7031	0	2877					
			7032	0	4741					
			7033	381	3911					
			7034	212	3250					
			7035	0						
B	75	300	31				337	7220	<10	<10
			32				318	6810	<10	<10
			33				293	6280	<10	<10
			34				273	5850	<10	<10
			35				262	5600	<10	<10
C	75	300	G11							
			G12							
			G13	64		275				
			G14							
			G15							
D	75	300	1531	62		1115				
			1532	66		1099				
			1533	59		1105				
			1534	60		1094				
			1535	56		1088				
E	430	1700	E5							Saturated
			E6							Saturated
			N7							986
			N8							1562
			N9							747
HMPD	75	300	G11	67		1720				
			G12	61		1888				
			G13	60		1333				
			G14	56		1995				
			G15	52		1368				
LLNL	430	1700	224	416		1600				
			225	399		1490				
			226	387		1340				
			227	373		1300				

Note: <10 means less than the detection limit of the dosimeter.

TABLE A.6. Neutron Dosimeter Data for Site G, Location 15

Vendor	CP mR, γ	SNOOPY mrem, n	Dosimeter ID Number	Gamma Response, mR	Neutron Counts	Response, mrem	D_2O-Cf Response, mrem	Bare-Cf Response, mrem	CR-39 Response, mrem	Polycarbonate mrem
A	600	2000	7036	0	7155					
			7037	0	7901					
			7038	0	8285					
			7039	0	10439					
			7040	445	6456					
B	110	350	36				496	10630	<10	<10
			37				518	11140	20	<10
			38				512	10970	<10	<10
			39				528	11300	<10	<10
			40				553	11830	<10	<10
C	110	350	G16							
			G17							
			G18	84		510				
			G19							
			G20							
D	110	350	1536	81		1203				
			1537	87		1201				
			1538	91		1199				
			1539	94		1219				
			1540	91		1243				
E	600	2000	E7							Saturated
			E8							Saturated
			N10							Saturated
			N11							3012
			N12							3552
HMPD	110	350	G16	93		2667				
			G17	88		2437				
			G18	100		2724				
			G19	96		2907				
			G20	98		2267				
LLNL	600	2000	28	553		2340				
			29	577		2380				
			30	580		2380				
			31	580		2460				

Note: <10 means less than the detection limit of the dosimeter.

TABLE A.7. Neutron Dosimeter Data for Site I, Location 4

Vendor	CP mR, γ	SNOOPY mrem,n	Dosimeter ID Number	Gamma Response, mR	Neutron Counts	Response, mrem	D_2O-Cf Response, mrem	Bare-Cf Response, mrem	CR-39 Response, mrem	Polycarbonate mrem
A	65	100	7001	65	232					
			7002	15	311					
			7003	54	239					
			7004	100	294					
			7005	25	231					
B	65	100	1				97	2077	20	<10
			2				98	2089	<10	<10
			3				100	2148	<10	<10
			4				98	2089	<10	<10
			5				93	1994	<10	<10
C	66	110	IT1							
			IT2							
			IT3	45		105				
			IT4							
			IT5							
D	66	110	1501	57		555				
			1502	57		593				
			1503	59		507				
			1504	56		572				
			1505	57		576				
E	65	100	E1							Saturated
			E2							Saturated
			N1							115
			N2							93
			N3							95
HMPD	66	110	1	46		582				
			2	45		640				
			3	48		506				
			4	50		601				
			5	53		369				
LLNL	65	100	204	56		111				
			205	66		108				
			206	67		107				

Note: <10 means less than the detection limit of the dosimeter.

TABLE A.8. Neutron Dosimeter Data for Site I, Location 8

Vendor	CP mR, γ	SNOOPY mrem,n	Dosimeter IO Number	Gamma Response, mR	Neutron Counts	Response, mrem	D_2O-Cf Response, mrem	Bare-Cf Response, mrem	CR-39 Response, mrem	Polycarbonate mrem
A	50	160	7006	112	217					
			7007	27	328					
			7008	13	318					
			7009	35	306					
			7010	23	311					
8	50	160	6				137	2926	<10	<10
			7				150	3210	<10	<10
			8				150	3210	<10	<10
			9				151	3233	20	<10
			10				152	3245	<10	<10
C	50	150	IT6							
			IT7							
			IT8	45		160				
			IT9							
			IT10							
D	50	150	1506	45		731				
			1507	43		737				
			1508	42		715				
			1509	44		781				
			1510	44		790				
E	50	160	E3							Saturated
			E4							Saturated
			N4							134
			N5							95
			N6							Saturated
HMPD	50	150	6	39		975				
			7	42		905				
			8	44		909				
			9	44		881				
			10	41		687				
LLNL	50	160	207	66		161				
			208	46		173				
			209	59	149					

Note: <10 means less than the detection limit of the dosimeter.

TABLE A.9. Neutron Dosimeter Data for Site I, Location 10

Vendor	CP mR, γ	SNOOPY mrem, n	Dosimeter ID Number	Gamma Response, mR	Neutron Counts	Response, mrem	D_2O-Cf Response, mrem	Bare-Cf Response, mrem	CR-39 Response, mrem	Polycarbonate mrem
A	240	1200	7011	340	1362					
			7012	603	1042					
			7013	262	1415					
			7014	338	1232					
			7015	505	1071					
B	240	1200	11				722	15470	<10	<10
			12				732	15680	35	<10
			13				755	16180	<10	<10
			14				738	15800	30	<10
			15				678	14510	<10	<10
C	270	1300	IT11							
			IT12							
			IT13	124		610				
			IT14							
			IT15							
D	270	1300	1511	103		1228				
			1512	109		1280				
			1513	105		1267				
			1514	108		1266				
			1515	108		1245				
E	240	1200	E5							Saturated
			E6							Saturated
			N7							386
			N8							1158
			N9							553
HMPD	270	1300	11	105		4132				
			12	104		4614				
			13	113		3885				
			14	105		4487				
			15	107		2746				
LLNL	240	1200	210	178		682				
			211	180		739				
			212	182		742				

Note: <10 means less than the detection limit of the dosimeter.

TABLE A.10. Neutron Dosimeter Data for Site I, Location 12A

Vendor	CP mR, γ	SNOOPY mrem, n	Dosimeter ID Number	Gamma Response, mR	Neutron Counts	Response, mrem	D_2O-Cf Response, mrem	Bare-Cf Response, mrem	CR-39 Response, mrem	Polycarbonate mrem
A	64	310	7016	208	508					
			7017	320	496					
			7018	177	517					
			7019	275	499					
			7020	154	609					
B	64	310	16				246	5275	<10	<10
			17				253	5428	<10	<10
			18				258	5534	<10	<10
			19				296	6340	<10	<10
			20				303	6490	<10	<10
C	76	370	IT16, IT17, IT18, IT19, IT20	94		355				
D	76	370	1516	85		1140				
			1517	86		1154				
			1518	84		1144				
			1519	90		1138				
			1520	84		1169				
E	64	310	E7							Saturated
			E8							Saturated
			N10							--
			N11							370
			N12							442
HMPD	76	370	16	94		1274				
			17	83		1738				
			18	80		1287				
			19	81		2025				
			20	79		2237				
LLNL	64	310	213	83		259				
			214	73		279				
			215	75		271				

Note: <10 means less than the detection limit of the dosimeter.

TABLE A.11. NBS Filtered Beam, Thermal Neutron Irradiation

Vendor	mrem,n	Dosimeter IO Number	Gamma Response, mR	Neutron Counts	Response, mrem	D_2O-Cf Response, mrem	Bare-Cf Response, mrem	CR-39 Response, mrem	Polycarbonate mrem
A	50	22	0	1590					
		23	0	1682					
		24	0	1620					
B	50	16				<1	<1	<10	<10
		17				<1	<1	<10	<10
		18				<1	<1	<10	<10
		19				<1	<1	<10	<10
		20				<1	<1	<10	<10
C	50	13	1		764				
		14	1		801				
		23	1		820				
		24	1		880				
HMPD	50	21	186		109				
		22	186		94				
		23	194		85				
		24	196		91				
		25	209		86				

TABLE A.12. NBS Filtered Beam, 2 keV Irradiation

Vendor	mrem,n	Dosimeter ID Number	Gamma Response, mR	Neutron Counts	Response, mrem	D_2O-Cf Response, mrem	Bare-Cf Response, mrem	CR-39 Response, mrem	Polycarbonate mrem
A	50	17	0	372					
		18	0	314					
		19	0	235					
		20	0	334					
B	50	21				84	1546	<10	<10
		22				93	1711	<10	<10
		23				82	1510	<10	<10
		24				83	1534	<10	<10
		25				102	1888	<10	<10
C	50	22			14				
		23			13				
		25			19				
		26			19				
HMPO	50	21	45		2805				
		22	49		1832				
		23	70		1818				

TABLE A.13. NBS Filtered Beam, 24 keV Irradiation

Vendor	mrem,n	Dosimeter ID Number	Gamma Response, mR	Neutron Counts	Response, mrem	D_2O-Cf Response, mrem	Bare-Cf Response, mrem	CR-39 Response, mrem	Polycarbonate mrem
A	50	0001	0	135					
		0006	0	117					
		0008	0	126					
		0010	0	194					
		0011	0	145					
8	50	8104				110	2120	<10	<10
		8105				80	1530	<10	<10
		8106				125	2360	<10	<10
		8107				100	1890	<10	<10
		8109				90	1650	<10	<10
C	50	2	0.6		98				
		6	0.5		282				
		7	0.5		275				
		11	0.6		188				
		12	0.5		393				
D	50	1504			176				
		1506			173				
		1508			182				
		1510			178				
		1511			178				
E	50	392							55
		393							50
		394							40
		395							50
		402							40
HMPD	50	NB01	62		1570				
		N802	58		1420				
		NB03	61		1310				
		N804	60		1130				
		NB05	55		1350				

Note: <10 means less than the detection limit of the dosimeter.

TABLE A.14. NBS Filtered Beam, 144 keV

Vendor	mrem,n	Dosimeter ID Number	Gamma Response, mR	Neutron Counts	Response, mrem	D_2O-Cf Response, mrem	Bare-Cf Response, mrem	CR-39 Response, mrem	Polycarbonate mrem
A	50	0018	19	26					
		0019	15	11					
		0020	21	22					
		0021	15	15					
		0024	17	2					
B	50	8123				25	470	30	<10
		8124				25	470	30	<10
		8125				25	470	30	<10
		8126				25	470	70	<10
		8127				31	590	120	<10
C	50	22	0.5		85				
		27	0.8		43				
		29	0.4		163				
		30	0.4		141				
		31	0.4		214				
D	50	1524			33				
		1525			157				
		1526			28				
		1528			39				
		1529			24				
E	50	458							70
		459							70
		460							60
		472							70
		476							70
HMPD	50	NB15	55		331				
		NB16	50		447				
		N817	63		472				
		NB18	52		465				

Note: <10 means less than the detection limit of the dosimeter.

TABLE A.15. Van de Graaff, 70 keV Irradiation

Vendor	mrem,n	Dosimeter ID Number	Gamma Response, mR	Neutron Counts	Response, mrem	D_2O-Cf Response, mrem	Bare-Cf Response, mrem	CR-39 Response, mrem	Polycarbonate mrem
A	46	0001	0	45					
		0002	0	45					
		0003	0	42					
B	46	1				31	566	30	<10
		2				34	625	60	<10
		3				33	614	<10	<10
C	46	1	1		57				
		3	1		86				
		5	1		53				
D	Did Not Participate								
E	46								30(12)
HMPD	46	JT01	13		473				
		JT02	15		343				
		JT03	13		536				

Note: <10 means less than the detection limit of the dosimeter.

TABLE A.16. Van de Graaff, 97 keV Irradiation

Vendor	mrem,n	Dosimeter ID Number	Gamma Response, mR	Neutron Counts	Response, mrem	D_2O-Cf Response, mrem	Bare-Cf Response, mrem	CR-39 Response, mrem	Polycarbonate mrem
A	50	0004	0	35					
		0005	0	35					
		0006	0	37					
B	50	4				26	484	<10	<10
		5				28	519	<10	<10
		6				28	519	30	<10
C	50	8	1		94				
		9	0		25				
		10	0		104				
D	Did Not Participate								
E	50								30(12)
HMPD	50	JT04	13		413				
		JT05	12		422				
		JT06	13		345				

Note: <10 means less than the detection limit of the dosimeter.

TABLE A.17. Van de Graaff, 110 keV Irradiation

Vendor	mrem,n	Dosimeter IO Number	Gamma Response, mR	Neutron Counts	Response, mrem	D_2O-Cf Response, mrem	Bare-Cf Response, mrem	CR-39 Response, mrem	Polycarbonate mrem
A	61	0002	0	58					
		0026	0	48					
		0009	0	59					
B	61	8131				38	708	140	<10
		8114				43	790	220	<10
		8136				36	660	160	<10
C	61	16	1		20				
		19	0		68				
		14	1		18				
D	61	1527			94				
		1518			75				
		1535			81				
E	61	7179							115
		7187							115
		7188							140
HMPD	61	RR9	18		344				
		RR10	19		257				
		RR4	17		337				

Note: <10 means less than the detection limit of the dosimeter.

TABLE A.18. Van de Graaff, 161 keV Irradiation

Vendor	mrem,n	Dosimeter ID Number	Gamma Response, mR	Neutron Counts	Response, mrem	D_2O-Cf Response, mrem	Bare-Cf Response, mrem	CR-39 Response, mrem	Polycarbonate mrem
A	35	0012	0	25					
		0027	0	16					
		0004	0	19					
B	35	8130				16	295	160	<10
		8110				15	283	120	<10
		8115				15	271	180	<10
C	35	21	1		7				
		26	1		5				
		25	1		19				
D	35	1520			3				
		1517			2				
		1503			28				
E	35	7173							60
		7184							55
		7486							80
HMPO	35	RR14	16		151				
		RR3	15		168				
		RR2	15		188				

Note: <10 means less than the detection limit of the dosimeter.

TABLE A.19. Van de Graaff, 264 keV Irradiation

Vendor	mrem,n	Dosimeter ID Number	Gamma Response, mR	Neutron Counts	Response, mrem	D_2O-Cf Response, mrem	Bare-Cf Response, mrem	CR-39 Response, mrem	Polycarbonate mrem
A	55	0017	0	15					
		0025	0	17					
		0022	0	0					
B	55	8108				19	342	120	<10
		8121				18	319	190	<10
		8118				20	366	210	<10
C	55	13	1		12				
		5	1		10				
		18	0		50				
D	55	1502			30				
		1507			26				
		1517			26				
E	55	7175							50
		7176							35
		7181							50
HMPD	55	RR20	17		123				
		RR6	16		115				
		RR17	16		136				

Note: <10 means less than the detection limit of the dosimeter.

TABLE A.20. Van de Graaff, 358 keV Irradiation

Vendor	mrem,n	Dosimeter ID Number	Gamma Response, mR	Neutron Counts	Response, mrem	D_2O-Cf Response, mrem	Bare-Cf Response, mrem	CR-39 Response, mrem	Polycarbonate mrem
A	67	0034	0	15					
	67	0023	0	12					
	68	0005	0	19					
B	67	8115				15	271	180	<10
	67	8133				14	260	160	<10
	68	8134				12	224	390	<10
C	67	3	2		7				
	67	23	1		11				
	68	17	1		11				
D	67	1513			23				
	67	1505			28				
	68	1512			31				
E	67	7189							50
		7190							55
		7191							80
HMPD	67	RR12	15		109				
	67	RR13	16		115				
	68	RR8	15		121				

Note: <10 means less than the detection limit of the dosimeter.

TABLE A.21. Van de Graaff, 448 keV Irradiation

Vendor	mrem,n	Dosimeter ID Number	Gamma Response, mR	Neutron Counts	Response, mrem	D_2O-Cf Response, mrem	Bare-Cf Response, mrem	CR-39 Response, mrem	Polycarbonate mrem
A	104	0000	0	22					
	116	0014	0	22					
	104	0031	0	15					
B	104	8116				17	307	250	<10
	116	8135				13	248	180	<10
	104	8120				19	342	230	<10
C	104	1	1		5				
	116	8	0		25				
	104	24	0		22				
D	104	1509			32				
	116	1516			27				
	104	1501			25				
E	104	7178							50
		7180							80
		7185							60
HMPD	104	RR11	16		181				
	116	RR15	17		100				
	104	RR18	16		131				

Note: <10 means less than the detection limit of the dosimeter.

TABLE A.22. Van de Graaff, 4.1 MeV Irradiation

Vendor	mrem,n	Dosimeter ID Number	Gamma Response, mR	Neutron Counts	Response, mrem	D_2O-Cf Response, mrem	Bare-Cf Response, mrem	CR-39 Response, mrem	Polycarbonate mrem
A	54	0007	0	7					
		0008	0	4					
		0009	0	2					
B	54	7				<1	<1	50	<10
		8				<1	<1	60	<10
		9				4	83	50	<10
C	54	17	1.1		3				
		18	1.1		1				
		19	2.2		1				
D	Did Not Participate								
E	54								30(12)
HMPD	54	JT07	10		59				
		JT08	10		38				
		JT09	10		39				

Note: <10 means less than the detection limit of the dosimeter.

TABLE A.23. Van de Graaff, 4.5 MeV Irradiation

Vendor	mrem,n	Dosimeter ID Number	Gamma Response, mR	Neutron Counts	Response, mrem	D_2O-Cf Response, mrem	Bare-Cf Response, mrem	CR-39 Response, mrem	Polycarbonate mrem
A	54	0010	0	0					
		0011	0	3					
		0012	0	7					
B	54	10				<1	24	20	<10
		11				<1	35	100	<10
		12				<1	35	50	<10
C	54	21	0.2		17				
		25	2.0		2				
		26	1.1		5				
E	54								30(12)
HMPD	54	JT10	10		40				
		JT11	11		34				
		JT12	10		48				

Note: <10 means less than the detection limit of the dosimeter.

TABLE A.24. Van de Graaff, 4.9 MeV Irradiation

Vendor	mrem,n	Dosimeter IO Number	Gamma Response, mR	Neutron Counts	Response, mrem	D_2O-Cf Response, mrem	Bare-Cf Response, mrem	CR-39 Response, mrem	Polycarbonate mrem
A	54	0013	0	6					
		0014	0	4					
		0015	0	1					
B	54	13				<1	<1	40	<10
		14				<1	<1	60	<10
		15				3	47	40	<10
C	54	28	1.3		7				
		29	0.7		1				
		30	1.2		3				
E	54								30(12)
HMPD	54	JT13	11		46				
		JT14	10		37				
		JT15	12		45				

Note: <10 means less than the detection limit of the dosimeter.

TABLE A.25. Summary of Average Neutron Dosimeter Measurements for Reactor Irradiations

Site	Location	Integrated Dose Equiv. SNOOPY mrem	Integrated Dose Equiv. TEPC mrem	Vendor A[a] Counts	Vendor B TLD D_2O: ^{252}Cf mrem	Vendor B TLD Bare: ^{252}Cf mrem	Vendor B CR-39 mrem	Vendor B Poly-Carbonate mrem	Vendor C mrem	Vendor D[b] mrem	Vendor E mrem	HMPD mrem	LLNL[c] mrem
E	First Irradiation:												
	1x-29	26	21	46 (4.5)	15 (1.2)	320 (28)	<10	<10	55 (26)		12 (2.7)		
	3x-29	15	9	29 (4.4)	8.8 (1.1)	190 (22)	<10	<10	8 (10)		12 (4.0)		
	Second Irradiation:												
	1x-29	32	22							97 (16)		110 (8.4)	34 (2.8)
	3x-29	15	9							66 (4.6)		41 (9.6)	16 (0.6)
G	First Irradiation:												
	2	40	8		27 (1.3)	580 (22)	<10	<10	10 (8)	140 (5.7)		160 (9.2)	
	3	47	19		46 (1.5)	980 (31)	<10	<10	1 (3)	180 (7.0)		290 (15)	
	9	300	110		300 (31)	6400 (670)	<10	<10	280 (28)	1100 (10)		1700 (300)	
	15	350	190		510 (21)	11200 (440)	4 (9)	<10	510 (76)	1200 (19)		2600 (250)	
	Second Irradiation:												
	2	220	42	330 (44)							150 (30)		130 (3.2)
	3	260	100	540 (88)							190 (30)		230 (4.1)
	9	1700	650	3700 (710)							1100 (420)		1400 (140)
	15	2000	1100	8000 (1500)							2200 (1900)[d]		2400 (50)
I	First Irradiation:												
	4	100	20	260 (38)	97 (2.6)	2100 (55)	4 (9)	<10			100 (12)		110 (2.1)
	8	160	33	300 (45)	150 (6.2)	3200 (134)	4 (9)	<10			76 (69)[d]		160 (12)
	10	1200	170	1200 (170)	730 (29)	15500 (630)	13 (18)	<10			700 (410)		720 (30)
	12A	310	67	530 (47)	270 (26)	5800 (560)	<10	<10			270 (240)[d]		270 (10)
	Second Irradiation:												
	4	110	22						110 (3)	560 (33)		540 (110)	
	8	150	32						160 (12)	750 (33)		870 (110)	
	10	1300	200						610 (56)	1300 (21)		4000 (740)	
	12A	370	80						360 (11)	1100 (13)		1700 (430)	

(a) Values are given as net neutron response in units of counts. Fast neutron dose equivalent cannot be evaluated from these results.
(b) Values given as mR equivalent. Fast neutron dose equivalent cannot be evaluated from these results.
(c) Corrected for spectral response using the 9 in. to 3 in. sphere ratio technique.
(d) "Saturated" dosimeter included in average as "0."
NOTE: Numbers in parentheses indicate one standard deviation. "<" numbers mean below the detection limit of the dosimeter.

TABLE A.26. Summary of Average Neutron Dosimeter Measurements for Monoenergetic Irradiations

Irradiation by Neutron Energy, keV	Integrated Dose Equiv. mrem	Vendor A[a] Counts	Vendor B				Vendor C mrem	Vendor D[b] mrem	Vendor E mrem	HMPD mrem
			TLD D_2O: ^{252}Cf mrem	TLD Bare: ^{252}Cf mrem	CR-39 mrem	Poly-Carbonate mrem				
Thermal (NBS)	50	1630 (47)	<1	<1	<10	<10	815 (49)	---	---	93 (9)
2 (NBS)	50	315 (60)	89 (9)	1640 (161)	<10	<10	16 (3)	---	---	2150 (566)
24 (NBS)	50	143 (30)	101 (17)	1910 (339)	<10	<10	247 (111)	177 (3)	47 (7)	1360 (161)
70 (PNL)	46	44 (2)	33 (2)	602 (31)	30 (30)	<10	65 (18)	---	30 (12)	451 (98)
97 (PNL)	50	36 (1)	27 (1)	507 (20)	10 (17)	<10	74 (43)	---	30 (12)	393 (42)
110 (PNL)	61	55 (7)	39 (4)	719 (66)	173 (42)	<10	35 (28)	83 (10)	23 (14)	313 (48)
144 (NBS)	50	15 (9)	26 (3)	494 (54)	56 (40)	<10	129 (67)	56 (57)	68 (4)	429 (66)
161 (PNL)	35	20 (5)	15 (1)	283 (12)	153 (31)	<10	10 (8)	29 (2)	65 (13)	169 (19)
264 (PNL)	55	11 (9)	19 (1)	342 (24)	173 (47)	<10	24 (23)	27 (2)	45 (8.7)	125 (11)
358 (PNL)	67	15 (4)	14 (2)	252 (25)	243 (127)	<10	10 (2)	27 (4)	62 (16)	115 (6)
448 (PNL)	104[c]	20 (4)	16 (3)	299 (48)	220 (36)	<10	17 (11)	28 (4)	63 (15)	137 (41)
4100 (PNL)	54	4 (3)	1 (2)	28 (48)	53 (6)	<10	2 (1)	---	30 (12)	45 (12)
4500 (PNL)	54	3 (4)	<1	31 (6)	57 (40)	<10	8 (8)	---	30 (12)	41 (7)
4900 (PNL)	54	4 (3)	1 (2)	16 (27)	47 (12)	<10	4 (3)	---	30 (12)	43 (5)

(a) Values are given as net neutron response in units of counts. Fact neutron dose equivalent dannot be evaluated from these results.
(b) Values are given as mR equivalent. Fact neutron dose equivalent cannot be evaluated from these results.
(c) One of the three irradiations was 116 mrem.
NOTE: Numbers in parentheses indicate one standard deviation. "<" numbers mean below the detection limit of the dosimeter.

NUREG/CR-2956
PNL-4471
RL-RH

DISTRIBUTION

No. of Copies

OFFSITE

315 U.S. Nuclear Regulatory Commission
Division of Technical Information and Document Control
7920 Norfolk Avenue
Bethesda, MD 20014

20 Margaret Federline
U.S. Nuclear Regulatory Commission
Office of Radiation Protection
NL-5650
Rockville, MD 20852

2 N. A. Dennis
U.S. Nuclear Regulatory Commission
Region 1
631 Park Avenue
King of Prussia, PA 19406

2 F. M. Costello
U.S. Nuclear Regulatory Commission
Region 1
631 Park Avenue
King of Prussia, PA 19406

2 R. B. Schwartz
U.S. National Bureau of Standards
Quince Orchard Rd.
Gaithersburg, MD 20760

2 A. Zirkes
Dosimeter Corporation
P.O. Box 42377
Cincinnati, OH 45242

No. of Copies

2 R. V. Wheeler
R. S. Landauer, Jr. and Co.
Glenwood Science Park
Glenwood, IL 60425

2 C. Distenfeld
Teledyne Isotopes
50 Van Buren Avenue
Westwood, NJ 07675

2 E. Geiger
Eberline Company
P.O. Box 2108
Santa Fe, NM 87501

2 Richard Griffith
Hazards Control Department
Lawrence Livermore National Laboratory
P.O. Box 5505
Livermore, CA 94550

ONSITE

50 F. M. Cummings (20)
L. W. Brackenbush
G. W. R. Endres
T. H. Essig
L. G. Faust
D. L. Haggard
J. J. Jech
R. I. Scherpelz
K. L. Soldat
Technical Information (5)
Publishing Coordination (2)

NRC FORM 335 (11 81)

U.S. NUCLEAR REGULATORY COMMISSION

BIBLIOGRAPHIC DATA SHEET

1. REPORT NUMBER (Assigned by DDC)
NUREG/CR-2956
PNL-4471

4. TITLE AND SUBTITLE (Add Volume No., if appropriate)
Neutron Dosimetry at Commercial Nuclear Plants
Final Report of Subtask B: Dosimeter Response

2. (Leave blank)

3. RECIPIENT'S ACCESSION NO.

7. AUTHOR(S)
F. M. Cummings, G. W. R. Endres, L. W. Brackenbush

5. DATE REPORT COMPLETED
MONTH: February YEAR: 1983

9. PERFORMING ORGANIZATION NAME AND MAILING ADDRESS (Include Zip Code)
Pacific Northwest Laboratory
Richland, WA 99352

DATE REPORT ISSUED
MONTH: March YEAR: 1983

6. (Leave blank)

8. (Leave blank)

12. SPONSORING ORGANIZATION NAME AND MAILING ADDRESS (Include Zip Code)
Division of Facility Operations
Office of Nuclear Regulatory Research
U.S. Nuclear Regulatory Commission
Washington, D.C. 20555

10. PROJECT/TASK/WORK UNIT NO.

11. FIN NO.
B2282

13. TYPE OF REPORT
Final Report on Subtask B

PERIOD COVERED (Inclusive dates)
October 1980 - February 1983

15. SUPPLEMENTARY NOTES

14. (Leave blank)

16. ABSTRACT (200 words or less)

As part of a larger program to evaluate personnel neutron dosimetry at commercial nuclear power plants, this study was designed to characterize neutron dosimeter responses inside the containment structure of commercial nuclear plants. In order to characterize those responses, dosimeters were irradiated inside containment at 2 pressurized water reactors and at pipe penetrations outside the biological shield at two boiling water reactors while the reactors were operating at full power. Additionally, the dosimeters were irradiated (1) using monoenergetic neutrons produced by an accelerator and (2) using the filtered reactor beams at the National Bureau of Standards research reactor. During the reactor irradiations simultaneous measurements were taken using a tissue equivalent proprotional counter and portable remmeters, SNOOPY, RASCAL and PNR-4.

The results of the analyses of dosimeter responses indicate that (1) the dosimeters irradiated inside containment of PWR's respond as if the dosimeters were irradiated using monoenergetic neutrons below 100 keV, (2) that the use of bare neutron sources for dosimeter calibration is inappropriate for the in-containment irradiations, (3) the TLD-albedo dosimeter is the only type of dosimeter available that demonstrated both adequate precision and sensitivity, (4) that the polycarbonate track etch dosimeter which uses (n,α) radiators was sensitive enough, but demonstrated inadequate precision for the reactor irradiations and that (5) CR-39 and polycarbonate track etch dosimeters which do not use (n,α) radiators were inadequate for use inside containment of nuclear power plants.

17. KEY WORDS AND DOCUMENT ANALYSIS

17a DESCRIPTORS
Neutron dosimetry, BWR, Personnel dosimeters, PWR, Tissue Equivalent Proportional Counter rem meter

17b IDENTIFIERS/OPEN-ENDED TERMS

18. AVAILABILITY STATEMENT
Unlimited

19. SECURITY CLASS (This report)
Unclassified

21. NO OF PAGES
99

20. SECURITY CLASS (This page)
Unclassified

22. PRICE
$

NRC FORM 335 (11 81)

* U.S. GOVERNMENT PRINTING OFFICE: 1983-381-297:3004